

Absorption Flattening Correction of Circular Dichroism Spectra of Particle Suspensions

Anna Gerdova

(200879589)



Department of Pure and Applied Chemistry

Thesis submitted for the degree of Master of Philosophy

March 2013

This thesis is the result of the author's original research. It has been composed by the author and has not been previously submitted for examination which has led to the award of a degree.

The copyright of this thesis belongs to the author under the terms of the United Kingdom Copyright Acts as qualified by University of Strathclyde Regulation 3.50. Due acknowledgement must always be made of the use of any material contained in, or derived from, this thesis.

Signed:

Date:

ABSTRACT

There are a number of theoretical models for correction for absorption flattening of circular dichroism (CD) measurements on particle suspensions. However, they have not been directly tested experimentally and there remains doubt as to whether the corrections are actually accurate. The aim of this thesis was to test the correction method recently developed by Halling (2009), by comparing corrected CD spectra with the expected ones. Proposed simulation method was applied to a test model containing different particles (both protein and non-protein nature). In case of non-protein containing particles corrections seem to work, but for protein-containing samples corrected CD spectra did not agree with the expected ones.

The alternative approach to solving the problem with effect of absorption flattening was tested. The use of intensive synchrotron source allowed collecting feasible CD spectra on single protein-containing particles (100 μm in diameter). This approach also revealed structural differences between particles in the same suspension.

ACKNOWLEDGEMENTS

I would like to express my sincere gratitude to my supervisor Prof. Peter Halling for his guidance, help, support, encouragement, patience and time. I could not wish for a better and friendlier supervisor.

A special thank you to Dr. Sharon Kelly who taught me a lot about the Circular Dichroism, and made me feel always welcome in her lab. Without her help and expertise, this thesis might not be accomplished.

I am grateful to the staff and students at IIT Delhi, for the wonderful opportunity of being a part of their lab during my visit. And also for the time afforded showing me around Delhi.

Biggest thanks to my lab colleagues: Lee (Apostolos Alissondratos), Anna Jawor-Baczynska, Cheska Gillespie, Lauren Bayne, John (Ikuba Ona). Thank you for your help and for keeping a good and friendly environment in the lab. It has been great working with you guys.

This thesis would not be possible without the support of my parents. They have always motivated, encouraged and inspired me. Special thanks to my husband Dr. Ivan Konoplev for his support and assistance. He was always there for me and ready to help in any possible way.

I would like to acknowledge ORSAS for the scholarship that allowed me to carry out this research, and also the financial support from UK India Education Research Initiative (UKEIRI). I offer my regards to all of those who supported me during this thesis.

I would like to dedicate this work to my daughters Taisia and Sophia who were born during this research. Thank you for bringing happiness and inspiration to go on in my work.

TABLE OF CONTENTS

Abstract	iii
Acknowledgements	iv
Table of Contents	v
Contribution Statement	x

LITERATURE REVIEW

Introduction	1
1. Immobilization of enzymes	2
1.1. Adsorption	3
1.2. Covalent binding	4
1.3. Entrapment	5
1.4. Encapsulation	6
1.5. Crosslinking	7
2. Methods to analyse state of protein in immobilized enzymes	7
3. Circular Dichroism measurements of proteins	9
3.1. Circular Dichroism Spectroscopy and its principles	9
3.2. Operation of CD spectropolarimeter	11
3.3. Information on protein structure obtained from Circular Dichroism	13
a) <i>Information available from the far UV region</i>	14
b) <i>Information available from the near UV region</i>	15

<i>c) Information available from near UV – Visible region</i>	17
3.4. Circular Dichroism measurements on proteins in particulate form	17
3.4.1. <i>Differential light scattering artefact</i>	18
3.4.2. <i>Absorption flattening artefact</i>	18
4. Synchrotron radiation Circular Dichroism	22
References	27

CHAPTER I

Absorption flattening correction for circular dichroism of particle suspensions in near UV – Visible region

Abstract	35
Introduction	36
Materials and Methods	38
Resolution of racemic tris(ethylenediamine)cobalt (III) chloride	38
Preparation of the samples	38
Circular dichroism	39
Estimation of volume of particles in the cell	40
Determination of the amount of λ -[Co(en) ₃] ³⁺ in the cell	41
Distribution of particle sizes	42
Correction of absorption flattening	42
Estimation of apparent absorbance of suspension	44
Correction of each point in CD spectra	45
Obtaining true CD spectra to compare with the corrected ones	46

Results and Discussions	46
Principles of test	46
Scattering contributions	47
Test of model corrections	49
Conclusions	55
References	56

CHAPTER II

Absorption flattening correction of CD spectra of large particle suspensions in UV region.

Introduction	59
Materials and Methods	60
Sample preparation	61
Circular dichroism measurements	61
Estimation of absorption flattening correction factor	62
Correction of CD spectra	68
Comparison of true CD spectra with the corrected ones	68
Results and Discussions	69
10-Camphorsulfonic acid sample	69
Trans-4-hydroxy-L-proline	71
D-(-)-Phenylglycine	73
L-Ascorbic acid	75
Conclusions	78
References	79

CHAPTER III

Absorption flattening correction of CD spectra of particles containing protein.

Introduction	81
Materials and Methods	82
Sample preparation	82
Circular Dichroism measurements	83
Estimation of absorption flattening correction factor	83
Correction of CD spectrum and its comparison to the true one	83
Results and Discussions	84
CD measurements of subtilisin Carlsberg suspensions	84
Correction of CD spectra for absorption flattening	87
Conclusions	92
References	93

CHAPTER IV

Circular dichroism measurements on individual 100 μm particles containing proteins using synchrotron light beam

Introduction	96
Materials and Methods	97
Methods	97
Results and Discussions	99

Sample presentation	99
Blank spectra	102
Amount of light reaching detector	104
Standard spectrum of solution	105
Protein-containing particles: ovalbumin prepared by TPP	106
Chymotrypsin EPRPs	110
Chymotrypsin CLEAs	111
Conclusions	113
References	114
CONCLUSIONS AND FUTURE WORK	117
APPENDIX	120

CONTRIBUTION STATEMENT

Chapter I: was previously published as an article in Chirality 2011; 23(7): 574-579, written by Gerdova A., Kelly S.M. and Halling P.J., named as “Experimental test of absorption flattening correction for circular dichroism of particle suspensions”. I therefore state that all the experimental work has been carried out by me. Description of these experiments with the results, conclusions and all the figures were done by me with the help and editing by my supervisor prof. Halling and S.M. Kelly. Abstract and introduction were written by prof. Halling and edited by S.M. Kelly.

Chapter IV: This work was done by Anna Gerdova, Kusum Solanki, Sharon M Kelly, Tamas Javorfi, Rohanah Hussain, Giuliano Siligardi, Gulam Mohmad, Munishwar N. Gupta, Peter J. Halling, and is ready to be submitted for publication. I therefore state that I have taken part in all the experimental work that has been carried out at the Diamond facilities, including preparation work at Strathclyde University. I was involved in designing and constructing of the sample holder; as well as collecting, processing and analyzing all the results. Description of these experiments with the results and conclusions were mainly written by my supervisor prof. Halling. I have plotted all the graphs, figures and pictures. The manuscript was edited by all authors and finalized by me.

Appendix: is an article that was submitted to the Analytical Biochemistry journal. It is a combined work carried out by me, Kusum Solanki and supervised by prof.Gupta and prof.Halling. I was involved in all the experiments and calculations. The manuscript was written by K. Solanki and edited by all authors.

All other material in the thesis has been written by me, with just the usual comments and advice from my supervisor.

Signature

LITERATURE REVIEW

INTRODUCTION

In last decades the use of enzymes as biocatalysts has grown remarkably. Enzymes are highly chemo-, regio- and enantioselective, therefore they are very attractive for pharmaceutical and agrochemical areas. Immobilised enzymes are in particular interest, because of their convenience in use, economy, and stability.

Due to their nature enzymes are thought to be restricted to aqueous reaction media. This significantly limits the scope of their application. Switching aqueous media to organic media might seem impossible because of the experience of enzymes denature in aqueous-organic mixture, but in the last 20 years scientists proved that many enzymes can work in neat organic solvents and organic solvents containing little water^{1, 2, 3}. Unfortunately not all the methods that prepare enzymes for use in such media give high catalytic activity (in comparison with aqueous media)^{4, 5}. To understand why it happens and to improve preparation methods it is important to look at the state of enzyme molecules.

Circular Dichroism is a valuable spectroscopic technique for examining structure of enzymes. This technique can be used not only for studying enzymes in solutions but is also applicable to protein-containing particle suspensions, like immobilized enzymes⁶.

1. IMMOBILIZATION OF ENZYMES.

Since the second half of the last century, numerous efforts have been devoted to the development of insoluble immobilized enzymes that have a wide range of applications⁷⁻¹⁰. For example, in industrial biocatalysis, immobilized enzymes are often preferred over free enzymes due to their easy handling and reusability; these can reduce the production cost. Immobilization has also been used to protect enzyme activity in low water organic media, to make the shelf life of dehydrated protein longer, and in the stabilization of vaccines preparations.

Immobilized enzymes have to perform two main functions: non-catalytical one, which helps separation (e.g. recycling) of biocatalyst and control the process; and the catalytical one, which helps the performance of the reaction itself (productivity, stability, selectivity, etc.).

There is a number of methods to immobilize enzyme: adsorption, covalent binding, entrapment, encapsulation, crosslinking (Fig.1.1).

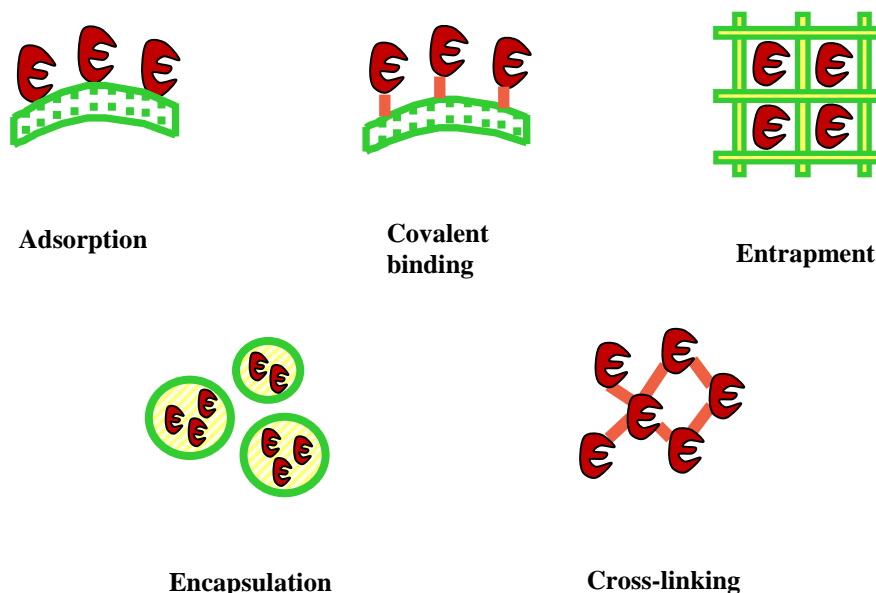


Fig.1.1. Methods of enzyme immobilization.

The choice of the immobilization method and the carrier depends on the nature of the enzyme and needs of the reaction; basically the main task is to select parameters at which both catalytical and non-catalytical needs of the reaction will be met.

1.1. Adsorption

Immobilization by adsorption is a low cost and simple technique, which allows re-use of the carrier. It enables enzyme to immobilize under mild conditions, and because there are no chemical modifications involved, adsorption method can possibly retain high activity of enzyme. The forces that allow binding are weak forces like ionic interactions, hydrogen bonds, van der Waals forces, etc. The procedure consists of mixing together biological components and a support with adsorption properties under suitable conditions for a period of incubation, followed by collection of the immobilized material and washing out the nonbound biological components.

The most significant disadvantage of this method is leakage of biocatalyst from the support⁸. There is a number of reasons behind desorption:

- environmental changes in pH, ionic strength, temperature;
- changes in conformation of protein because of substrate binding, binding of contaminants presenting in the substrate, or other conditions;
- physical factors, such as flow rate, particle agitation, particle-particle abrasion.

Another problem of this method is the absence of suitable spacer between the support and the enzyme can produce problems related to steric hindrance.

1.2. Covalent binding

Another method of immobilization is by covalent binding the enzyme and the support material, by forming a bond between functional groups on the surface of the support and functional groups of amino acid of the enzyme (that are not essential to catalytic action). There are many support materials available. The most important factor for maintaining enzyme activity in the support environment is hydrophilicity⁹. Thus, polysaccharide polymers, which contain hydroxyl groups, are very popular supports: cellulose, dextran (Sephadex), starch, agarose (sepharose). But because they are mechanically weak they are not good for large scale applications. Other popular supports that have high stability are inorganic carriers, like porous silica and porous glass¹¹.

Formation of covalent bond between enzymes and support can be done by a range of reactions; most of them involve coupling through protein amino groups, thiol groups, carboxy groups or aromatic rings of L-tyrosine and L-histidine. The major classes of coupling reactions are¹⁰:

- Diazo linkage between amino groups of proteins and aryl-diazonium electrophilic groups of the carrier;
- Amide bond formation method is based on the attack of amino groups of protein at an activated functional group on the carrier ;
- Alkylation and arylation reactions are based on the alkylation of amino, phenolic or thiol groups of a protein with reactive supports containing active halides, oxirane, vinylsulfonyl, or vinylketo groups;
- Schiff's base formation is based on the formation of a Schiff's base (aldimine) linkage between carbonyl groups of the activated support and free amino groups of the protein;

- Ugi reaction – four functional groups react simultaneously – carboxylate, amine, aldehyde, isocyanide – resulting in formation of an N-substituted amide;
- Amidation – supports containing imidoester functional groups are attacked by nucleophiles and react selectively with amino groups of protein;
- Thiol-disulfide interchange – protein bonding via thiol groups of both carrier and protein;
- Mercury enzyme interactions based on interaction of mercury derivatives carriers and thiol groups of the protein;
- γ -Irradiation-induced coupling based on coupling proteins to agarose and dextran by γ -irradiation of the protein in the presence of the carrier. The radicals formed on both components combine, giving rise to the covalent bond.

When choosing the binding method it is important to find one that will not deactivate the enzyme by reacting with amino acids at the active site.

1.3. Entrapment

Physical entrapment of enzymes in polymeric gels¹² or fibers¹³ is another simple and effective method of immobilization. It does not include binding of enzyme to the matrix, and provides uniform distribution of enzyme throughout the entire volume of the carrier¹⁴. Gel matrixes are high in chemical and biological stability and allow reusing enzymes entrapped in them. Typical supports are synthetic polymers like polyacrylamide, polyvinyl alcohol, polyvinylpyrrolidone, etc. Natural polymers like carrageenan, alginate, gelatine, etc. have large pore size to entrap enzymes, therefore they are widely used when entrapping whole cells.

Disadvantages of this method include high cost of immobilization, diffusion limitations, leakage of small molecular weight enzymes from the support, low loading capacity¹⁵. Also conditions of polymerization reaction are relatively severe; therefore enzyme loses its activity.

1.4. Encapsulation

Encapsulation of the enzymes is another immobilization method that involves separation of enzyme solution from substrate solution by the use of semipermeable membrane. In this method enzymes are not attached to the carrier and are restricted in space by the membrane walls. Through this membrane wall low molecular weight substrates and cofactors can penetrate inside the capsule, at the same time keeping bigger enzyme molecules inside. One of the major disadvantages of the method is that it requires a very strict pore size control. It is not suitable for big substrate molecules, as well as for enzymes that are similar in size to the product molecules, as it will cause leakage¹⁰.

Advantages of this technique are:

- It is easy and simple;
- It enables the preparation of multi-enzyme systems and the sequential enzyme reaction;
- There is no chemical modification during the entrapment process and membrane protects biocatalyst from the harsh environment, therefore enzyme should retain its activity.

Capsules in this method can be made of cellulose, alginic acid, chitosan and maltodextrin. Also double-layered microcapsules made of two different polymers are popular and can be coated with gelatine, boric acid, κ -carrageenan, chitosan, polyvinylacetate¹⁰.

1.5. Crosslinking

This type of immobilization is achieved by cross-linking the enzymes to each other to form large three-dimensional complex structures. This method doesn't require support. Method of protein cross-linking (CLE) appeared 50 years ago and was based on the reaction of glutaraldehyde with the NH₂ groups on the protein surface ¹⁶. However this method showed loss in activity, low stability and low reproducibility. In 1992 F.A. Quioco et al. ¹⁷ improved CLE by cross-linking of crystalline enzymes (CLEC's). CLEC's proved to be much more resistant to denaturation caused by heat, organic solvents and proteolysis ¹⁸. However this method required enzyme crystallization and therefore enzymes had to be of a very high purity. Thus a new improved method emerged – CLEA. It is based on forming enzyme aggregates by adding salts, organic solvents, or non-ionic polymers. Because precipitation is often used as a purification method, CLEA combines purification and immobilization in one operation unit. These aggregates help to maintain enzymes activity and increases stability and tolerance to organic solvents. CLEA is also a much cheaper and easier method than CLEC with a wide range of application. *Combi-CLEA* preparation (that contains two or more enzymes) is also available, allowing catalytic cascade processes ¹⁹.

2. METHODS TO ANALYSE STATE OF PROTEIN MOLECULES IN IMMOBILIZED ENZYMES.

A wide range of different physico-chemical techniques are applied to understand protein behaviour in solution. But methods to analyze immobilized enzymes are rather limited. Application of spectroscopic methods is difficult because of the light scattering artefacts that arose from measurements on large particles of tens to hundreds micron in diameter. The carrier materials themselves may introduce

background signals due to the absorption of the incident radiation, which doesn't allow to properly identify structural information from the sample²⁰. Calorimetry measurements have complications of the heat input from stirring needed to maintain particles in suspension. There are three main spectroscopic methods that can give interpretable data of immobilized enzymes structure. They are: CD, fluorescence and diffuse reflectance infrared (DRIFT).

Solid-state NMR, when suitably adapted (e.g. Magic-angle spinning) can predict structural information of proteins in particulate form like: membrane proteins^{21,22}, macromolecular assemblies^{23,24}, fibrils^{25,26}, biomaterials²⁷.

Also some studies on immobilized enzymes structure were done by using electron paramagnetic resonance (EPR)²⁸.

Intrinsic Fluorescence Spectroscopy analyzes fluorescence from the sample (which is an emission of light occurring because of the de-excitation of electrons). This method is applicable for proteins due to the fluorescence ability of aromatic aminoacids, mainly tryptophan. Therefore when the change in protein structure occurs it changes the fluorescence properties of the protein. In 1995 T. Kijima *et al.*^{29, 30} studied correlation between the fluorescence emission wavelength and the catalytic activity of proteases in aqueous-organic media. In 2009 Ganesan *et al.*²⁰ showed that the intrinsic fluorescence spectroscopy can be used to understand structure of immobilized enzymes by studying subtilisin Carlsberg immobilized on silica gel.

Infrared spectroscopy detects vibrational characteristics of functional groups in the sample. This is another method for examining secondary structure of enzymes in solution, suspension and in the solid state^{20, 31-33}. The amide groups in protein give rise to 9 vibrational bands based on frequency associated with specific vibration. One of them, the amide I band is sensitive to protein conformation and provides direct information on the secondary structure. The amide I band is primarily due to C=O stretching, coupled slightly with CN stretching, CCN deformation and NH bending. The C=O stretching frequency is sensitive to the H-bonding associated with it, which in turn is determined by the secondary structure such as α -helix, β -sheet, β -turn and

random coil. Thus, changes in amide I peak maximum shows the change in the structure of the protein.

Circular Dichroism is another spectroscopic technique that is used to study secondary structure of proteins in solutions and in particulate forms. This method is easy to use; it doesn't require a large amount of sample; and can be used for different solvent conditions, varying temperatures and pH.

3. CIRCULAR DICHROISM MEASUREMENTS OF PROTEINS

3.1. Circular Dichroism spectroscopy and its principles.

Circular Dichroism is observed when optically active (chiral) molecule absorbs left and right circular polarized light to a different extent. Chiral molecules are asymmetric in such way that they cannot be superimposed on their own image³⁴. CD follows Beer-Lambert-Bouguer law, which describes absorbance as:

$$A = \log_{10}(I^0/I) = \epsilon Cl \quad (1)$$

where I^0 and I are, respectively, the intensity of the incident light and the transmitted light, l is a pathlength through a medium (in cm) containing the molar concentration C of the chiral solute (in M), and ϵ is the molar extinction coefficient of the solute (in $M^{-1} \cdot cm^{-1}$)³⁵. From this equation CD can be described as:

$$\Delta A = A_L - A_R = \epsilon_L Cl - \epsilon_R Cl = \Delta \epsilon Cl \quad (2)$$

where L is left and R is right.

If left- and right-circularly polarised light have equal intensities their resultant will lie in a plane. Difference in intensities, when light is absorbed to different extent, results in elliptically polarized light (Fig.3.1) ³⁶.

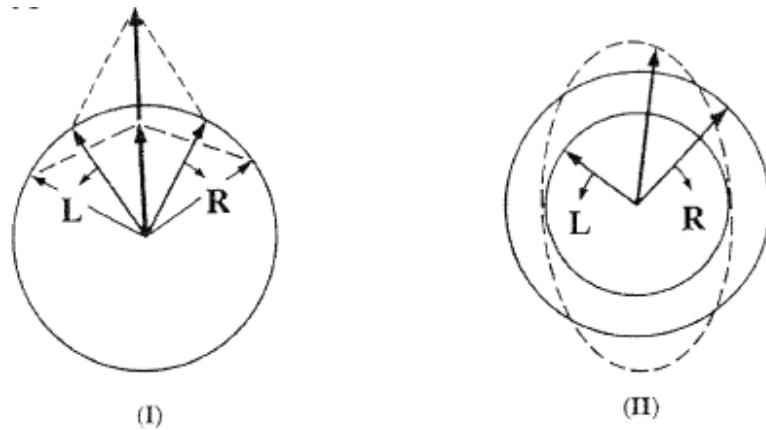


Fig. 3.1. Plane polarised light resolved in two circularly polarized components, R and L. (I) the two components have equal intensities and when combined the resultant lies in the plane; (II) the components are of different intensities and the resultant is elliptically polarized. This figure was taken from ³⁶.

CD can also be described in terms of the ellipticity (θ) in degrees:

$$\theta = \tan^{-1} (b/a) \quad (4)$$

where b and a are the minor and major axes of the resulting ellipse (Fig. 3.1). Relationship between ΔA and ellipticity can be expressed as:

$$\theta = 180 \cdot \ln 10 \cdot \Delta A / 4\pi = 32.98\Delta A \quad (5)$$

3.2. Operation of CD spectropolarimeter.

Operation of a modern CD spectropolarimeter begins from a Xe lamp emitting light with a wide range of wavelengths including UV, visible and IR (163-1100 nm for Jasco J-810); this light then passes through the monochromator, which transmits only a narrow spectral band. Special optics (mirrors, prisms) ensure that light is polarized and direct it through the photoelastic modulator (PEM), which generates circular polarized light. This circular polarized light passes through the sample and then reaches the detector. The schematic diagram of the modern CD spectropolarimeter Jasco J-810 is shown below on Fig. 3.2³⁷:

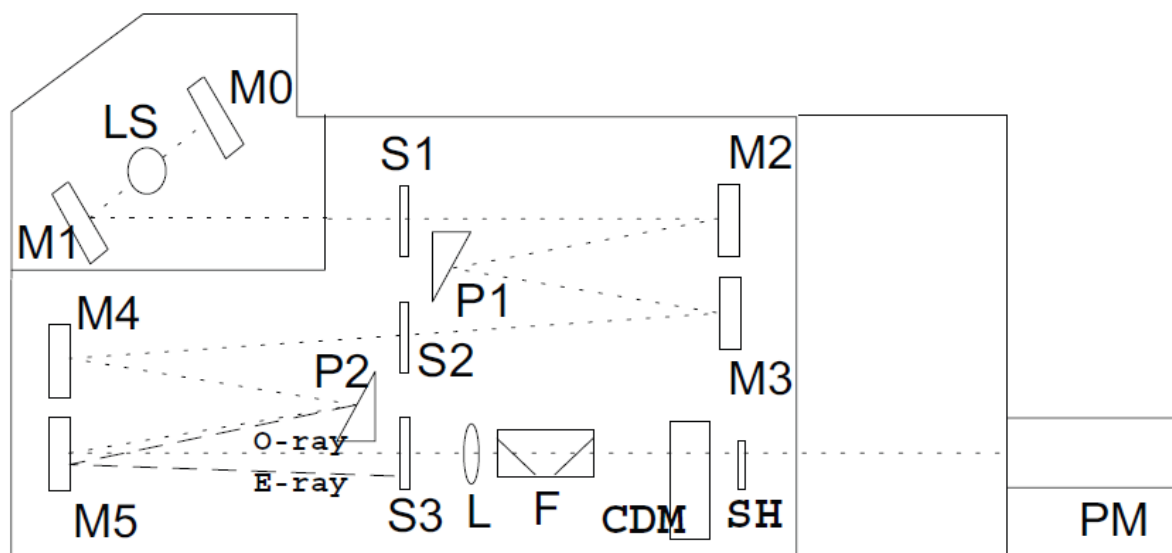


Fig.3.2. Schematic diagram of Jasco J-810 spectropolarimeter. Fig. taken from³⁷.

This diagram shows how light from the 150W Xe-light source (LS) by passing through a number of mirrors (M0-M5), prisms P1 and P2 and slits (S1-S3) gets plane polarized. Prisms P1 and P2 act as a double monochromator and make light that

passes through them not only monochromated but linearly polarized and oscillated in the horizontal direction – ordinary ray, O-ray (extraordinary ray, E-ray, has crossed polarization). Then O-ray collimated by the focusing lens L and filtered by a series of 45° quartz plates F becomes circularly polarized by passing through the photoelastic modulator crystal CDM. This circularly polarized light goes through the shutter (SH), where if necessary it gets cleared from the radiation. Then passes through the sample in the sample chamber, and gets detected by the photomultiplier tube (PM).

To get reliable data when using a CD spectropolarimeter it is important to follow a number of rules. Instrument should be constantly purged with Nitrogen for two reasons: 1) oxygen in the air absorbs light below 200nm so measurements cannot be performed at short wavelengths; 2) presence of oxygen leads to formation of ozone, which can damage the optics.

CD instrument should be regularly calibrated. Most commonly standards include: Camphorsulfonic acid (CSA) and ammonium salt of camphorsulfonic acid (ACS); Pantolactone; Epiandrosterone; Tris(ethylenediamine)Co complex³⁷.

When preparing a sample, it is important to make a right choice of buffer, as some buffers absorb light at the same wavelength range as the compound of interest, therefore masking the main CD signal. For example, buffers containing carboxylates absorb light below 200 nm, therefore if possible they should be avoided. Most commonly used buffer is the phosphate buffer, which has low absorbance at the wavelengths higher than 190 nm. It is important to remember that Cl⁻ ions distort CD signal below 195 nm. Therefore NaCl should not be used when preparing buffers; instead it can be replaced with Na₂SO₄ or NaF³⁶.

Determination of protein concentration is very important when obtaining the secondary structure from the CD spectra. The most popular methods to calculate concentration are:

- The Biuret method, based on formation of purple complex between substances containing peptide bonds and copper salts under alkaline conditions;

- Lowry method, is based on the Biuret reaction (above) combined with the Folin-Ciocalteu chemistry where a complex mixture of inorganic salts react with Tyr and Trp residues giving a strong green-blue color;
- The bicinchoninic acid (BCA) method combines reduction of Cu(II) to Cu(I) by protein in alkaline conditions with colorimetric detection of Cu(I) by bicinchoninic acid, which gives a yellow-green product;
- The Coomassie Blue (Bradford) method is based on the change of the absorbance maximum when dye binds to the protein in acidic media;
- Absorbance at 280 nm method is based on measuring absorbance of protein at 280 nm, which arises due to the amino acids with aromatic rings.

Cells and cuvettes used for CD measurements should be made from high quality quartz, to perform good light transmission. To avoid optical artefacts strain free cells are also available. It is important before each CD run to make sure that cells are clean and have no scratches.

3.3. Information on protein structure obtained from Circular Dichroism.

Circular Dichroism is a valuable technique which gives information not only on the secondary structure of proteins but also is sensitive to changes in the tertiary structure; it gives structural information about the cofactor sites^{38, 39}; and can detect structural changes caused by binding of ligands⁴⁰. Wavelength at which CD measurements are carried out can be split into three groups: a) far UV region (ranges between 180-250 nm); b) near UV region (250-350 nm); and c) near UV-Visible region (300-700 nm)⁴¹. In each group different chromophores absorb, giving information about the structure of the molecule.

a) Information available from the far UV region:

Chromophore responsible for absorption in the far UV region is the peptide bond. Absorption occurs here because of the two low energy electron transitions happening in the peptide bond: $n-\pi^*$ transition and $\pi-\pi^*$ transition (Fig.3.3)⁴². $n-\pi^*$ transition is forbidden electronically, but it is allowed magnetically, therefore this transition has a weak and broad absorption band, which is centred at around 210 nm; and $\pi-\pi^*$ transition gives a stronger and narrower band at around 190nm.

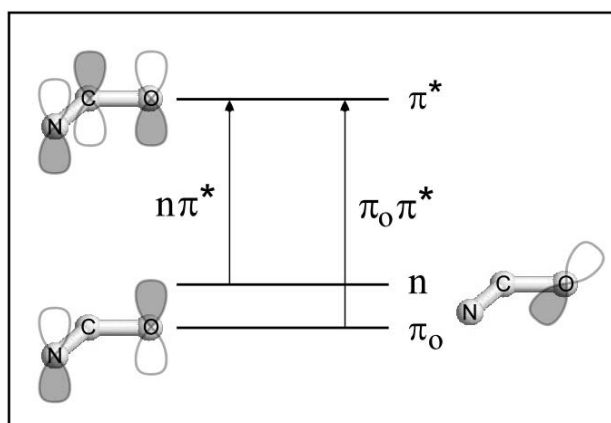


Fig.3.3. Electron transitions in the peptide bond. This picture was taken from⁴².

Typical structural forms like α -helices, β -sheets and random coils give rise to different CD signals in the far UV region. These characteristic signals are illustrated on the Fig.3.4 for poly-lysine:

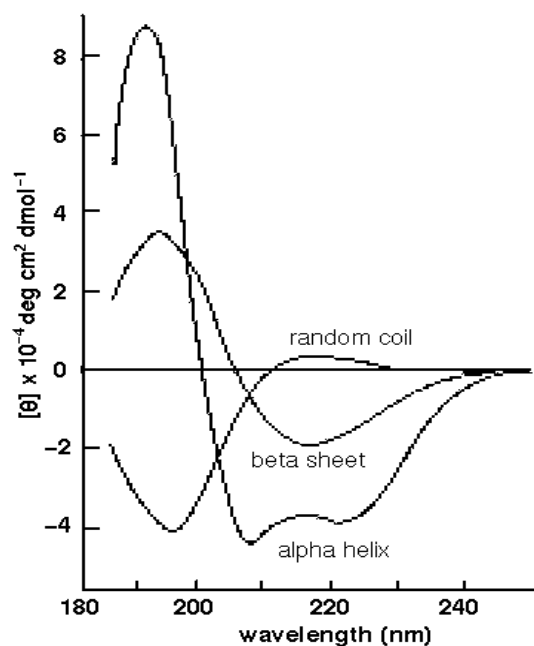


Fig. 3.4. Far-UV CD spectra of α -helix, β -sheet and random coil for poly-lysine. These spectra are available online ⁴³.

CD spectra don't identify the residues involved, but determine fractions of α -helices, β -sheets and random coils in proteins. Once CD spectra are recorded, secondary structure can then be analysed by a number of different algorithms: SELCON ^{44, 45}, CONTIN-CD ⁴⁶, CDSSTR ^{47, 48}, K2d ^{49, 50}, etc. These methods are based on the use of reference proteins with solved structure by X-ray crystallography. A web site DICHROWEB (<http://www.cryst.bbk.ac.uk/cdweb/html/home.html>) ^{51, 52} allows to analyze CD data in different formats, using a wide range of algorithms.

b) Information available from the near UV region:

CD bands in near UV region arise due to the absorption by the aromatic residues of Trp, Tyr, Phe, as well as contribution from disulfide bonds. In a folded protein these aromatic rings are placed in a chiral environment therefore they induce a CD signal.

But when protein denaturates chirality is lost and CD signal cannot be observed. Thus near UV spectra can give an idea about the tertiary structure of proteins. Position of CD bands of above chromophores has been studied in details^{53, 54}, and can be summarized below:

- Peaks from disulfide bonds are strong and wide, and can be detected by the long tail extending above 310 nm;
- Trp gives fine CD structure between 288 and 305 nm;
- Tyr gives CD bands between 275 and 282 nm;
- Phe gives fine sharp CD structure at 255-270 nm.

Absorption of aromatic residues in these wavelengths happens because of the vibrational $\pi_0 - \pi^*$ transitions. Kelly et al.³⁶ in their work demonstrated a near UV CD spectrum for type II dehydroquinase from *Streptomyces coelicolor* (Fig.3.5.):

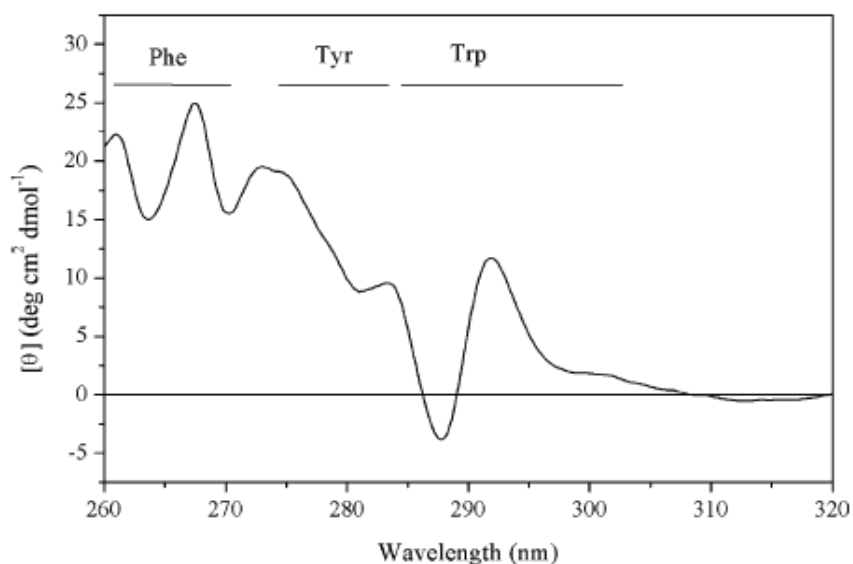


Fig. 3.5. The near UV CD spectrum for type II dehydroquinase from *Streptomyces coelicolor*. Figure taken from³⁶.

There are three main factors established by Strickland et al.⁵³ that influence the intensity of aromatic CD bands. They are:

- 1) Rigidity of protein;
- 2) Interaction of aromatic ring with its surroundings;
- 3) Number of aromatic residues.

Although intensity of CD bands is very variable, near UV CD spectra is still very important for getting information about tertiary structure of proteins.

c) Information available from the near UV - Visible region:

CD signals at near UV - Visible region (300-700nm) give information about the environment of the non peptide groups, e.g. ligands or cofactors like pyridoxal-5'-phosphate, flavins, haem groups, chlorophyll moieties, etc. Free ligands and cofactors do not usually have a CD signal (or a very small one), but when they are in complex with protein CD signal arises indicating presents of chirality in binding sites⁵⁵. Changes in the CD signal can indicate loss of integrity of binding sites.

3.4. Circular Dichroism measurements on proteins in particulate form.

CD can be a useful technique to understand structure of many proteins that are in the particulate form. There has been done a significant amount of work on measuring and analyzing CD spectra of membrane proteins⁵⁶⁻⁵⁸, protein-containing nanoparticles⁵⁹⁻⁶¹, and other small protein particles in suspensions^{62, 63}. Recently Ganesan et al.⁶ showed that CD measurements are also possible on larger particles (many micrometers in size), like immobilized enzymes.

All above studies showed that the major difficulties with obtaining and solving CD spectra of particle suspensions are two optical effects: absorption flattening and differential scattering. These artefacts produce distortions of the spectral shapes and magnitudes^{6, 56-58, 62-65}.

3.4.1. Differential light scattering artefact.

Differential light scattering occurs when left and right circularly polarised light is scattered with different intensities out of the measuring beam of a CD spectropolarimeter. If the particle is achiral and scatters light in equal intensities for both circular polarizations, transmission of light will be reduced but at the same extent for left and right polarized light, therefore CD spectra will not be changed. But if the light scatters with different intensities then distortions of CD spectra are observed. Due to the decrease in the number of photons reaching the photomultiplier, light scattering causes a reduction in the signal to noise ratio of the spectra. The effects of differential light scattering can be minimized by using suitable experimental techniques. The main experimental approach, suggested in 1973 by Dorman et al., is to increase the solid angle of detection, therefore maximizing the collection efficiency of the photomultiplier. This may be done by increasing the size of the detector, decreasing the distance from sample cell to detector, or both⁶⁵. Another method of reducing scattering losses in suspensions, used by Barer⁶⁶, is to match medium and particle refractive indices, due to the fact that light scattering can be caused by the refractive index gradient between particle and the mounting medium.

3.4.2. Absorption flattening artefact.

Measurements of light absorption or circular dichroism (CD) on suspended particles may differ compared with the same amount of chromophore uniformly distributed in solution. Because of the random distribution of particles in suspensions

chromophore concentration varies from light beam to light beam, which passes through the sample. And the less absorption particles are in the suspension the larger the variations are. In a homogeneously distributed solution the chromophore concentration is the same for all light beams that pass through. The average of absorbance for homogeneous solution will be the same as for the suspension, but CD measures not the absorbance but the intensities. According to Beer-Lambert-Bouguer law the intensity of the light decreases exponentially through the sample:

$$I = I_0 \cdot 10^{-\varepsilon c l} \quad (6)$$

where ε is molar absorptivity of the particle (molar extinction coefficient), c is molar concentration of the particles, l – cell length. Hence, if calculate absorption for suspension from the mean intensity it will be less than mean absorption for solution.

In the case of particle suspensions containing protein absorption flattening is considered to be the most significant factor contributing to the CD spectra distortions⁶⁷. The quantitative effects of absorption flattening are not easily estimated. First theoretical methods to estimate absorption flattening effect on suspensions of solid cubes and spheres were introduced by Duysens in 1956⁶⁸. Then in 1971 Gordon & Holzwarth⁶⁹ extended these methods to use for spherical shells, and in 1987 Teeters⁵⁷ applied similar theoretical methods for calculations of membrane sheets. Since then there were a number of analytical approaches^{56-58, 67, 69-73}, that resulted in equations based on number of assumptions and simplifications (e.g. uniform size, very low volume fraction, spherical particles, etc.).

Corrected for absorption flattening CD spectra (CD_{corr}) can be obtained from the observed CD spectra (CD_{obs}) by using absorption flattening coefficient (Q_{CD}). In this thesis as in many other papers^{57, 69, 71} Q_{CD} is defined as CD_{corr} divided by the CD_{obs} . Therefore :

$$CD_{corr} = \frac{CD_{obs}}{Q_{CD}} \quad (7)$$

In some papers^{6,56} authors define absorption flattening coefficient as $(1-Q_{CD})$. This depends on the value that is chosen for the no flattening case, which can be 0 or 1.

In 2006 Ganesan et al.⁶ corrected CD spectra for absorption flattening of suspension containing immobilized enzymes, using a semiempirical model suggested by Wallace and Mao⁵⁶. This model is based on the assumption that absorption flattening coefficient is linearly proportional to the derived absorbance (here absorption flattening coefficient was defined as $(1-Q_{CD})$).

In 2009 Halling suggested an alternative computer based simulation approach that can be suitable for any type of particle suspensions⁷¹. The idea of his work was to simulate the passage of light through a part of the sample with known amount of randomly located particles (Fig.3.6). Simulation input parameters were only dependant on the volume fraction of particles, size of the particles and size distribution.

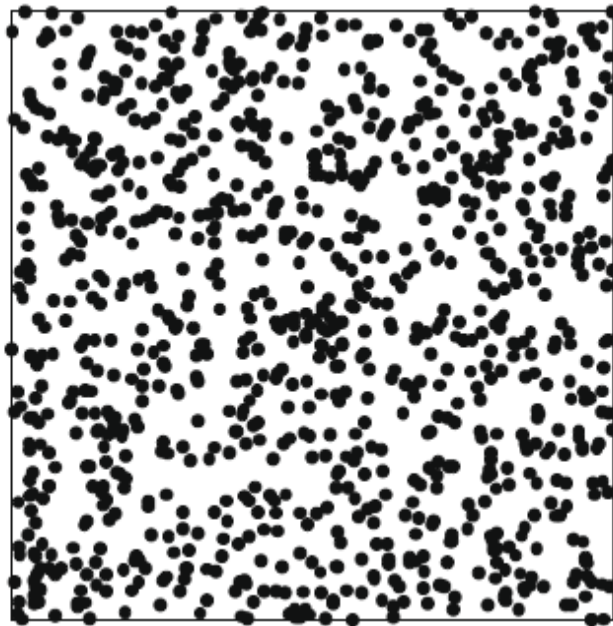


Fig.3.6. Sample of simulated appearance of suspension with volume fraction equals to 0.01; pathlength divided by the particle diameter equals to 2; and 20% standard deviation of particle diameters. Figure modified from Halling, 2009⁷¹.

Each light path through the sample was examined; and pathlength when passing through one or more particles was calculated as $= 2\sqrt{R^2 - r^2}$, where R is radius of the particle and r is the distance from a light ray with (x_r;y_r) coordinates to the particle centre.

After this, the intensity of emerging light was determined for each path as 10^{-A} , where A is absorbance and can be calculated by multiplying absorbance measured through a diameter of the particle (A_{part}) by the total pathlength through particles. The transmitted fractions of left and right polarized light were measured the same way replacing A_{part} with $A_{part,L}$ and $A_{part,R}$, respectively, where:

$$A_{part,L} = A_{part} + \log\left(\frac{1+10^{CD_{part}}}{2}\right) \quad (8)$$

$$A_{part,R} = A_{part} + \log\left(\frac{1+10^{-CD_{part}}}{2}\right) \quad (9)$$

Sum of the transmitted intensity for all of the light paths was then used to calculate the absorbance (A_{sus}) and circular dichroism (CD_{sus}) signals for suspension, where:

$$CD_{sus} = A_{sus,L} - A_{sus,R} \quad (10)$$

These A_{sus} and CD_{sus} values were then compared to the ones that would have been obtained if the same amount of chromophore was uniformly distributed throughout the sample volume, named A_{sol} and CD_{sol} . In order to compare these values, A_{sol} and CD_{sol} were determined by multiplying the average of light paths of the pathlength through particles by the A_{part} or CD_{part} values.

Finally, flattening coefficients Q_A and Q_{CD} were determined using standard equations:

$$Q_A = \frac{A_{sus}}{A_{sol}} \quad (11)$$

$$Q_{CD} = \frac{CD_{sus}}{CD_{sol}} \quad (12)$$

Halling⁷¹ showed that this simulation method to correct for absorption flattening can be applied to particles with unequal diameters (unlike other approaches); and it is also easy to use when handling experimental data.

4. SYNCHROTRON RADIATION CIRCULAR DICHROISM

Synchrotron Radiation Circular Dichroism (SRCD) is a new technique that allows obtaining CD signals in the vacuum UV region (from 190 nm down to 120 nm). Miles & Wallace⁷⁴ showed SRCD spectra (Fig.4.1) of three proteins with different structures measured to 160 nm: red line represents myoglobin with mostly helical structure; blue line represents concanavalin with mostly β -sheets; and yellow line represents collagen with mostly polyproline helix (PPII) structure. With the black line they separated two areas: the longer wavelength area above 190 nm where measurements can be done on a conventional CD; and below 190 nm (shaded with green) – area available only for measurements on the SRCD. It can be seen that below 190 nm there is a significant difference between spectra of each protein; therefore SRCD measurements can provide more information on the protein structure.

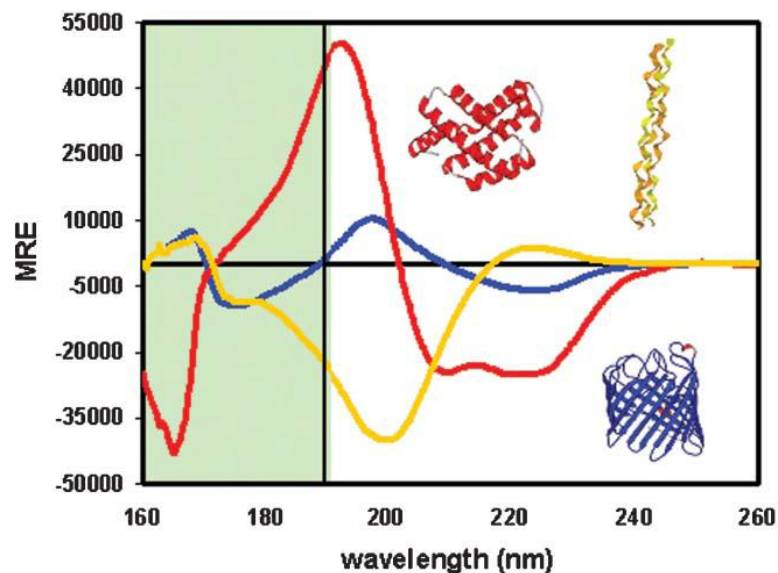


Fig.4.1. SRCD and CD spectra of three proteins: red line – myoglobin; blue line – concanavalin; yellow line – collagen. Green area represents data available only for SRCD measurements. MRE stands for mean residue ellipticity. Figure is taken from⁷⁴.

Conventional CD instruments cannot do measurements at such low wavelengths. This is due to the flux of the SRCD source being much higher than the flux of the Xe lamp, which is used in the conventional CD machines. Clarke & Jones⁷⁵ showed a Figure (Fig.4.2) comparing flux of a Xe lamp to a low-flux and high-flux synchrotron radiation (SR) sources. It can be seen that in a conventional CD instrument a high light flux of 10^{10} photons/sec is available only at the wavelengths longer than 220nm, and there is a significant drop in flux below 200 nm. Whereas for SR sources at 200 nm the flux is higher than 10^{13} photons/sec; and remains constant to about 140nm, allowing good measurements at low wavelengths.

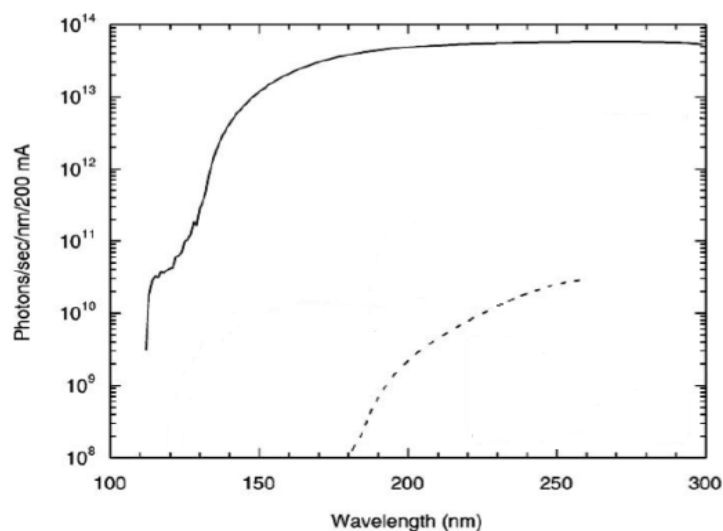


Fig.4.2. Comparison of the light flux of the conventional CD (dashed line) with SRCD (solid line). Figure was adapted from Clarke & Jones ⁷⁵.

The high flux of SRCD leads to a number of applications and advantages over conventional CD ⁴¹:

- 1) An improved signal-to-noise ration. This can be very useful when comparing structural changes of wild-type and mutant protein, because noise can mask the differences between spectra, therefore changes will not be detected. Good signal-to –noise ration also means that only small amount of sample is required and data can be collected much faster than with the conventional CD.
- 2) Wider range of buffers and solvents can be used, including salts and high concentrated buffers, which are not suitable for measurements on conventional CD (as discussed previously in Chapter 3). This is because of the light being so intensive, that despite the highly absorbing solution, enough still reaches the detector.
- 3) Accurate and reliable measurements in aqueous solutions in the low wavelength region allows to get better information about proteins, DNA

samples and even some sugars that cannot be seen with the conventional CD. SRCD can also be used to detect interaction between two protein molecules, when changes occur only at low wavelengths and cannot be detected with the conventional instrument.

SRCD are constructed similarly to a conventional CD and include: a number of mirrors, an ultra-high vacuum monochromator, a photoelastic modulator, a sample compartment and a detector. The main difference with the conventional CD is that all optical windows are made from a material that is transparent to light in the low wavelengths, like: magnesium, calcium or lithium fluorides⁷⁶.

A light source of SR is an electron storage ring. Electrons are generated by the electron gun and then accelerated to almost the speed of light with the help of three particle accelerators: linear accelerator called linac, booster synchrotron and storage ring. Path of the electrons is bent with the use of powerful dipole bending magnets. When electron passes through each magnet it loses energy producing very intense X-rays, ultra-violet, visible and infra-red light. The latest generation of synchrotrons also have the insertion devices magnets (wigglers and undulators) in the straight sections of the ring. By passing through them light gets even more intense and tuneable. Figure 4.3 shows a schematic diagram of the synchrotron radiation source.

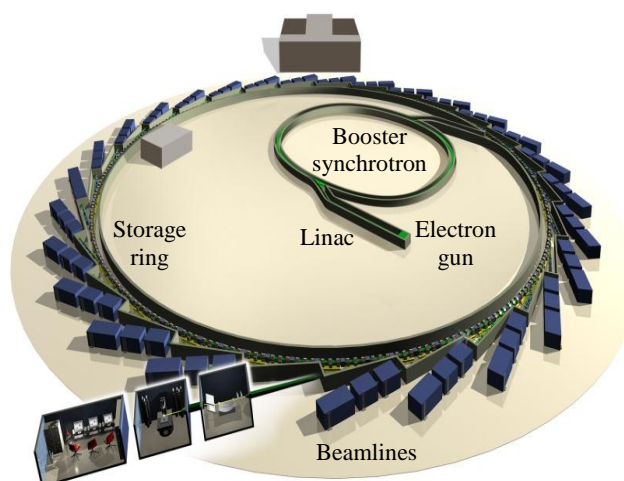


Fig. 4.3. Schematic diagram of SR facilities in Diamond, UK. Picture is adapted from⁷⁷.

Due to high running costs, there are not many SR sources available around the world. SRCD beamline can be found in synchrotron facilities in USA (NSLS), UK (Diamond), Denmark (ISA), Japan (HISOR, TERAS), China (BSRF), Germany (BESSY 2), Taiwan (NSRRC), France (SOLEIL).

REFERENCES

1. Klibanov A.M. Improving enzymes by using them in organic solvents. *Nature* 2001;409: 241-246.
2. Klibanov A.M. Enzymatic catalysis in anhydrous organic solvents. *Trends Biochem. Sci.* 1989;14:141-144.
3. Fitzpatrick P.A., Steinmetz A.C.U., Ringe D., Klibanov A.M. Enzyme crystal structure in a neat organic solvent. *Proc. Natl. Acad. Sci. USA* 1993;90:8653-8657.
4. Klibanov A.M. Why are enzymes less active in organic solvents than in water? *Trends Biotechnol.* 1997;15:97-101.
5. Lee M.Y., Dordick J.S. Enzyme activation for nonaqueous media. *Curr. Opin. Biotech.* 2002;13:376-384.
6. Ganesan A., Price N.C., Kelly S.M., Petry I., Moore B.D., Halling P.J. Circular dichroism studies of subtilisin Carlsberg immobilised on micron sized silica particles. *Biochim. Biophys. Acta* 2006;1764:1119-1125.
7. Cao L. Immobilised enzymes: science or art? *Current Opinion in Chemical Biology* 2005;9:217-226.
8. Bickerstaff G.F. Immobilization of enzymes and cells. *Methods in Biotechnology*, vol.1. Humana Press Inc., Totowa, NJ, 1997.
9. Gemeiner P. (1992). Materials for enzyme engineering. *Enzyme Engineering*, Ellis Horwood, New York, 1992:13-119.
10. Cao L. Carrier-bound immobilised enzymes. Wiley-VCH, 2005.
11. Tischer W., Wedekind F. Immobilized enzymes: methods and applications. *Top.Curr.Chem.* 1999;200:95-126.

12. Bernfeld P. and Wan J. Antigens and enzymes made insoluble by entrapping them into lattices of synthetic polymers. *Science* 1963;142:678–679.
13. Dinelli D., Marconi W., and Morisi F. Fiber-entrapped enzymes. In: *Methods in Enzymology*, volume XLIV, (Mosbach, K., ed.), Academic Press, New York, NY, 1976:227–243.
14. Brena B.M., Batista-Viera F. Immobilization of enzymes. From: *Methods in Biotechnology: Immobilization of Enzymes and Cells*, Second Edition. Edited by: J. M. Guisan © Humana Press Inc., Totowa, NJ, 2006:15-30.
15. Gorecka E., Jastrzebska M. Immobilization techniques and biopolymer carriers. *Biotechnol. Food Sci.* 2011;75:65-86.
16. Cao L., van Langen L.M., Sheldon R.A. Immobilised enzymes: carrier-bound or carrier-free? *Curr. Opin. Biotechnol.* 2003;14:387-394.
17. Quijcho F.A., Richards F.M. Intermolecular cross-linking of a protein in the crystalline state: carboxypeptidase A. *Proc. Natl. Acad. Soc. USA* 1992;114:7314-7316.
18. Sheldon R.A. Cross-linked enzyme aggregates (CLEA's): stable and recyclable biocatalysts. *Biochemical society transactions* 2007;35:1583-1587.
19. Patel R.N. *Biocatalysis in the Pharmaceutical and Biotechnology Industries*. CRC Press, Taylor & Francis Group 2007: 353-360.
20. Ganesan A., Moore B.D., Kelly S.M., Price N.C., Rolinski O.J., Birch D.J.S., Dunkin I.R., Halling P.J. Optical spectroscopic methods for probing the conformational stability of immobilized enzymes. *Chem. Phys. Chem.* 2009;10:1-9.
21. Opella S.J., Marassi F.M. Structure determination of membrane proteins by NMR spectroscopy. *Chem Rev.* 2004;104(8):3587-3606.

22. Hong M., Su Y. Structure and dynamics of cationic membrane peptides and proteins: Insights from solid-state NMR. *Protein Sci.* 2011;20(4):641-655.
23. Baldus M. Molecular interactions investigated by multi-dimensional solid-state NMR. *Curr.Opin. Struct. Bio.* 2006;16(5):618-623.
24. Egawa A., Fujiwara T., Mizoguchi T., Kakitani Y., Koyama Y., Akutsu H. Structure of the light-harvesting bacteriochlorophyll c assembly in chlorosomes from *Chlorobium limicola* determined by solid-state NMR. *Proc. Natl. Acad. Sci.* 2007;104(3):790-795.
25. Petkova A.T., Yau W.M., Tycko R. Experimental constraints on quaternary structure in Alzheimer's b-amyloid fibrils. *Biochemistry* 2006,45:498-512.
26. Tycko R. Molecular structure of amyloid fibrils: insights from solid-state NMR. *Quart. Rev. Biophys.* 2006;39(1):1-55.
27. McDowell L.M., Schaefer J. High-resolution NMR of biological solids. *Curr. Opin. Struct. Biol.* 1996,6:624-629.
28. Ganapathi-Desai S., Butterfield D.A., Bhattacharyya D. Kinetics and active fraction determination of a protease enzyme immobilized on functionalized membranes: mathematical modelling and experimental results. *Biotechn. Proc.* 1998;14(6):865-873.
29. Kijima T. Fluorescence spectroscopic study of subtilisins as relevant to their catalytic activity in aqueous-organic media. *Bull. Chem. Soc. Jpn.* 1994;67:2819-2824.
30. Kijima T., Yamamoto S., Kise H. Study on tryptophan fluorescence and catalytic activity of α -chymotrypsin in aqueous-organic media. *Enzyme Microb. Technol.* 1996;18:2-6.
31. Quiroga E., Marchese G.C.J., Barberis S. Organic solvents effect on the secondary structure of araujiain hI, in different media. *Biochemical Engineering Journal* 2007;35,:198-202.

32. Dong A., Meyer J.D., Kendrick B.S., Manning M.C., Carpenteret J.F. Effect of secondary structure on the activity of enzymes suspended in organic solvents. *Arch. Biochem. Biophys.* 1996;334,:406-414.
33. Griebenow K., Klibanov A.M. Can conformation changes be responsible for solvent and excipient effects on the catalytic behaviour of subtilisin Carlsberg in organic solvents? *Biotechnol. Bioeng.* 1997;53,351-362.
34. Jones G., Clarke D.T. Applications of extended ultra-violet circular dichroism spectroscopy in biology and medicine. *Faraday Discuss.* 2004;126:223-236.
35. Fasman G.D. Circular dichroism and the conformational analysis of biomolecules. Springer-Verlang New York, LLC, 1996.
36. Kelly S.M., Jess T.J., Price N.C. How to study proteins by circular dichroism. *Biochimica et Biophysica Acta* 2005;1751:119-139.
37. Castiglioni E. CD spectropolarimetry. The instrumental approach; 2001. Can be find online at <http://www.jasco.hu/konyvtar/bozza%20testo1.pdf>
38. Andersson L.A., Peterson J.A. Active-site analysis of ferric P450 enzymes: hydrogen-bonding effects on the circular dichroism spectra. *Biochem. Biophys. Res. Commun.* 1995;211:389-395.
39. Alden R.G., Johnson E., Nagarajan V., Parson W.W., Law C.J., Cogdell R.J. Calculations of spectroscopic properties of the LH2 bacteriochlorophyll-protein antenna complex from *Rhodospseudomonas acidophila*. *J. Phys. Chem. B* 1997;101:4667-4680.
40. Boxer D.H., Zhang H., Gourley D.G., Hunter N.W., Kelly S.M., Price N.C. Sensing of remote oxyanion binding at the DNA binding domain of the molybdate dependent transcriptional regulator, ModE. *Org. Biomol. Chem.* 2004;2:2829-2837.

41. Berova N., Nakanishi K., Woody R.W. Circular dichroism: Principles and Applications. 2nd edition, Wiley-VCH, New York, 2000.
42. Wallace B.A., Janes R.W. Modern Techniques for circular dichroism and synchrotron radiation circular dichroism spectroscopy. Advances in biomedical spectroscopy – vol.1, IOS Press 2009.
43. This figure can be found at
http://www.cryst.bbk.ac.uk/PPS2/assignments/A1/CD_info.html
44. Sreerema N., Woody R.W. A self-consistent method for the analysis of protein secondary structure from circular dichroism. Anal. Biochem.1993; 209:32-44.
45. Sreerama N., Woody R.W. Computation and analysis of protein circular dichroism spectra. Methods Enzimol. 2004;383:318-351.
46. Provencher S.W. and Glockner J. Estimation of globular protein secondary structure from circular dichroism. Biochem. 1981;20: 33-37.
47. Toumadje A., Alcorn S.W., Johnson W.C.Jr. Extending CD spectra of proteins to 162nm improves the analysis for secondary structure. Anal. Biochem. 1992;200:321-331.
48. Compton L.A., Johnson W.C., Jr. Analysis of protein circular dichroism spectra for secondary structure using a simple matrix multiplication. Anal. Biochem. 1986;155:155-167.
49. Andrade M.A., Chacón P., Merelo J.J., Morán F. Evaluation of secondary structure of proteins from UV circular dichroism using an unsupervised learning neural network. Prot. Engineering 1993;6:383-390.
50. Sreerama N., Woody R.W. Estimation of protein secondary structure from CD spectra: Comparison of CONTIN, SELCON and CDSSTR methods with an expanded reference set. Anal. Biochem. 2000;287(2):252-260.

51. Whitmore L., Wallace B.A. DICHROWEB: an online server for protein secondary structure analyses from circular dichroism spectroscopic data. *Nucleic Acids Research* 2004;32:668-673.
52. Whitmore L., Wallace B.A. Protein Secondary Structure Analyses from Circular Dichroism Spectroscopy: Methods and Reference Databases. *Biopolymers* 2008;89:392-400.
53. Strickland E.H. Aromatic contributions to circular dichroism spectra of proteins. *Crit. Rev. Biochem.* 1974;2(1):113-175.
54. Woody R.W., Dunker A.K. Aromatic and cystine side-chain circular dichroism in proteins. In "Circular dichroism and the conformational analysis of biomolecules" edited by Fasman G.D., Plenum Press, New York, 1996: 25-67.
55. Kelly S., Price N. The use of circular dichroism in the investigation of protein structure and function. *Curr.Prot.Pept.Sci.* 2000;1:349-384.
56. Wallace B.A., Mao D. Circular dichroism analysis of membrane proteins: an examination of light scattering and absorption flattening in large membrane vesicles and membrane sheets. *Anal. Biochem.* 1984;142:317-328.
57. Teeters C.L., Eccles J., Wallace B.A. A theoretical analysis of the effects of sonication on differential absorption flattening in suspensions of membrane sheets. *Biophys. J.* 1987;51:527-532.
58. Wallace B.A., Teeters C.L. Differential absorption flattening optical effects are significant in the circular dichroism spectra of large membrane fragments. *Biochemistry* 1987;26:65-70.
59. Sarmiento B., Ferreira D.C., Jorgensen L., van de Weert M. Probing insulin's secondary structure after entrapment into alginate/chitosan nanoparticles. *Eur. J. Pharm. Biopharm.* 2007;65:10-17.

60. Wangoo N., Raman Suri C., Shekhawat G. Interaction of gold nanoparticles with protein: A spectroscopic study to monitor protein conformational changes. *Appl. Phys. Lett.* 2008;92:133104.
61. Sahoo D., Bhattacharya P., Patra H.K., Mandal P., Chakravorti S. Gold nanoparticle induced conformational changes in heme protein. *J. Nanopart. Res.* 2011;13:6755-6760.
62. Schneider A.S., Harmatz D. An experimental method correcting for absorption flattening and scattering in suspensions of absorbing particles: circular dichroism and absorption spectra of haemoglobin in situ in red blood cells. *Biochemistry* 1976;15:4158-4162.
63. Tinoco I.Jr., Mickols W., Maestre M.F., Bustamante C. Absorption, scattering and imaging of biomolecular structures with polarized light. *Annu. Rev. Biophys. Biophys. Chem.* 1987;16:319-349.
64. Bustamante C., Tinoco I.Jr., Maestre M.F. Circular differential scattering can be an important part of the circular dichroism of macromolecules. *Proc. Natl. Acad. Sci. USA* 1983;80:3568-3572.
65. Dorman B.P., Maestre M.F. Experimental differential light-scattering correction to the circular dichroism of bacteriophage T2. *Proc. Natl. Acad. Sci. USA* 1973;70:255-259.
66. Barrer R. Spectrophotometry of clarified cell suspensions. *Science* 1955;121:709-715.
67. Urry D.W. Protein conformation in biomembranes: optical rotation and absorption of membrane suspensions. *Biochim. Biophys. Acta* 1972;265:115-168.
68. Duysens L.N.M. The flattening of the absorption spectrum of suspensions, as compared to that of solutions. *Biochim. Biophys. Acta* 1956;19:1-12.
69. Gordon D.J., Holzwarth G. Artifacts in the measured optical activity of membrane suspensions. *Arch. Biochem. Biophys.* 1971;142:481-488.

70. Castiglioni E., Lebon F., Longhi G., Gangemi R., Abbate S. An operative approach to correct CD spectra distortions due to absorption flattening. *Chirality* 2008;20:1047–1052.
71. Halling P.J. Estimation of flattening coefficient for absorption and circular dichroism using simulation. *Anal. Biochem.* 2009;387:76-81.
72. Castiglioni E., Abbate S., Longhi G., Gangemi R. Wavelength shifts in solid-state circular dichroism spectra: a possible explanation. *Chirality* 2007;19:491-496.
73. Bustamante C., Maestre M.F. Statistical effects in the absorption and optical activity of particulate suspensions. *Proc. Natl. Acad. Sci. USA* 1988;85:8482-8486.
74. Miles A.J., Wallace B.A. Synchrotron radiation circular dichroism spectroscopy of proteins and applications in structural and functional genomics. *Chem. Soc. Rev.* 2006;35:39-51.
75. Clarke D.T., Jones G.R. CD12: a new high-flux beamline for ultraviolet and vacuum-ultraviolet circular dichroism on the SRS, Daresbury. *J. Synchr. Rad.* 2004;11:142-149.
76. Sutherland J.C. Measurement of circular dichroism and related spectroscopies with conventional and synchrotron light sources: theory and instrumentation. In *Modern Techniques for Circular Dichroism and Synchrotron Radiation Circular Dichroism Spectroscopy* (edited by Wallace B.A., Janes R.W.). IOS Press Amsterdam, 2009:19-72.
77. Figure can be found at www.diamond.ac.uk

CHAPTER I

Absorption flattening correction for circular dichroism of particle suspensions in near UV-Visible region*

Anna Gerdova¹, Sharon M. Kelly², Peter Halling¹

¹*WestCHEM, Department of Pure & Applied Chemistry, University of Strathclyde, Glasgow G1 1XL, UK*

²*Faculty of Biomedical and Life Sciences, University of Glasgow, Glasgow G12 8QQ*

ABSTRACT There are well established theoretical models for correction for absorption flattening of circular dichroism (CD) measurements on particle suspensions. However, these have not been directly tested experimentally. We describe a test system with the chiral tris (ethylenediamine) Co(III) complex dissolved in water trapped inside Sephadex particles, suspended in 1-butanol. Independent measurements of particle size distribution, volume fraction and the absorbance of the suspension are used to calculate the required CD correction. The corrected CD signal is found to agree rather well with that for the same amount of Co complex dispersed uniformly throughout the sample cell. This holds for different

particle volume fractions and Co complex concentrations inside the particles. The correction seems to work despite a substantial scattering contribution to the absorbance, which is not considered in the theoretical models.

KEY WORDS: circular dichroism; absorption flattening; scattering; simulation programme; tris(ethylenediamine) cobalt III chloride; Sephadex

INTRODUCTION

Circular dichroism (CD) measurements give useful information about many chiral materials. CD studies of proteins are particularly useful, with the far UV spectrum being related to secondary structure composition, while the near UV signals are sensitive to tertiary structure changes.¹ Many interesting samples containing proteins are in particulate form. There has been considerable attention to membrane proteins contained within vesicle preparations,^{2,3,4} and some studies of other protein-containing nanoparticles.^{5,6} However, there are also a wide range of larger particles (many micrometres in size) in which proteins are found, and for which CD study would be informative. These include biopharmaceutical formulations, immobilised enzymes, forms used for protein storage and some natural biological samples like cartilage. We have recently shown that it is possible to make useful CD measurements on such particles.^{7,8} These made use of a rotating sample cell to keep particles in suspension, and placement close to the detector to minimise scattering effects.

All CD measurements on particle suspensions may be affected by the artefact of absorption flattening. A simple picture of the origin is that some light paths through the sample may meet fewer particles, or even none at all, because of their random distribution in the suspension. These light paths contribute disproportionately to the transmitted intensity that is measured, and hence reduce the apparent magnitude of an absorbance-related measure like the CD signal. Various theoretical treatments

have been presented to quantify the size of absorption flattening,⁹⁻¹⁶ and these may be used to correct the measured CD signal, given measurements of other relevant suspension properties. The phenomenon of absorption flattening got its name from affecting the measured absorbance spectra by characteristic flattening of the peaks. This phenomenon also affects measurements of CD spectra in a different and maybe even more severe way. In this work we are not studying the effect of absorption flattening on the absorbance spectra, but we are attempting to correct the effect of flattening on the CD spectra.

The results of correction for absorption flattening may be plausible CD spectra, agreeing with the expected structures of protein molecules in the sample. But in the absence of other methods to determine the structure experimentally, there remains doubt as to whether the corrected spectra are actually accurate. It is desirable to make some tests with samples in which the true spectrum can be known more confidently, and be used to compare with that obtained after correction for flattening (and perhaps other artefacts). The chiral tris (ethylenediamine) Co(III) complex may be used for this purpose as a chromophore whose CD spectrum should be determined simply by the nature of the medium in which it is present. Castiglioni et al¹⁷ have recently used this complex to test corrections for the effects of flattening in a divided sample cell. In this cell, only part of the beam passes through the chromophore solution, while the remainder passes through the solvent medium alone. This results in an absorption flattening effect, and the experiments showed that it could be correctly estimated by the appropriate model (which is rather simpler than that for particle suspensions). We now describe a method to have the Co(en)₃ complex dispersed in small particles (of around 100 μm size), suspended in a chromophore free medium. This allows test of the more complicated corrections for absorption flattening in such particle suspensions, including the measurements of parameters on which they depend, the particle size distribution and volume fraction. The test shows that substantial flattening corrections (changing CD intensities of the major band up to 50%) can be made correctly using the test procedure.

MATERIALS AND METHODS

Racemic tris(ethylenediamine)cobalt (III) chloride dihydrate, potassium sodium tartrate tetrahydrate, 99%, A.C.S. reagent, Sephadex G-75 (Cat. No G75120) and 1-butanol, 99.4%, A.C.S. reagent, were purchased from Sigma-Aldrich, GmbH.

Resolution of racemic tris(ethylenediamine)cobalt (III) chloride

A method for the resolution of racemic tris(ethylenediamine)cobalt (III) chloride was obtained from an internet version of the Laboratory manual for inorganic chemistry, Chemistry department, written by Helm M.L., Fort Lewis College, Durango, Colorado. A mixture of 7 g (18 mmol) of $[\text{Co}(\text{en})_3]\text{Cl}_3 \cdot 2\text{H}_2\text{O}$ and 21 ml of water was heated to boiling. After the solute had dissolved, 5.42 g (19 mmol) of potassium sodium tartrate tetrahydrate was added to the boiling solution. This solution was allowed to cool on ice. When orange crystals of λ -tris(ethylenediamine)cobalt (III) d-tartrate chloride pentahydrate had formed they were filtered and washed with 40% aqueous ethanol. Crystals were then recrystallized by dissolving them in hot water, around 70°C, (1 ml of water per g of crystals), and cooling first to room temperature and then in an ice bath. Crystals were filtered, washed with 16 ml of 40% aqueous ethanol, 16 ml of absolute ethanol and 16 ml of ether, and dried in air. Purity of obtained λ - $[\text{Co}(\text{en})_3]^{3+}$ salt was 96% ($\Delta\epsilon_{493\text{nm}} = 1.81$, in comparison with literature value of 1.89).¹⁸

Preparation of the samples

Sephadex G-75 (0.1 g) was added to 2 mL of an aqueous solution of λ - $[\text{Co}(\text{en})_3]^{3+}$ tartrate (0.012 or 0.015 M), and left to swell for 2 days at room temperature. Obtained $[\text{Co}(\text{en})_3]^{3+}$ -Sephadex suspensions were centrifuged at 2232 x g for 5

minutes. Supernatants were removed, and pellets were re-suspended in 1-butanol. In preliminary experiments a number of other solvents were tested. 1-dodecanol, 1-heptanol and butyl butyrate have limited capacity to dissolve water, and the Sephadex beads tended to form aggregates, which did not break up even after 10 washes and applying ultrasound, so an even distribution of particles in the cell could not be obtained. On the other hand 2-propanol dissolved too much water, including that inside the particles. 1,1,1,3,3,3-hexafluoro-2-propanol was observed to dissolve the $[\text{Co}(\text{en})_3]^{3+}$ -complex itself.

Circular dichroism

CD measurements of samples were carried out in a Jasco J-810 spectropolarimeter operating at 20 °C. To avoid sedimentation of $[\text{Co}(\text{en})_3]^{3+}$ -Sephadex particles a specially constructed motor driven rotating sample cell holder was used.⁷ Rotation speed was set at 75 rpm. (This was found to be optimal to obtain even distribution of particles in the suspension samples. Results were not affected for limited changes around this value, but much higher or lower speeds gave reduced signals, as particles were concentrated at the rims or at the bottom of the cell.). Samples were introduced into a quartz cylindrical cell with 0.1cm path length (Hellma UK Ltd.). Two samples were prepared with varying concentrations of particles within the cell, as well as with different concentrations of $[\text{Co}(\text{en})_3]^{3+}$ within the particles: the first sample had a low concentration of Co-complex and high volume fraction of particles, the second sample had a higher concentration of Co-complex and lower volume fraction of particles. CD and high-tension voltage (HT) spectra were obtained at a scan rate of 50 nm min⁻¹, a response time of 0.5 s, and a bandwidth of 1nm. Spectra of 1-butanol saturated with water, and spectra of Sephadex particles filled with water and dispersed in 1-butanol were also recorded using the same conditions.

Estimation of volume of particles in the cell

In order to determine the weight of particles, after CD and HT spectra were measured, samples were carefully washed out from the rotating cell into plastic tubes using 1-butanol saturated with water (to prevent further removal of water from inside the particles). Suspensions were centrifuged; supernatants removed; and precipitates washed three times with petroleum ether (40-60 °C). Residues of this very volatile solvent could be removed selectively by evaporation from open topped tubes. The washed pellets were then weighed every 30sec, to detect the transition between rapid weight loss due to petroleum ether evaporation and much slower loss of water (Fig.1).

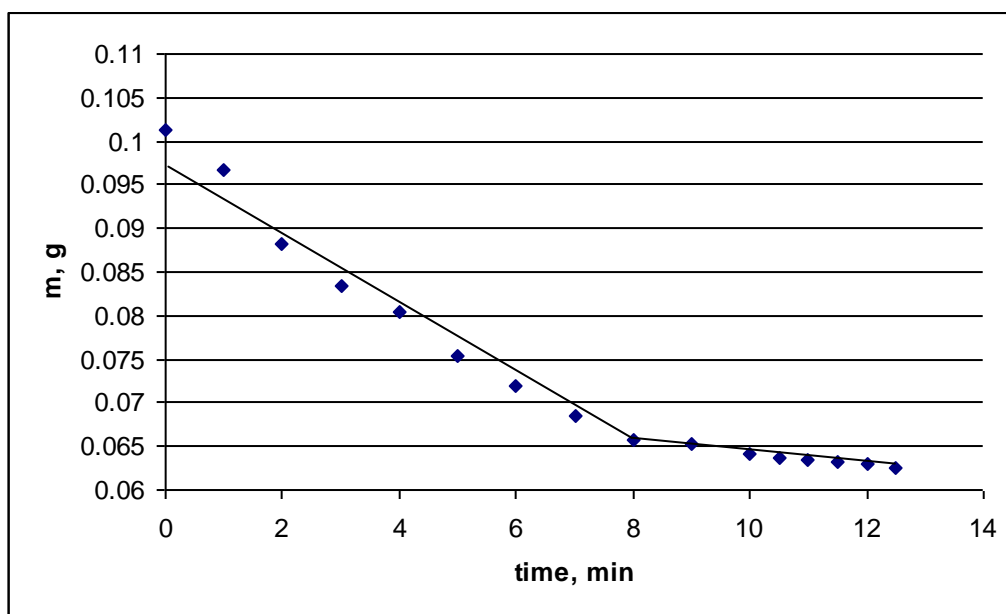


Fig.1. Determination of water content in the cell. The break point is the transition between evaporation of petroleum ether and loss of water; and is considered to be the weight of water inside the sample. (The plot was not extrapolated back to zero time, because it is not clear if water evaporates as well during evaporation of petroleum ether.)

The transitional point is the weight of the particles, mainly water, from each sample. To estimate the particle volume, we need an estimate of their density. The particles are largely water (as it swells, Sephadex takes up about 13 g water per g dry), so we use a value of 1 g/mL. Actually the particles density must be slightly higher, as they sediment slowly in water, but this will be counterbalanced by a slight underestimate of their mass, because of butanol lost during washing with petroleum ether, or water that evaporates along with the solvent. Because the liquid inside the particles will exchange with the medium, density cannot be measured by buoyancy or displacement methods. Finally, the volume fraction was determined by dividing the volume of the particles by the total volume of the cell, resulting in 0.25 and 0.18 for the first and second sample, respectively.

Determination of the amount of λ -[Co(en)₃]³⁺ in the cell

The amount of [Co(en)₃]³⁺ inside the measured samples was determined in a spectrophotometer. Particles, obtained from previous water content measurements, were re-suspended in 2 ml of water, thoroughly mixed and absorption spectra for the supernatants were taken. UV measurements were carried out in a Beckman Coulter DU 800 spectrophotometer operating at 20 °C. Samples were introduced into a quartz rectangular cell with 1cm path length; spectra were recorded at a scan speed of 1200 nm min⁻¹ and a bandwidth of 1 nm. Using calibration curve of aqueous solutions with known concentrations of Co-complex, and knowing the total amount of water in which particles were re-suspended (2 ml + measured volume of water inside particles), amount of λ -[Co(en)₃]³⁺ in both samples was calculated. Controls with freshly loaded particles showed that Co complex was quantitatively recovered on suspension in water. And knowing volume of water inside each sample during CD measurements, concentrations of Co-complex within particles were obtained (0.044M and 0.081M in the first and second sample). Therefore, in each case, average concentration of dye in the cell was calculated by multiplying concentration of λ -[Co(en)₃]³⁺ in particles by volume fraction of particles (0.25 and 0.18), resulting in 0.011M and 0.0146M.

Distribution of particle sizes

To determine distribution of particle sizes, diameters of 300 Sephadex particles from the suspension were measured under the microscope (Olympus, Vanox, M10, Japan). Particles sizes were fitted to a normal distribution, and the volume mean diameter and standard deviation of sizes were estimated from this.

Correction of absorption flattening

The correction for absorption flattening was estimated using the recently published simulation method.¹⁶ This approach generates random patterns of particles consistent with input values of pathlength, the volume fraction of particles in the cell, the mean particle size and its fractional standard deviation. Then a large array of possible light paths through the suspension are considered to calculate the expected transmission of light, and hence the absorbance and CD signals. The results from the simulation agree with the predictions of equations first derived by Gordon & Holzwarth,⁹ for the limit of low volume fraction and uniform particle size where they apply. The equations are shown here using alternative symbols, as explained in reference¹⁶. The correction factor for absorption flattening of the CD signal, (Q_{CD}), is given by:

$$Q_{CD} = \frac{3}{\alpha} [\beta - \exp(-\alpha)] \quad (1)$$

where $\alpha = A_{\text{part}} * \ln 10$, A_{part} is the absorbance through the diameter of a single particle, and β is given by:

$$\beta = \frac{2[1-(1+\alpha)e^{-\alpha}]}{\alpha^2} \quad (2)$$

To apply this to experimental data we need a way to calculate α or A_{part} from readily available measurements.

We can use the corresponding expression for the correction factor for flattening of absorbance itself (Q_A):

$$Q_A = \frac{3(1-\beta)}{2\alpha} \quad (3)$$

and we also use the definition of Q_A as the ratio of the measured absorbance of the suspension (A_{SUS}) to that which would be found if the chromophore were uniformly distributed through the solution. This absorbance is simply shown to be $A_{part} * \phi * l / d$, where ϕ is the volume fraction of particles, l the cell pathlength, and d the particle diameter. Hence:

$$Q_A = \frac{A_{SUS} \times d \times \ln 10}{\alpha \times \phi \times l} \quad (4)$$

Now if d , ϕ and l are known, combination of equations 3 and 4 allows β to be calculated from a measured value of A_{SUS} . Equation 2 then gives an implicit calculation of α , and finally equation 1 gives Q_{CD} .

In the present study we used the simulation method, which can take account of a range of particle sizes and $\phi \gg 0$, and generates a table of A_{SUS} and corresponding Q_{CD} values. These are nearly, but not quite exactly, linearly related, and a 3rd degree polynomial was used for interpolation (Fig. 2).

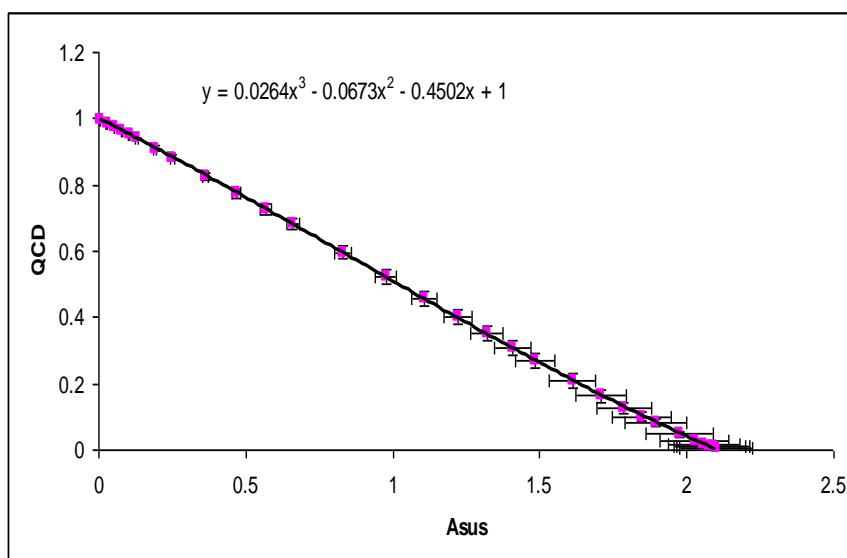


Fig. 2. Relationship between the correction factor for absorption flattening and absorbance. This plot is for the sample with 0.25 volume fraction of particles in the cell, volume mean particle diameter 69.4 nm, and standard deviation 0.22. The fitted cubic equation is used purely for interpolation, and has no theoretical significance.

Estimation of apparent absorbance of suspension

According to Arvinte et al.¹⁹ absorbance values can be measured from changes in high tension (HT) voltage signal on the spectropolarimeter, using equation:

$$A = Z \times [\log (HT_{\text{sample}}) - \log (HT_{\text{blank}})] \quad (5)$$

where Z is an instrument constant to be determined by standardization, and varies by instrument.

To calculate Z of the spectropolarimeter used in these experiments, HT spectrum of 0.04M $[\text{Co}(\text{en})_3]^{3+}$ aqueous solution was measured on spectropolarimeter (Jasco J-810) and absorbance spectrum on spectrophotometer (Beckman Coulter DU 800), using exactly the same sample and cell in both instruments (a quartz cylindrical cell with 0.1cm path length (Hellma UK Ltd.) fixed in a rotating cell holder set at 60 rpm

speed). A water blank sample was also measured in both instruments. For every data point in the spectrum $\log [(HT_{\text{sample}}) / (HT_{\text{blank}})]$ was then plotted against ΔA (difference in absorbance between sample and blank) (Fig.3). It can be seen in Fig.3 that the data are in good agreement with a line extrapolated to the origin, whose gradient is the value of $1/Z$.

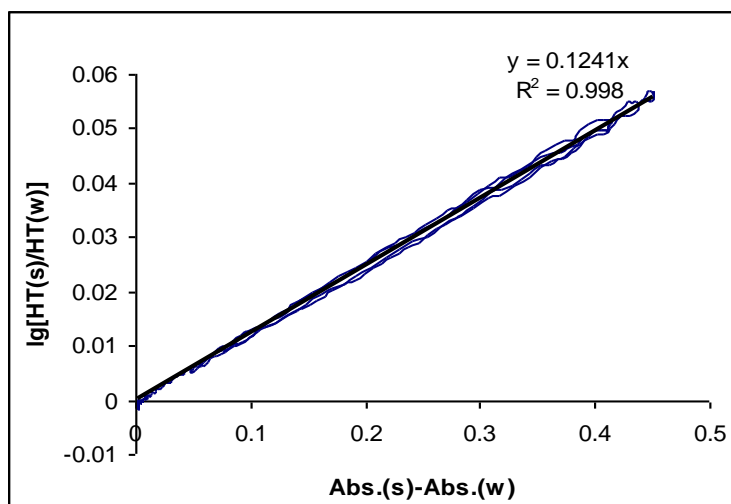


Fig. 3. Conversion plot of HT to absorbance for 0.04 M aqueous solution of $[\text{Co}(\text{en})_3]^{3+}$.

The instrument software will also output “Absorbance” values. By subtracting these reported values for the blank from those for the sample, we found absorbance values similar to those obtained as above, but tending to be slightly lower where absorbances are highest. Because the method used by the instrument software is not described, we preferred not to use these values.

Correction of each point in CD spectra

Knowing the instrument’s constant, absorbance for every point of HT spectra of samples was calculated using equation (1), where blank is 1-butanol saturated with water. From the absorbance (A_{SUS}), the absorption flattening correction factor (Q_{CD})

was calculated for each point in the spectrum, using the previously obtained polynomial relationship between the two (Fig.2). Finally, corrected CD spectrum was obtained by dividing raw CD data of the test suspension by Q_{CD} and subtracting CD spectrum of the blank.

Obtaining true CD spectra to compare with the corrected ones

A series of CD spectra were measured for different concentrations of Co-complex (0.0064M, 0.034M and 0.049M) in aqueous solutions saturated with 1-butanol. The intensities were found to be proportional to concentration. Hence these standard spectra were scaled to give the expected spectra of solutions having the same average concentration of $[\text{Co}(\text{en})_3]^{3+}$ in the cell as in the suspensions (i.e. 0.011M and 0.0146M). These spectra were compared with the corrected spectra of the suspensions.

RESULTS AND DISCUSSION

Principles of test

To test the correction for absorption flattening of CD spectra, we need a system in which the CD chromophores can be dispersed at known concentration in particles of defined volume fraction and size distribution. To generate stable particles we took beads of cross-linked dextran, the commercial product Sephadex. These can be swollen in water, where they will take up 12-15 times their weight of water. By adding the chiral λ -tris(ethylenediamine)cobalt (III) complex to the water, this will also become evenly dispersed within the internal water of the beads. To obtain a suspension of the water-wet Sephadex beads, in which the chromophore was

confined to the bead interiors, they were suspended in water-immiscible organic solvents. It was found necessary to use a relatively polar solvent to disperse the beads, probably because it is necessary to dissolve excess water from the spaces between them. 1-butanol was found to be an effective choice, which also avoided excessive problems of evaporation, and of high viscosity which make it difficult to load the suspension into the measurement cell. Examination by the naked eye and microscope confirmed that the beads were completely dispersed, and that the visibly red $[\text{Co}(\text{en})_3]^{3+}$ was confined to the bead interiors.

The theoretical models for absorption flattening indicate that the required correction to the CD signal can be determined, given: a) the particle size and size distribution; b) the volume fraction of particles; and c) the absorbance of the suspension. The particle size distribution was estimated by microscopic examination of a representative selection of particles in the suspension before CD measurements. The volume fraction of particles was estimated from the mass of water contained in particles recovered from the cell after CD measurements. The absorbance of the suspension (A_{SUS}) was estimated from the HT signal of the spectropolarimeter, compared with the HT of a suitable blank. The aim of corrections for absorption flattening is to recover the spectrum that would have been obtained if the same amount of chromophore were uniformly distributed throughout the measurement cell. Hence, to test whether the corrected CD spectrum is accurate, it is necessary to know this amount of $[\text{Co}(\text{en})_3]^{3+}$. So particles recovered from the cell after the CD measurement were resuspended in a known additional volume of water. The $[\text{Co}(\text{en})_3]^{3+}$ then leaves the particles and becomes distributed throughout the entire water volume, and its concentration in the supernatant can be measured spectrophotometrically.

Scattering contributions

The theoretical models for absorption flattening are based entirely on the effects of light absorption, and take no account of possible scattering. Visual examination of the $[\text{Co}(\text{en})_3]^{3+}$ -Sephadex suspensions showed that they gave considerable

scattering. Part of the technique for making CD measurements on these suspensions is the placement of the sample cell very close to the detector. Thus the maximum fraction of scattered light still reaches the detector. However, scattering still makes a major contribution to the measured apparent absorbance, as indicated by the substantial A_{SUS} values at wavelengths where $[\text{Co(en)}_3]^{3+}$ does not absorb significantly (e.g. 650 nm, Fig. 5). Note that there is usually also considerable scattering from protein-containing particles for which CD studies are of interest. Hence the scattering particles used here are a relatively good model for them.

The scattering of light by particles is a much studied phenomenon, and theoretical treatments exist for many cases.²⁰⁻²² However, the larger protein-containing particles of interest usually do not have uniform internal refractive index, as assumed in most theoretical treatments. Instead they will have multiple internal refractive index boundaries, at the surfaces of pores and similar internal structures. The Sephadex particles were chosen to mimic this structure – with multiple internal regions of different refractive index due to the polysaccharide chains – although there will also be a significant refractive index boundary where the organic solvent and water phases meet near the bead external surface.

It is possible to analyse the effects for a simple but plausible model of scattering in a bead with multiple refractive index boundaries. Scattering may simply reduce the intensity on onward transmitted light by a fixed proportion for a given distance travelled through the bead. This would result from a fixed probability that any given photon is scattered during progress through the next distance element along the path through the bead. It is also necessary to assume that any photon scattered by a large enough angle to prevent it reaching the detector can be permanently disregarded – in other words, that multiple scattering is negligible. If these conditions are met, then scattering affects transmission in exactly the same way as does absorption within the bead. Hence we would expect the relationship between A_{SUS} and the flattening coefficient for CD (Q_{CD}) to be the same as if the absorbance was due entirely to true absorption.

It is of course also possible that samples containing chiral material may scatter left and right polarised light to different extents. This differential scattering is a potential

further artefact in CD measurements on scattering samples,²³⁻²⁵ and cannot be corrected for by the method used here.

The apparent absorbance due to scattering will depend on the instrument used to measure it, as light scattered through small angles may still reach the detector. Hence it is important for correction of CD signals that A_{SUS} is measured on the spectropolarimeter at the same time. By obtaining A_{SUS} values from the HT signal we achieve this.

Test of model corrections

Samples were prepared with two different concentrations of $[\text{Co}(\text{en})_3]^{3+}$ within the beads (0.012 and 0.015 M in the initial aqueous solution), and two different volume fractions of beads (0.25 and 0.18) (Fig.4).

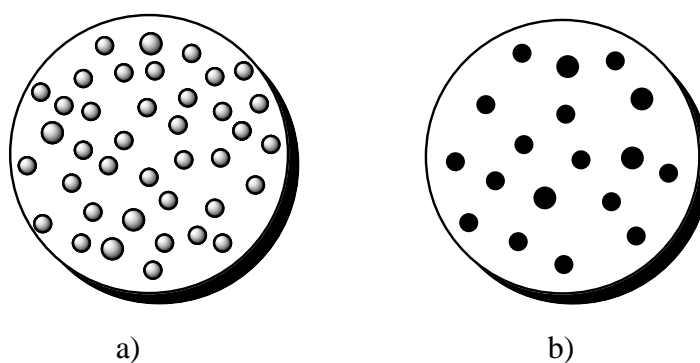
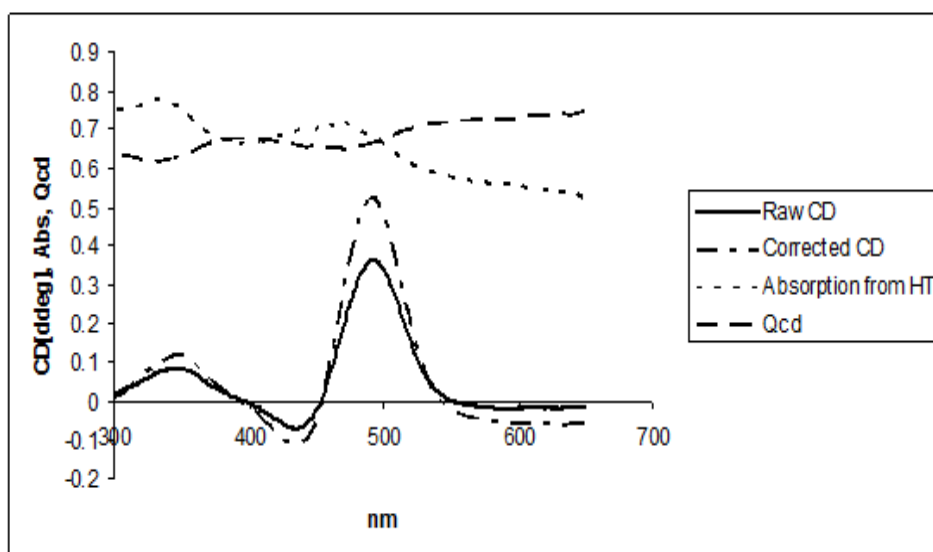


Fig. 4. Diagrammatic representation of analyzed suspensions. a) Sample with small concentration of $[\text{Co}(\text{en})_3]^{3+}$ within the particles and high volume fraction of particles in the cell; b) sample with high concentration of $[\text{Co}(\text{en})_3]^{3+}$ within the particles and small volume fraction of particles in the cell.

In each case the relationship between the absorbance of the suspension (A_{SUS}) and the flattening coefficient for CD (Q_{CD}) was calculated by the simulation method previously reported, using as inputs the measured volume fractions and particle size distributions. Then this relationship was used to estimate Q_{CD} values from measured A_{SUS} values. The Q_{CD} values were used to correct the measured CD signals from the suspension samples. Fig.5 shows how this correction works, with a complete spectrum of measured A_{SUS} and CD intensity, estimated Q_{CD} , and calculated corrected CD. (Note that we are not attempting to study correction for flattening of the absorbance spectrum itself, we are just using A_{SUS} as an experimental data input to estimate Q_{CD} .) The model for absorption flattening predicts different relationships between Q_{CD} and absorbance for the two samples, due to the difference in volume fraction of particles in the CD cells. As seen on Fig.5 corrections for absorption flattening are quite significant, the lower Q_{CD} , the bigger the corrections.

a)



b)

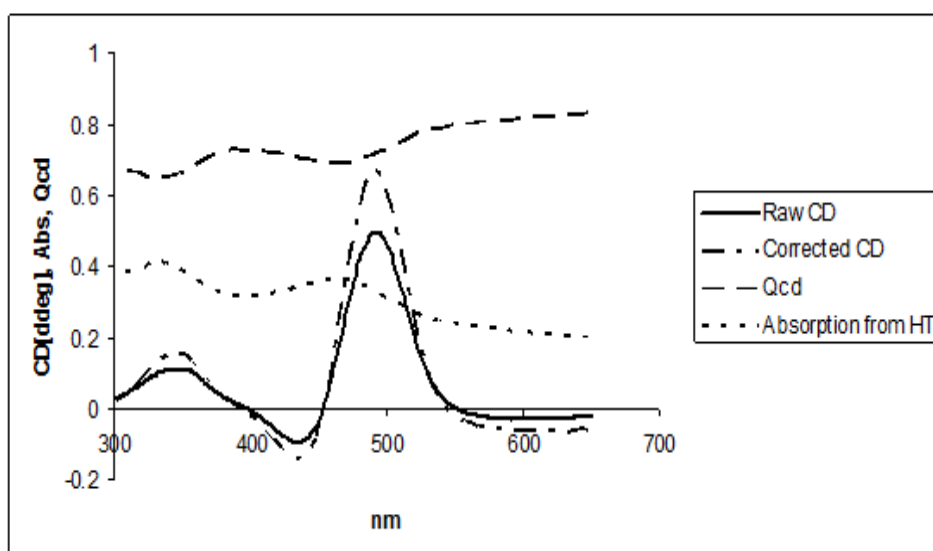


Fig.5. Plots of raw and corrected CD data, absorbance calculated from HT spectra and determined correction factor (Q_{CD}), for: a) sample with 0.011M average concentration of Co-complex and with 0.25 volume fraction of particles in the cell ; b) sample with 0.0146M average concentration of Co-complex and with 0.18 volume fraction of particles in the cell.

In parallel, the measured amount of $[\text{Co}(\text{en})_3]^{3+}$ in the suspended particles is used to scale the measured CD spectrum of $[\text{Co}(\text{en})_3]^{3+}$ in solution, to give the CD spectrum expected if the same amount of $[\text{Co}(\text{en})_3]^{3+}$ was uniformly distributed throughout the sample cell. Because in the suspension samples the water inside the Sephadex particles is likely to be saturated with 1-butanol, for better comparison, aqueous solutions of $[\text{Co}(\text{en})_3]^{3+}$ were also saturated with 1-butanol. (In fact, the presence of 1-butanol was found to have very little effect on the CD spectrum.) Measured CD spectra were blanked against water saturated with 1-butanol. The expected CD signal scaled from solution measurements should agree with the corrected CD of the suspension, if the correction method works properly. The expected and corrected CD spectra are compared in Fig.6.

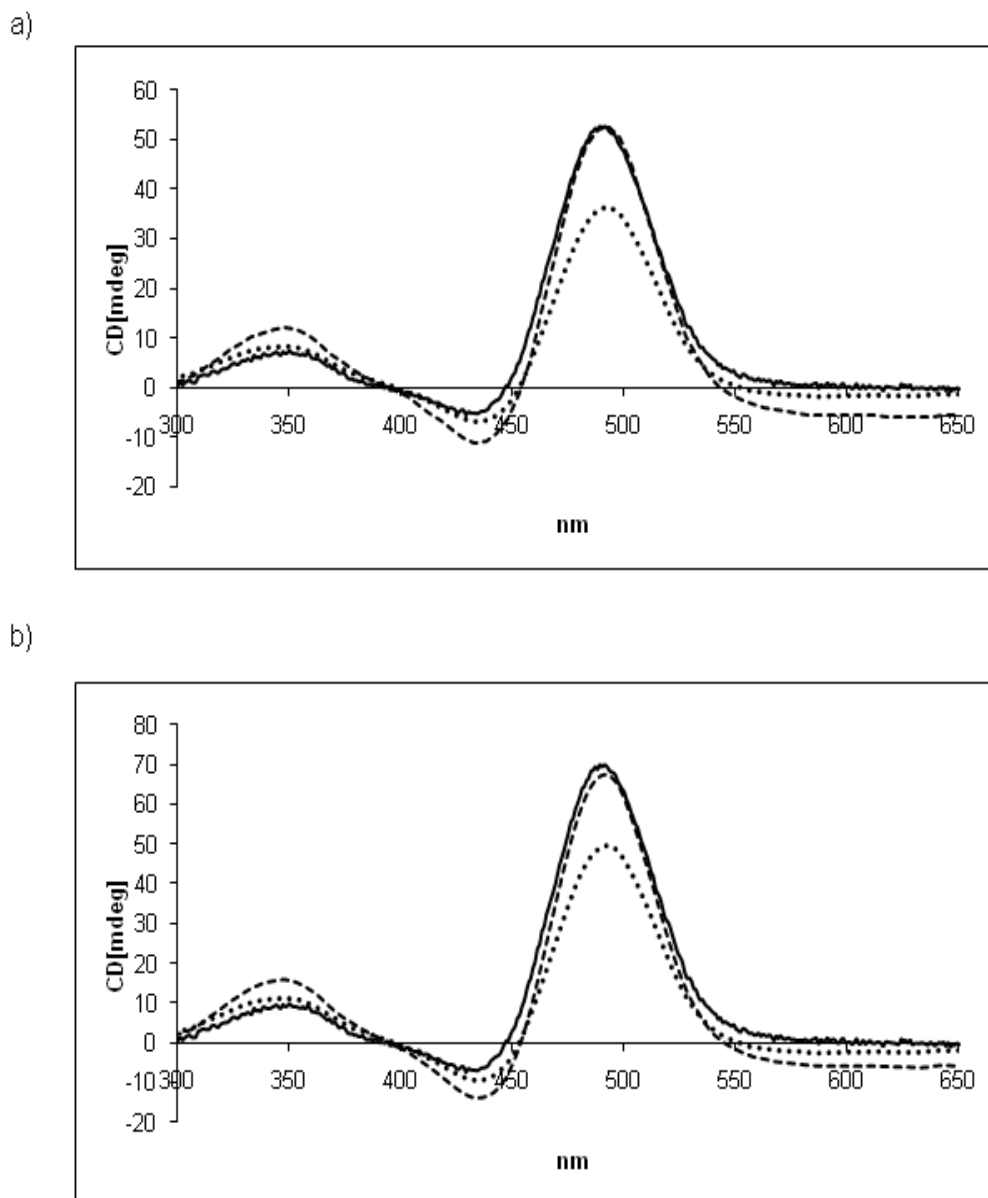


Fig.6. a) comparison of expected CD spectrum of 0.011M aqueous solution of $[\text{Co}(\text{en})_3]^{3+}$, saturated with 1-butanol, scaled from 0.0064M solution (—), with raw (.....) and corrected CD spectrum of sample with the same average concentration of $[\text{Co}(\text{en})_3]^{3+}$ in the sample cell (---); b) comparison of expected CD spectrum of 0.0146M aqueous solution of $[\text{Co}(\text{en})_3]^{3+}$, saturated with 1-butanol, scaled from 0.0064M solution (—), with raw (.....) and corrected CD spectrum of sample with the same average concentration of $[\text{Co}(\text{en})_3]^{3+}$ in the sample cell (---). All the measurements were performed under the same conditions, using the same sample cell.

It would be good to test a system where the true absorption peaks are larger, and show the characteristic distortion in shape due to flattening. We tried to achieve this with higher concentrations of $[\text{Co}(\text{en})_3]^{3+}$ in the particles. However, it was observed in the microscope that in such samples undissolved crystals (probably of Co complex) tend to gather on the surface of Sephadex beads (Fig.7).

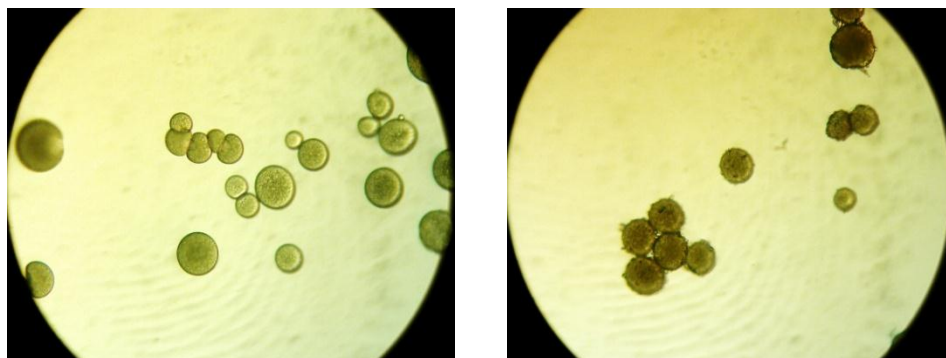


Fig.7. Sephadex beads with different concentration of Co-complex within them: left – 0.015M, right – 0.084M.

With these particles at higher $[\text{Co}(\text{en})_3]^{3+}$ concentration, the corrected CD spectra no longer agreed so well with those expected, and there was a significant red-shift in the maximum. A limited effect of this type may lie behind a very small red-shift (1-2 nm) of the corrected spectra in Fig. 6.

As noted, the corrected and expected spectra at lower concentrations of $[\text{Co}(\text{en})_3]^{3+}$ in the particles agree well. This shows that the rather strong assumptions about scattering must be quite realistic. Interestingly, suspensions of Sephadex particles containing just water were much less strongly scattering. For example, at 650nm the apparent absorbance of a suspension of particles containing water was 0.028, whereas for a suspension of particles containing $[\text{Co}(\text{en})_3]^{3+}$ solution it was 0.566. It may be that the presence of $[\text{Co}(\text{en})_3]^{3+}$ in the water increases the refractive index sufficiently to make a large difference from that of the polysaccharide matrix. In an

alternative data treatment approach, the absorbance of a corresponding suspension of water-filled Sephadex particles was subtracted from absorbance of the sample (A_{sus}) before estimating Q_{CD} . Because particles containing no $[\text{Co}(\text{en})_3]^{3+}$ show only small scattering it made very little difference for calculations and shape of the spectra.

CONCLUSIONS

In this paper we attempted to correct the effect of absorption flattening on the CD spectra. The experiments and measurements carried out show that absorption flattening correction can be correctly estimated by the appropriate theoretical model. This is despite the presence of significant scattering, at least of the type presented by the test particles. However, it must be acknowledged that the tests we were able to apply did not cover the most extreme conditions, in particular high true absorbance. This will require further study. However we can now have more confidence in results when the correction method is applied to suspensions of protein-containing particles, where the correct spectrum cannot usually be independently determined.

REFERENCES

1. Kelly S.M., Jess T.J., Price N.C. How to study proteins by circular dichroism. *Biochim. Biophys. Acta* 2005;1751:119-139.
2. Sreerama N., Woody R.W. On the analysis of membrane protein circular dichroism spectra. *Protein Sci.* 2004;13:100-112.
3. Wallace B.A., Lees J.G., Orry A.J., Lobley A., Janes R.W. Analyses of circular dichroism spectra of membrane proteins. *Protein Sci.* 2003;12(4):875-884.
4. Laird D.J., Mulvihill M.M., Whiles Lillig J.A. Membrane-induced peptide structural changes monitored by infrared and circular dichroism spectroscopy. *Biophys. Chem.* 2009;145(2-3):72-78.
5. Sarmiento B., Ferreira D.C., Jorgensen L., van de Weert M. Probing insulin's secondary structure after entrapment into alginate/chitosan nanoparticles. *Eur. J. Pharm. Biopharm.* 2007;65:10-17.
6. Wangoo N., Raman Suri C., Shekhawat G. Interaction of gold nanoparticles with protein: A spectroscopic study to monitor protein conformational changes. *Appl. Phys. Lett.* 2008;92:133104.
7. Ganesan A., Price N.C., Kelly S.M., Petry I., Moore B.D., Halling P.J. Circular dichroism studies of subtilisin Carlsberg immobilised on micron sized silica particles. *Biochim. Biophys. Acta* 2006;1764:1119-1125.
8. Ganesan A., Moore B.D., Kelly S.M., Price N.C., Rolinski O.J., Birch D.J.S., Dunkin I.R., Halling P.J. Optical spectroscopic methods for probing the conformational stability of immobilised enzymes. *Chem. Phys. Chem.* 2009;10:1-9.
9. Gordon D.J., Holzwarth G. Artifacts in the measured optical activity of membrane suspensions. *Arch. Biochem. Biophys.* 1971;142:481-488.

10. Urry D.W. Protein conformation in biomembranes: optical rotation and absorption of membrane suspensions. *Biochim. Biophys. Acta* 1972;265:115-168.
11. Wallace B.A., Mao D. Circular dichroism analyses of membrane proteins: an examination of light scattering and absorption flattening in large membrane vesicles and membrane sheets. *Anal. Biochem.* 1984;142:317-328.
12. Teeters C.L., Eccles J., Wallace B.A. A theoretical-analysis of the effects of sonication on differential absorption flattening in suspensions of membrane sheets, *Biophys. J.* 1987;51:527-532.
13. Wallace B.A., Teeters C.L. Differential absorption flattening optical effects are significant in the circular dichroism spectra of large membrane fragments. *Biochemistry* 1987;26:65-70.
14. Bustamante C., Maestre M.F. Statistical effects in the absorption and optical activity of particulate suspensions. *Proc. Natl. Acad. Sci. USA* 1988;85:8482-8486.
15. Castiglioni E., Lebon F., Longhi G., Gangemi R., Abbate S. An operative approach to correct CD spectra distortions due to absorption flattening. *Chirality* 2008;20:1047-1052.
16. Halling P.J. Estimation of flattening coefficient for absorption and circular dichroism using simulation. *Anal. Biochem.* 2009;387:76-81.
17. Castiglioni E., Abbate S., Longhi G., Gangemi R. Wavelength shifts in solid-state circular dichroism spectra: a possible explanation. *Chirality* 2007;19:491-496.
18. McCaffery A.J., Mason S.F. The electronic spectra, optical rotatory power and absolute configuration of metal complexes the dextro-tris(ethylenediamine) cobalt (III) ion. *Mol. Phys.* 1963;6:359-371.

19. Arvinte T., Bui T.T.T., Dahab A.A., Demeule B., Drake A.F., Elhag D., King P. The multi-mode polarization modulation spectrometer: part1: simultaneous detection of absorption, turbidity, and optical activity. *Anal. Biochem.* 2004;33:46-57.
20. van de Hulst H.C. *Light scattering of small particles.* New York: John Wiley & Sons, Inc.; 1957.
21. Asano S., Yamamoto G. Light scattering by a spheroidal particle. *Appl. Opt.* 1975;14:29-49.
22. Bohren C.F., Huffman D.R. *Absorption and scattering of light by small particles.* Wiley VCH, 1998.
23. Bustamante C., Tinoco I.Jr., Maestre M.F. Circular differential scattering can be an important part of the circular dichroism of macromolecules. *Proc. Natl. Acad. Sci. USA* 1983;80:3568-3572.
24. Dorman B.P., Maestre M.F. Experimental differential light-scattering correction to the circular dichroism of bacteriophage T2. *Proc. Natl. Acad. Sci. USA* 1973;70:255-259.
25. Schneider A.S., Hartz D. An experimental method correcting for absorption flattening and scattering in suspensions of absorbing particles: circular dichroism and absorption spectra of haemoglobin in situ in red blood cells. *Biochemistry* 1976;15:4158-4162.

CHAPTER II

Absorption flattening correction of CD spectra of large particle suspensions in UV region.

INTRODUCTION

CD is a valuable technique that gives information on structure of proteins. Information on the different types of secondary structure can be obtained from CD spectra in the far UV region (240nm and below), whilst near UV region (260-320nm) is responsible for tertiary structure fingerprints¹. There is a considerable interest in samples where enzymes are present in large particles (many micrometers in size), such as immobilized enzymes, biopharmaceutical formulations and different forms used for storage, etc. One of the major artefacts of CD measurements of particle suspensions is absorption flattening of CD signals^{2, 3, 4}. This doesn't allow determination of protein structure inside particles. Hence it is very important to find a way to correct for absorption flattening in such samples and also experimentally prove that these corrections are true.

Previous work⁵ on CD measurements of particles containing chiral tris (ethylenediamine) Co(III) complex showed that it is possible to correctly estimate absorption flattening correction of CD spectra of suspension samples using

appropriate theoretical model. Tris (ethylenediamine) Co(III) complex gives CD signals between 300 and 600nm. To see whether proposed theoretical model ⁶ can be applied to CD measurements in lower 200nm to 300nm range of wavelengths useful for protein CD measurements, measurements on suspension particles containing chromophore that absorbs below 300nm were carried out in this work. Here Co complex inside Sephadex particles was replaced with Ascorbic acid (AA), but all the preparations, measurements and calculation methods were done the same way. Other compounds (Camphorsulfonic acid, Phenylglycine and 4-hydroxy-proline) were also tested, but unfortunately, they appeared to be not suitable for the proper calculations.

Work on suspensions containing Co complex solution and Ascorbic acid solution show that proposed theoretical model for absorption flattening correction can be applied to a broad range of particle suspensions containing chromophore solutions that give CD signal anywhere between 200nm and 600nm.

MATERIALS AND METHODS

L-Ascorbic acid, BioXtra, $\geq 99.0\%$ (Cat. No A5960); (1S)-(+)-10-Camphorsulfonic acid, 99% (Cat. No C2107); D-(-)-Phenylglycine 99% (Cat. No P25485); trans-4-hydroxy-L-proline, BioXtra, $\geq 99.0\%$ (Cat. No 56250); Subtilisin Carlsberg (protease from *Bacillus licheniformis*), Type VIII, lyophilized powder, 7-15 units/mg solid (Cat. No. P5380); α -Chymotrypsin from bovine pancreas, Type II, lyophilized powder, ≥ 40 units/mg protein (Cat.No. C4129); Sephadex G-75 (Cat. No G75120); 1-butanol, ACS reagent, $\geq 99.4\%$ (Cat. No 360465) were purchased from Sigma-Aldrich, GmbH.

Sample preparation

Four different solution samples were prepared as follows:

- 1) Aqueous solution of 1.4M 10-camphorsulfonic acid;
- 2) Aqueous solution of 0.019M D-(-)-phenylglycine;
- 3) 0.16M solution of trans-4-hydroxy-L-proline in 0.02M sodium phosphate buffer pH11;
- 4) 0.019M solution of L-ascorbic acid in 0.02M sodium phosphate buffer pH2.0.

To these solutions Sephadex G-75 beads were added and left to swell for couple minutes at room temperature. Obtained suspensions were then centrifuged at 704 x g for 3 minutes. Supernatants were removed and pellets re-suspended in 1-butanol.

Measurements of L-ascorbic acid sample were carried out straight away, to avoid oxidation.

Circular dichroism measurements

CD measurements of samples were carried out in a Jasco J-810 spectropolarimeter warmed up for half an hour before measurements and operating at 20 °C. Spectra were obtained at a scan rate of 20 nm min⁻¹, a response time of 0.5 s, and a bandwidth of 1nm. To avoid sedimentation of particles samples were introduced into cylindrical cell fixed in the rotating at 60 rpm cell holder⁴. Same quartz cylindrical cell with 0.1cm path length (Hellma UK Ltd.) was used for all the experiments. For measurements in far UV to achieve better signal to noise ratio it is common to use cells with smaller pathlengths (i.e. 0.02 cm), but in these experiments only 0.1 cm pathlength cells could be used due to the large particle size (there should be enough space for particles to move around for their even distribution in the cell during measurements).

Samples with varying volume fraction of particles in the cell were measured. Spectra of buffer/water (depending on the sample) saturated with 1-butanol, and spectra of Sephadex particles filled with buffer/water and dispersed in 1-butanol

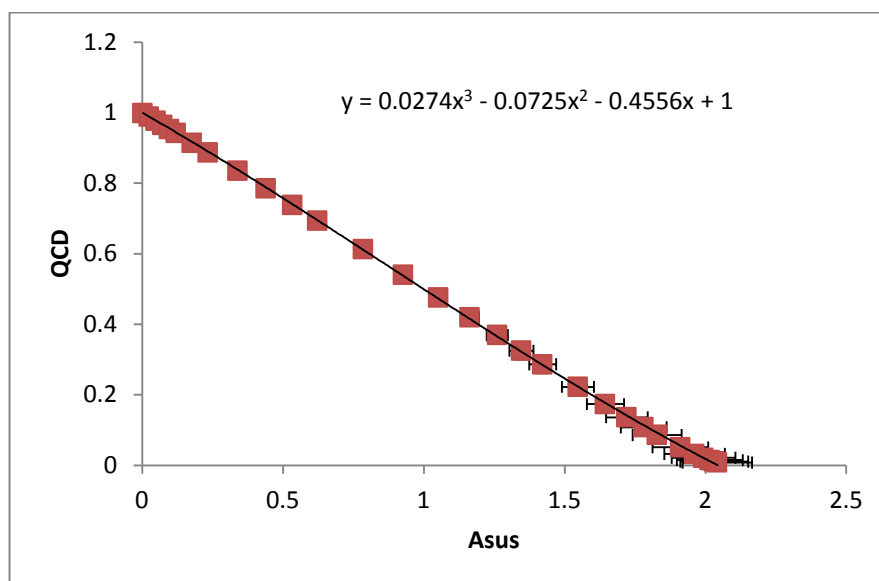
were also recorded using the same conditions. Spectra of samples supernatants were also recorded to check if any chromophore leaked into the organic media (i.e. 1-butanol).

Estimation of absorption flattening correction factor

Calculations below were done only to samples containing Ascorbic acid (AA), as CD data of other compounds were not suitable for absorption flattening simulation method suggested by Prof. Halling⁶. Details and reasons why other compounds were not suitable will be discussed in full in Results and Discussions part.

The result of the simulation programme is a table of absorbance of suspension (A_{SUS}) values and corresponding absorption flattening correction factor (Q_{CD}) values. This method depends on three inputs: volume fraction of particles; pathlength to particle size ratio; and standard deviation of particle size. Estimation of these parameters was described in details in previous work⁵ and was done exactly the same way in these experiments, therefore will not be discussed here. Thus, for two AA samples volume fractions were calculated to be 0.28 and 0.23; mean particle size 80.4 μm and fractional standard deviation of particle size 0.24. For both sets of parameters simulation programme generated polynomial relationship between A_{SUS} and Q_{CD} (Fig.1):

A



B

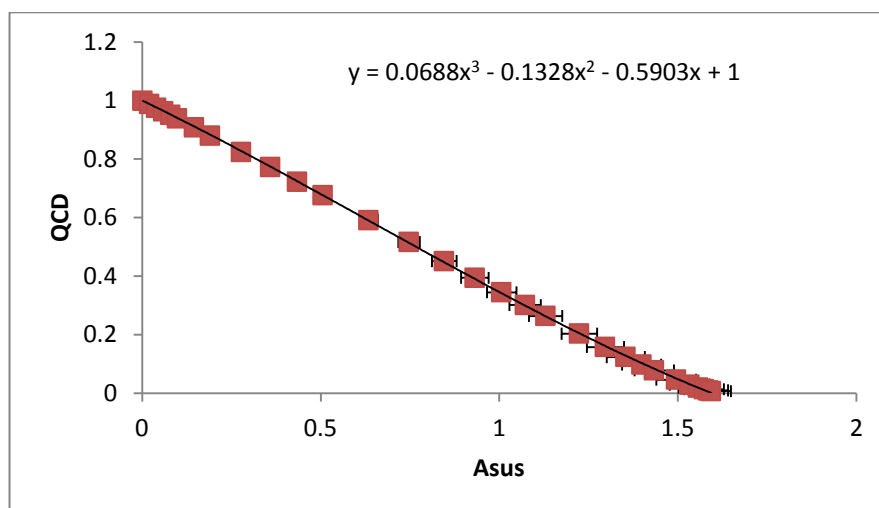


Fig.1. Relationship between absorbance of suspension and absorption flattening correction factor for: A – sample with particles volume fraction 0.28, and B – sample with particles volume fraction 0.23.

Knowing this relationship to calculate correction factor (Q_{CD}) for each point of CD spectra corresponding absorbance of suspension (A_{SUS}) values have to be estimated.

There is an established relationship^{7, 8} between photomultiplier high tension voltage (HT) in CD spectrometer and absorbance:

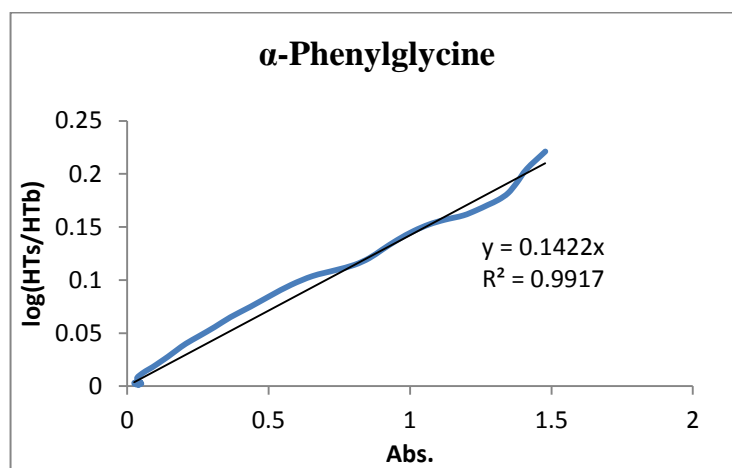
$$A = Z \times [\log (\text{HT}_{\text{sample}}) - \log (\text{HT}_{\text{blank}})] \quad (1)$$

where A – Absorbance, $\text{HT}_{\text{sample}}$ – voltage generated by the sample, HT_{blank} – voltage generated by the blank, Z – photomultiplier constant, and varies by instrument.

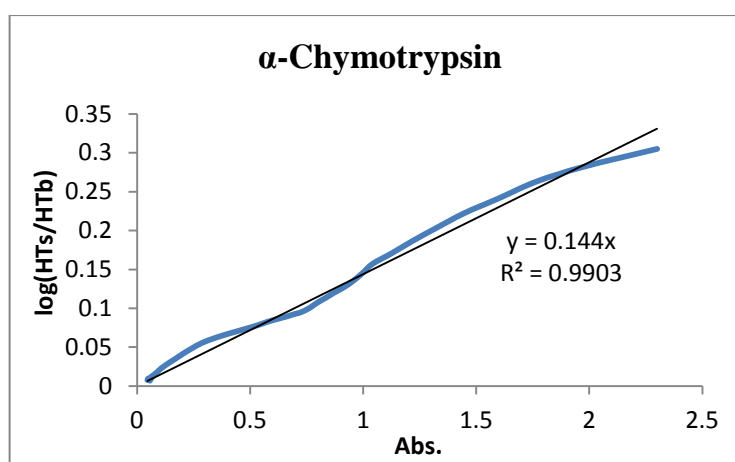
To calculate Z for the CD spectrometer used in these experiments three different samples were prepared by dissolving 5mg of α -Phenylglycine, 2.5mg of α -Chymotrypsin and 5mg of Subtilisin in 10mL of 20mM sodium phosphate buffer, pH 7.8. For each of them HT and absorbance spectra were recorded. Buffer spectra were also measured and subtracted from the relevant solution spectra to compensate for any buffer absorbance. Samples were introduced into cylindrical quartz cell with 0.1cm path length (Hellma UK Ltd.) fixed in a rotating cell holder set at 60 rpm speed. Same cylindrical cell was used for all the measurements. HT spectra were obtained at Jasco J-810 spectropolarimeter using the same settings as for the particles measurements. Absorbance spectra were measured at Beckman Coulter DU 800 spectrophotometer at a scan speed of 1200 nm min⁻¹ and a bandwidth of 1 nm. Both instruments were warmed up for half an hour before measurements and operated at 20°C.

For every data point between 200-260nm in each sample's CD spectrum $\log [(\text{HT}_{\text{sample}}) / (\text{HT}_{\text{blank}})]$ was calculated and plotted against corresponding difference of absorbance between sample and buffer (Fig.2). There is a good agreement between data and lines extrapolated to the origin, whose gradient is the value of 1/Z. Thus for α -phenylglycine $Z = 7.03$, for α -chymotrypsin $Z = 6.94$, and for subtilisin $Z = 6.75$.

A



B



C

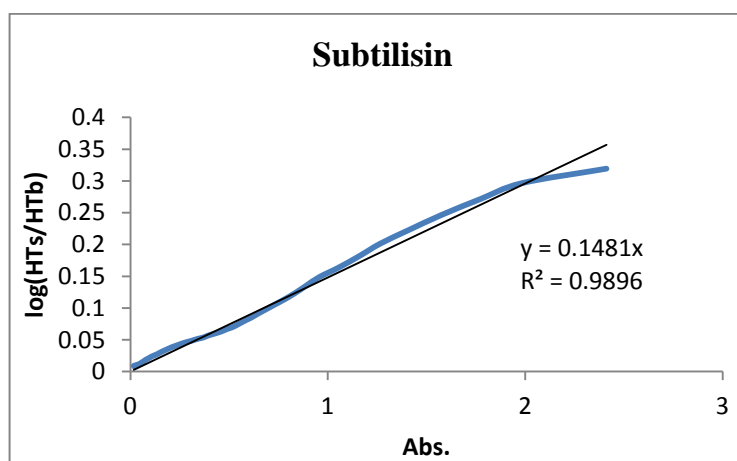
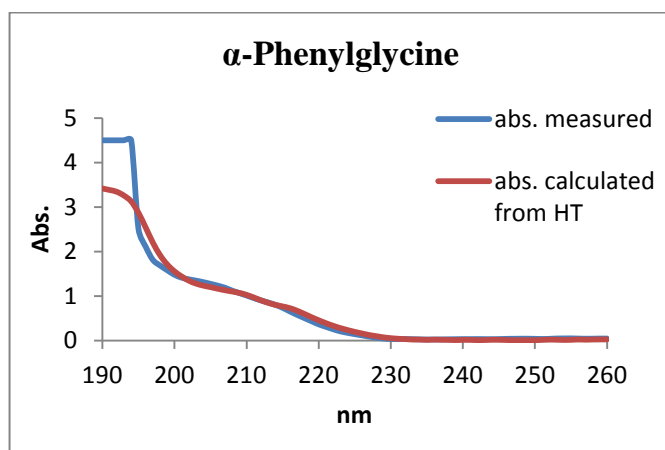


Fig.2. Conversion plots of HT values from CD spectrometer to Absorbance for: A) α -phenylglycine; B) α -chymotrypsin; C) Subtilisin.

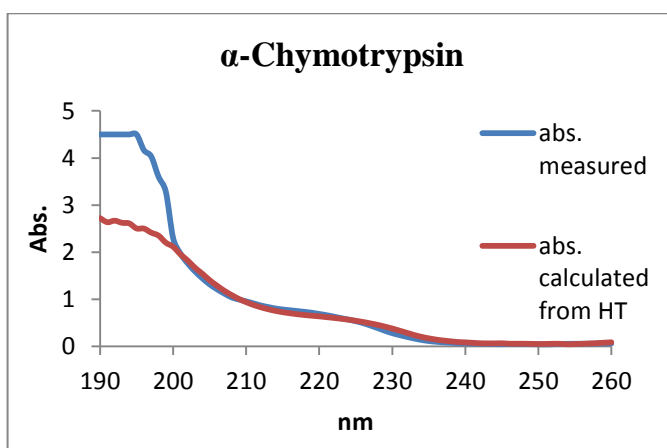
For each sample using values of Z from corresponding plot Absorbance can be calculated using equation (1) and compared to the one measured on the spectrophotometer (Fig.3). For each sample there is a good agreement between measured and calculated absorbance from 200nm to 260nm. Below 200nm spectra do not agree, because spectrophotometer used in these experiments is not purged with nitrogen, thus there is significant oxygen absorption below 200nm (which is not the case for the nitrogen purged CD spectrometer).

Thereby all further calculations of apparent absorbance of suspensions will start from 200nm, using the average value of Z equals to 6.91.

A



B



C

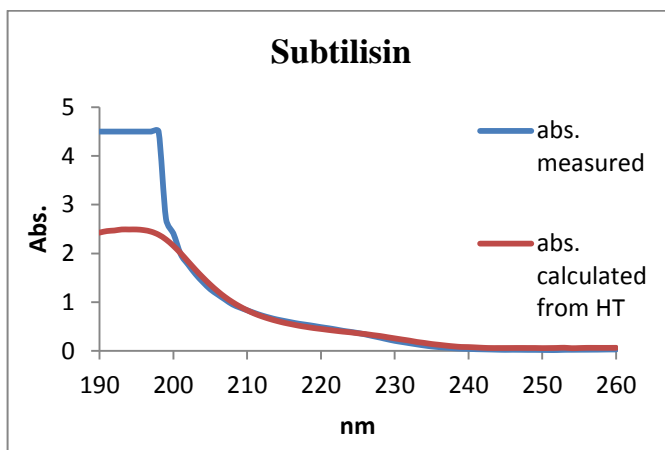


Fig.3. Comparison of Absorbance measured on spectrophotometer (blue line) and Absorbance calculated from HT values of CD spectrometer (red line) for: A) α -phenylglycine; B) α -chymotrypsin; C) subtilisin.

Correction of CD spectra

For each AA sample, knowing the instrument's constant, absorbance for every point of HT spectrum was calculated using equation (1). From the absorbance (A_{SUS}), the absorption flattening correction factor (Q_{CD}) was calculated for each point in the spectrum, using the previously obtained polynomial relationship between the two (Fig.). Finally, corrected CD spectrum was obtained by dividing raw CD data of the test suspension by Q_{CD} and subtracting CD spectrum of the blank. The alternative approach of data treatment where the absorbance of a corresponding suspension of water-filled Sephadex particles is subtracted from absorbance of the sample (A_{SUS}) before estimating Q_{CD} did not show any significant difference for calculations and shape of the spectra.

Comparison of true CD spectra with the corrected ones

In order to compare corrected CD spectra to the true one, it is essential to know concentration of Ascorbic acid in the cell during the CD measurements of suspensions. Amount of AA present in the measured samples was determined exactly the same way as in the previous work ⁵ (with the only difference of re-dispersing particles in 3 ml of the original buffer instead of in 2 ml of water), where it was described in details, therefore will not be discussed here. Hence, average concentration of Ascorbic acid in the sample with 0.28 volume fraction of particles was calculated to be $7.13 \cdot 10^{-3}$ M, and in the sample with 0.23 particles volume fraction – $5.6 \cdot 10^{-3}$ M.

CD spectra were measured for 2 control samples with $2.7 \cdot 10^{-3}$ M and $1.9 \cdot 10^{-3}$ M concentrations of ascorbic acid in buffer. The intensities of the spectra showed to be proportional to concentration. Therefore, they were scaled up to give the expected spectra of the samples with the same concentration of ascorbic acid as in suspension samples ($7.13 \cdot 10^{-3}$ M and $5.6 \cdot 10^{-3}$ M). These spectra were then compared with the corrected for absorption flattening ones of the suspensions.

RESULTS AND DISCUSSIONS

In previous work with λ -tris(ethylenediamine)cobalt (III) complex ⁵ it has been shown that in the visible light region absorption flattening correction can be correctly estimated by the appropriate theoretical model ⁶. It is based on creating a system in which the CD chromophores are dispersed at known concentration in particles with specific size distribution and volume fraction. The aim of this work is to see whether the same correction method can be applied to CD spectra obtained in UV light region. For this reason, suspensions of Sephadex beads, in 1-butanol, filled with various chromophore solutions that give CD signal in UV region (10-camphorsulfonic acid ⁹, hydroxyl-L-proline ¹⁰, phenylglycine ¹¹, ascorbic acid ^{12, 13}) were studied.

Experiments on estimation of photomultiplier constant Z showed that reliable values of absorbance can only be calculated from HT data at wavelengths higher than 200nm. It is hard to say which reading is wrong below 200nm: the one from the spectrophotometer or the one calculated from the HT spectra. Therefore all measurements and calculations in this work are done starting from 200nm and upwards.

10-Camphorsulfonic acid sample:

10-Camphorsulfonic acid is a common compound used for calibration of CD spectropolarimeters, therefore its spectra is very well studied ⁹. Fig.4 shows CD and HT measurements of suspension sample containing 10-camphorsulfonic acid aqueous solution (CSA). They are compared to the spectra of 0.02M CSA aqueous solution saturated with 1-butanol. Because in the suspension samples the water inside the Sephadex particles is likely to be saturated with 1-butanol, for better comparison, aqueous solutions of CSA were also saturated with 1-butanol. Note that concentration of CSA solution is not the same as inside the Sparticles of suspension sample, therefore this figure only shows similarity in the shape between solution and suspension, but does not compare their intensity. Spectra of Sephadex beads filled

with aqueous solution and dispersed in 1-butanol were also recorded to get the base line. To see if there is any leakage of CSA from the beads into the organic media spectra of supernatant from the suspension sample was also measured.

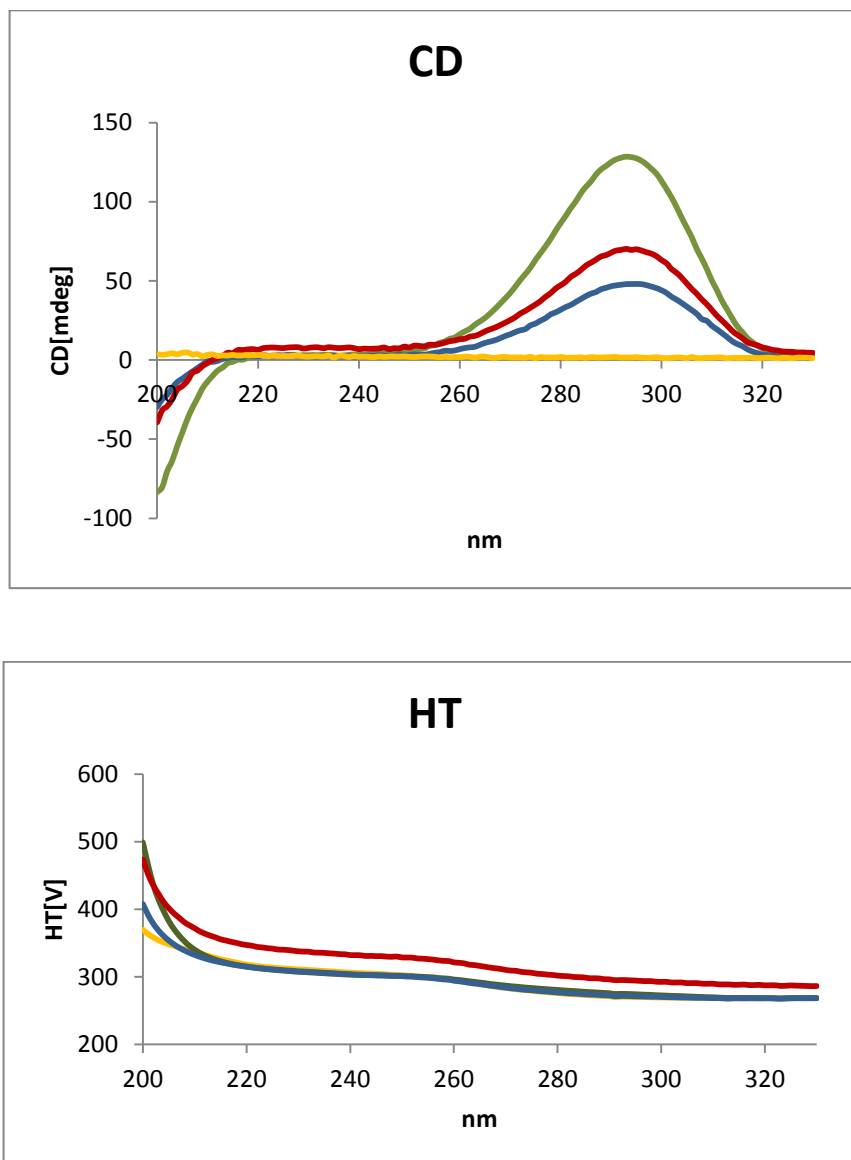


Fig.4. CD and HT spectra of: 1) 0.02M 10-camphorsulfonic acid solution in water saturated with 1-butanol (green line); 2) suspension sample containing 10-camphorsulfonic acid solution (red line); 3) supernatant from the suspension sample (blue line); 4) Sephadex beads filled with water and dispersed in 1-butanol (yellow line).

Fig.4 shows that unfortunately CSA sample is not suited for checking the adequacy of the suggested absorption flattening correction model for two reasons:

- 1) One of the requirements of the absorption flattening correction model is determination of absorbance of the suspension sample from the HT spectrum. On the Fig.4 HT spectrum of the CSA suspension sample is very similar to the HT spectrum of the blank (Sephadex beads filled with water and dispersed in 1-butanol), except for the scattering. Concentration of CSA is not enough for absorption peaks to appear. Calculations show that CSA concentration has to be at least 15 times higher compared to the used one in order to distinguish any peak at all. But if one will use such concentrated sample then readings for the CD spectrum will be too high, as the instrument's cut off is at 200mdeg. Sample with current CSA concentration has CD maximum at around 60mdeg. Therefore sample with 15 times higher chromophore concentration will be way beyond the cut off line (height of samples CD peaks is more or less linear proportional to its concentration).
- 2) CD spectrum of samples supernatant shows that there is a significant leakage of CSA from the Sephadex beads into the organic media.

Hence, CSA is not suitable for checking proposed absorption flattening correction model.

Trans-4-hydroxy-L-proline:

For the next experiment CSA was replaced with trans-4-hydroxy-L-proline (HYP) dissolved in 0.02M sodium phosphate buffer pH11. pH11 was chosen to help HYP to stay inside the Sephadex particles and not to leak out. Indeed, CD measurements of the same sample dissolved in buffer pH7.8 showed presence of small amount of HYP in supernatant. When CD spectrum of supernatant of the sample with pH11 (Fig.5) shows that there is no HYP in it, hence there is no leakage from particles into the organic media.

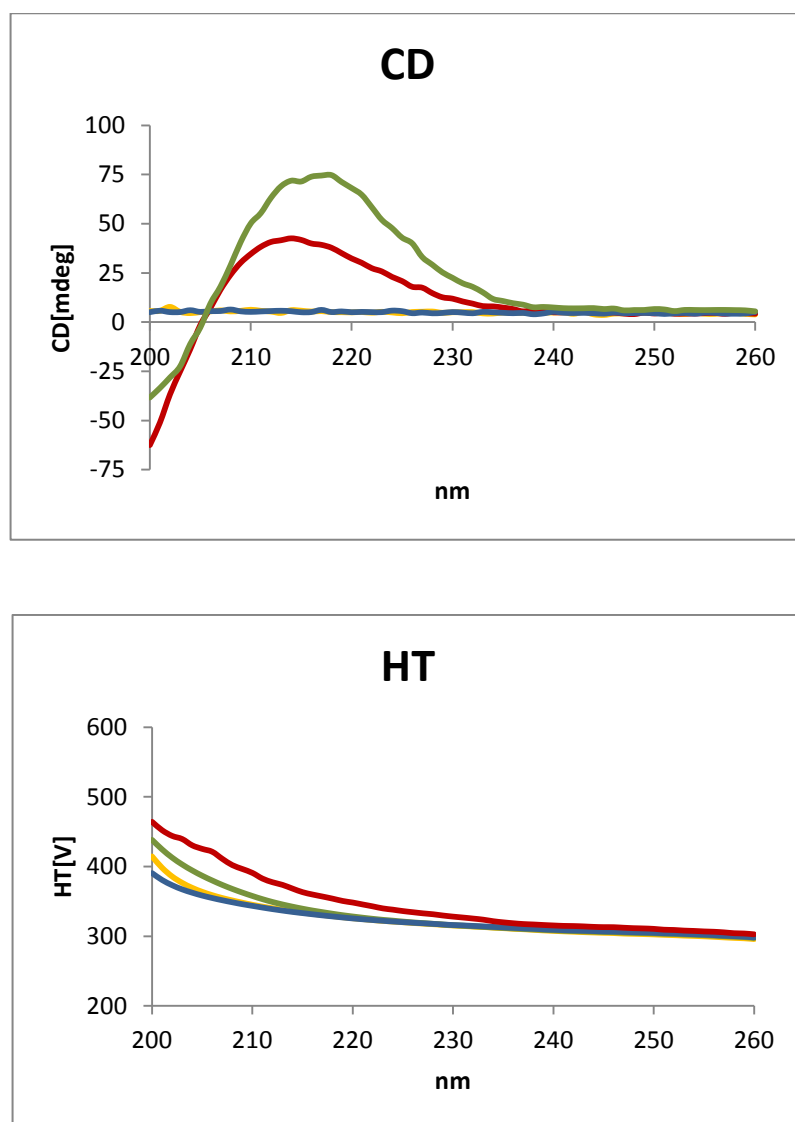


Fig.5. CD and HT spectra of: 1) 0.04M HYP solution in water saturated with 1-butanol (green line); 2) suspension sample containing HYP solution (red line); 3) supernatant from the suspension sample (blue line); 4) Sephadex beads filled with water and dispersed in 1-butanol (yellow line).

Fig.5 shows CD and HT spectra of suspension sample of Sephadex particles filled with HYP solution (suspended in 1-butanol). They are compared to HYP aqueous solution spectra (saturated with 1-butanol), spectra of supernatant from the suspension sample and spectra of Sephadex particles filled just with water (no HYP) and dispersed in 1-butanol (blank).

HT spectra of HYP suspension sample slightly differs from the blank spectra below 235nm (where the CD peak is observed). Correction model for this sample predicted very small corrections, which doesn't agree with the spectra obtained if the same amount of chromophore was uniformly distributed in the cell (called control spectrum) (Fig.6).

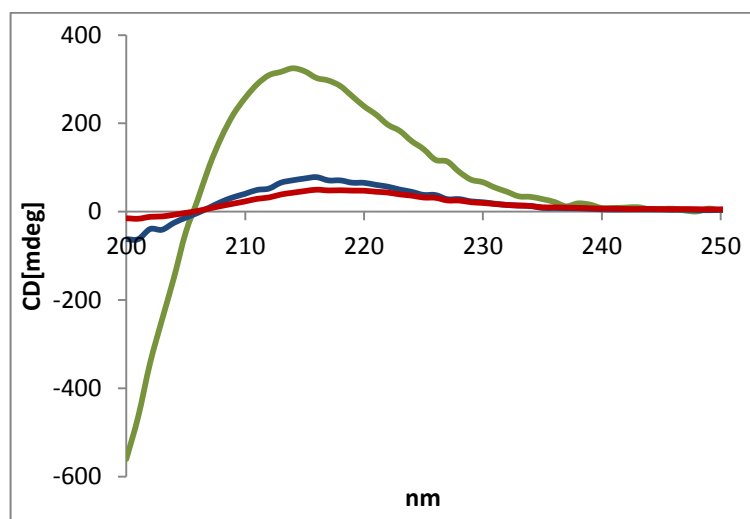


Fig.6. Comparison of original CD spectrum of HYP suspension sample (red line) with corrected spectrum (blue line) and scaled control spectrum (green line).

Therefore for this sample proposed theoretical model doesn't work.

D-(-)-Phenylglycine:

When preparing suspension sample maximum possible concentration of Phenylglycine in water was used (solubility in water: 0.3g/100mL¹⁴). Despite this CD and HT spectra of the sample didn't show any distinguishable peaks. Fig.7 shows their comparison to the spectra of 4*10⁻³M D-Phenylglycine solution in water saturated with 1-butanol. Spectra of Sephadex beads filled with aqueous solution and dispersed in 1-butanol were also recorded to get the base line:

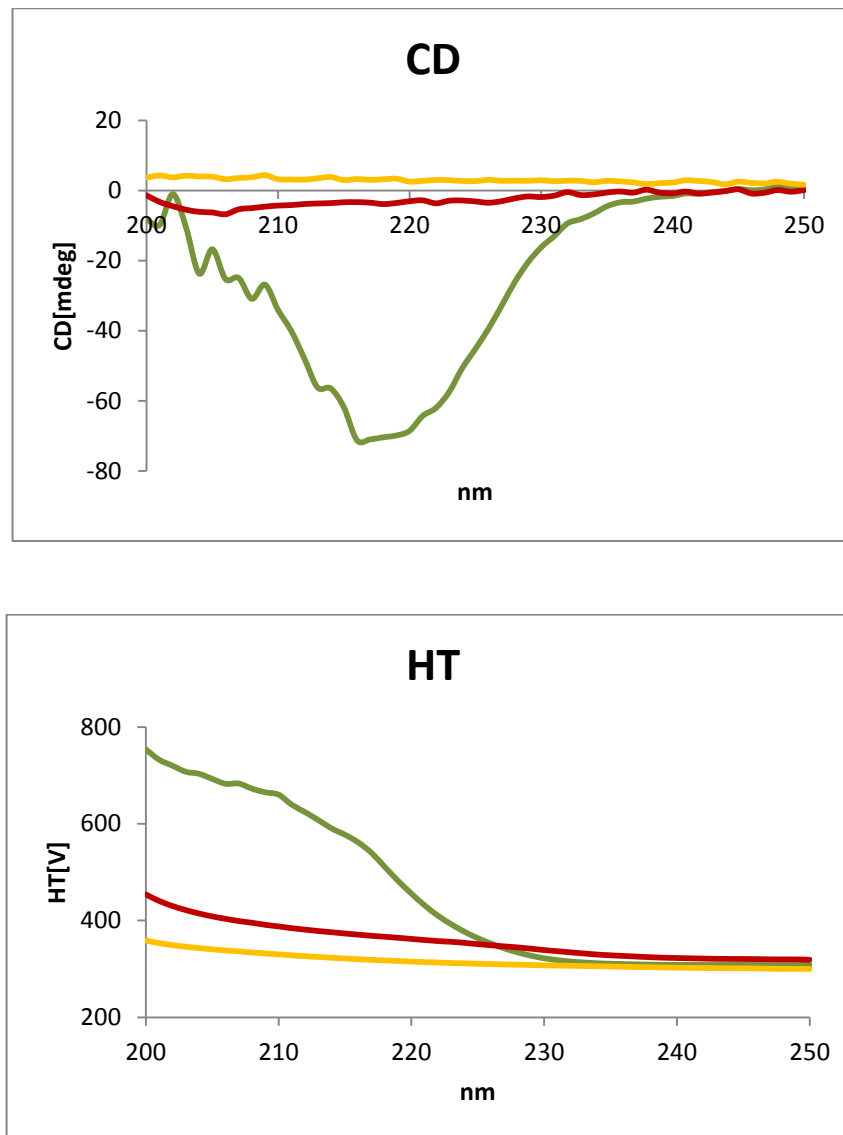


Fig.7. CD and HT spectra of: 1) $4 \cdot 10^{-3}$ M D-Phenylglycine solution in water saturated with 1-butanol (green line); 2) suspension sample containing D-Phenylglycine solution (red line); 3) Sephadex beads filled with water and dispersed in 1-butanol (yellow line).

HT spectrum of D-Phenylglycine solution has a visible peak below 230 nm. But because concentration of D-Phenylglycine in suspension sample cannot be raised any higher this compound is not suitable for testing the correction model.

L-Ascorbic acid:

Ascorbic acid (AA) is easily oxidized to dehydroascorbic acid. The higher the pH the faster is oxidation reaction and loss of AA. For this reason samples here were prepared at pH2.0. At acidic pH, when AA is undissociated, absorption maximum is at 244-245nm; at pH higher than 5.0 maximum is at 265nm; and fully dissociated AA has absorption maximum at 300nm¹⁵. All the measurements of the suspension and solution samples were taken straight after their preparation to minimize oxidation with time.

AA is a very polar compound, it prefers to stay in water solution rather than dissolve in butanol. Therefore, there is no leakage of the AA from the Sephadex particles.

Unlike previous samples, HT spectrum of the AA suspension sample shown on Fig.8 has a clear peak with maximum around 250nm. Hence AA is a suitable compound to test the absorption flattening correction model.

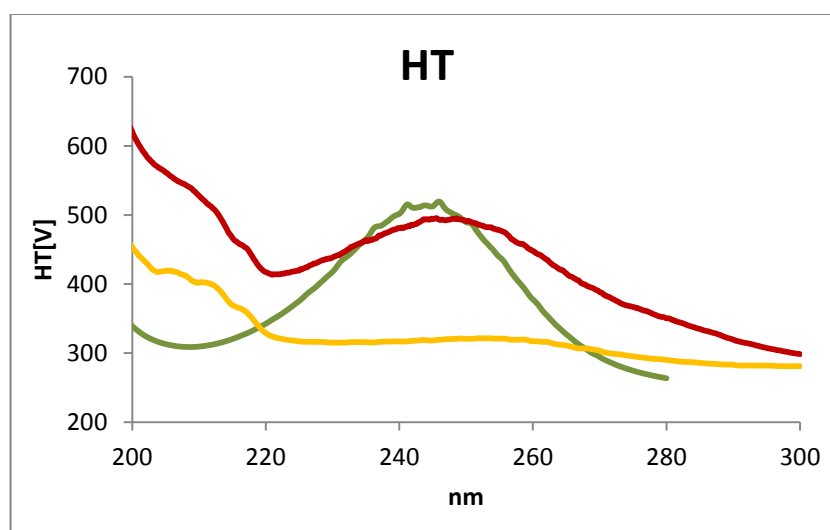


Fig.8. HT spectra of: 1) 1.9×10^{-3} M L-ascorbic acid solution in water saturated with 1-butanol (green line); 2) suspension sample containing L-ascorbic acid solution (red line); 3) Sephadex beads filled with water and dispersed in 1-butanol (yellow line).

. Samples with two different volume fractions of particles within the measuring cell were prepared and CD and HT spectra measured. Correction model requires determination of: a) the particle size and size distribution; b) the volume fraction of particles; and c) the absorbance of the suspension. Once all these parameters for each sample were obtained, corrected CD spectra were calculated (Fig.9). The original CD spectrum for both samples is a little bit noisy and the peak maximum (expected at around 245nm) is quite flat. But changing the concentration of the AA solution inside the particles and raising the volume fraction of Sephadex particles inside the sample only led to a very high HT (higher than 600 V), making the CD data even noisier and not reliable ¹.

To test if corrected spectra is accurate, it is necessary to recover the spectrum expected if the same amount of chromophore was distributed uniformly throughout the cell. Therefore, amount of AA presented inside Sephadex beads during CD measurements had to be determined. This was done by recovering particles after the CD measurements and resuspending them in known amount of buffer. AA comes out from the particles into the buffer and uniformly distributes throughout the entire volume, making possible to determine its concentration spectrophotometrically. Now the control AA solution spectrum can be scaled up to get the expected spectrum if the same amount of chromophore was distributed uniformly throughout the cell.

Fig.9 shows the comparison between the corrected for absorption flattening CD spectra and the scaled control spectra (spectra expected if the same amount of chromophore was distributed uniformly throughout the cell). Original CD spectra of two samples are also depicted. It can be seen that there is quite a significant correction for absorption flattening. In each sample the maximum peak of the original spectrum is more than 3 times flatter than the maximum peak of the control spectrum.

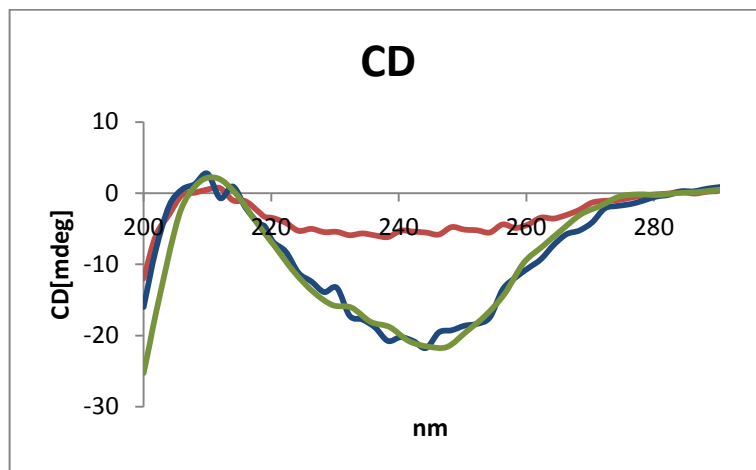
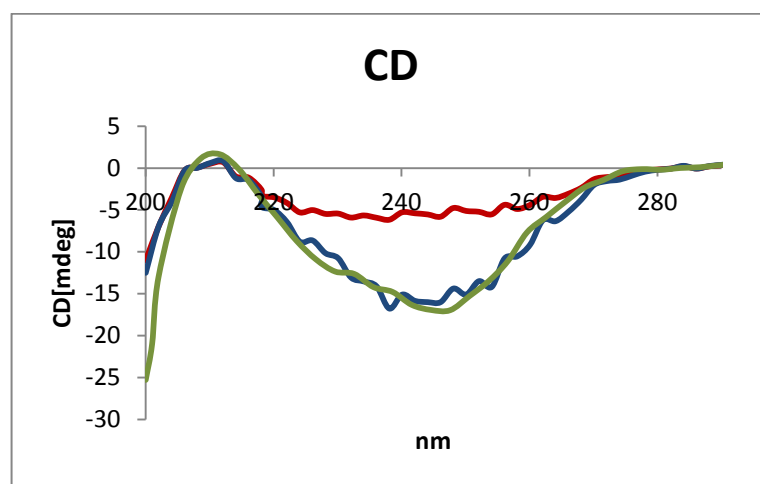
A**B**

Fig.9. Comparison of original CD spectrum (red line) with corrected spectrum (blue line) and scaled control spectrum (green line) for two samples: **A** – sample with 0.28 volume fraction of particles and concentration of AA inside the particles $7.3 \cdot 10^{-3} \text{M}$; **B** - sample with 0.23 volume fraction of particles and concentration of AA inside the particles $5.6 \cdot 10^{-3} \text{M}$.

Fig.9 shows that despite the corrected spectra being slightly noisy the agreement between it and the expected CD spectra is very good for both samples. All bandshapes are very similar, with the peak maximum at around 245nm agreeing almost perfectly within the noise. There is a slight disagreement below 210nm which

could be a result of spectropolarimeter getting less sensitive at such low wavelengths and HT of suspension sample getting high (around 600nm). Therefore accuracy of the CD spectrum at this wavelength is not trustable.

Overall comparison of corrected CD spectrum and the expected one if the same amount of chromophore was distributed uniformly throughout the entire volume shows that suggested model for absorption flattening correction does give reasonable data at the UV-light region.

CONCLUSIONS

The experiments and measurements using L-Ascorbic acid as a chromophore show that it is possible to get a reliable correction for absorption flattening of CD spectra using proposed theoretical model at UV-light region.

REFERENCES

1. Kelly S.M., Jess T.J., Price N.C. How to study proteins by circular dichroism. *Biochim. Biophys. Acta* 2005;1751:119-139.
2. Kuroda R., Berova N., Nakanishi K., Woody R.W., editors. Solid-state CD: application to inorganic and organic chemistry. *Circular dichroism: Principles and applications*, New York:Wiley;2000:159–184.
3. Castiglioni E., Lebon F., Longhi G., Gangemi R., Abbate S. An operative approach to correct CD spectra distortions due to absorption flattening. *Chirality* 2008;20:1047–1052.
4. Ganesan A., Price N.C., Kelly S.M., Petry I., Moore B.D., Halling P.J. Circular dichroism studies of subtilisin Carlsberg immobilised on micron sized silica particles. *Biochim. Biophys. Acta* 2006;1764:1119-1125.
5. Gerdova A., Kelly S.M., Halling P.J. Experimental test of absorption flattening correction for circular dichroism of particle suspensions. *Chirality* 2011;23(7):574-579.
6. Halling P.J. Estimation of flattening coefficient for absorption and circular dichroism using simulation. *Anal. Biochem.* 2009;387:76-81.
7. Arvinte T., Bui T.T.T., Dahab A.A., Demeule B., Drake A.F., Elhag D., King P. The multi-mode polarization modulation spectrometer: part1: simultaneous detection of absorption, turbidity, and optical activity. *Anal. Biochem.* 2004;33:46-57.
8. Dahab A.A., El-Hag D., Drake A.F. Simultaneous determination of photometric accuracy during circular dichroism measurements. *Anal. Methods* 2010;2:929-935.
9. Chen G.C., Yang J.T. Two-point calibration of circular dichrometer with d-10-camphorsulfonic acid. *Anal. Letters* 1977;10(14):1195-1207.

10. Brahmachari S.K., Bansal M., Ananthanarayanan V.S., Sasisekharan V. Structural investigations on poly(4-hydroxy-L-proline).2. Physicochemical studies. *Macromolecules* 1979;12(1):23-28.
11. Takagi S., Nomori H., Hatano M. Circular Dichroism of D-phenylglycine. *Chem. Letters* 1974;611-616.
12. Purdie N., Swallows K.A. Direct determination of water-soluble vitamins by circular dichroism. *J. Agric. Food Chem.* 1991;39(12):2171-2175.
13. Wittine K., Gazivoda T., Markus M., Mrvos-Sermek D., Hergold-Brundic A., Cetina M., Zihir D., Gabelica V., Mintas M., Raic-Malic S. Crystal structures, circular dichroism spectra and absolute configurations of some L-ascorbic derivatives. *J. Mol. Struct.* 2004;687:101-106.
14. Web site <http://www.chemicaland21.com/lifescience/phar/D-alpha-PHENYLGLYCINE.htm>
15. Eitenmiller R.R., Ye L., Landen W.O., Jr., editors. *Vitamin analysis for the health and food sciences.* CRC press, Taylor & Francis Group 2008;231-290.

CHAPTER III

Absorption flattening correction of CD spectra of particles containing protein.

INTRODUCTION

Circular Dichroism (CD) is a valuable technique that gives information on the structure of protein. CD of protein solutions as well as protein-containing nanoparticles^{1,2} and membrane proteins^{3,4,5} has been well studied. There is a considerable interest in samples with larger protein-containing particles (many micrometers in size), such as: immobilized enzymes, biopharmaceutical formulations, enzymes used for storage, etc. One major artefact that appears in CD measurements on such particles is absorption flattening. Therefore it is important to find a way to correct it to get true CD spectra of suspensions.

In previous works two models were tested: one with Co complex⁶ and second with ascorbic acid; both compounds were dispersed in Sephadex particles and suspended in chromophore free solution. These models showed that by using appropriate simulation programme⁷ CD spectra can be accurately corrected for absorption flattening.

The aim of this work is to see if the same correction method can be applied to particles containing proteins. For the experiment subtilisin Carlsberg and α -chymotrypsin - proteins from the serine protease group were chosen. They are very common enzymes with well studied CD spectra^{8,9,10}. To test whether corrections are accurate the final spectra were compared to the spectra obtained if the same amount of chromophore was uniformly dispersed throughout the entire cell volume, so called control spectrum. Unfortunately, after all measurements and corrections the above comparison showed a significant disagreement in intensity between corrected CD spectra and control ones. Therefore demonstrating that in the case of protein-containing particle suspensions absorption flattening can't be accurately corrected by the proposed simulation method.

MATERIALS AND METHODS

Subtilisin Carlsberg (protease from *Bacillus licheniformis*), Type VIII, lyophilized powder, 7-15 units/mg solid (Cat. No. P5380); α -Chymotrypsin from bovine pancreas, Type II, lyophilized powder, ≥ 40 units/mg protein (Cat.No. C4129); Sephadex G-75 (Cat. No G75120); 1-butanol, ACS reagent, $\geq 99.4\%$ (Cat. No 360465) were purchased from Sigma-Aldrich, GmbH.

Sample preparation

4mg, 10mg and 14mg of Subtilisin Carlsberg were dissolved in 3mL of 20mM sodium phosphate buffer, pH 7.8. Also a solution with 15mg of α -chymotrypsin dissolved in 3mL of 20mM sodium phosphate buffer, pH 7.8, was prepared. To these solutions Sephadex G-75 was added and left to swell for several minutes at room temperature. Obtained suspensions were then centrifuged at 704 x g for 3 minutes. Supernatants were removed and pellets re-suspended in 1-butanol.

Circular Dichroism measurements

Circular Dichroism measurements were carried out in Jasco J-810 spectropolarimeter, operating at 20°C. Samples were introduced into cylindrical quartz cell with 1mm pathlength (Hellma UK Ltd.), fixed in rotating at 60 rpm cell holder. For each protein concentration samples with various particle volume fractions were measured. CD and high-tension voltage (HT) spectra were obtained at a scan rate of 20 nm min⁻¹, a time constant of 0.5 s, and a bandwidth of 0.2nm. Spectra of 1-butanol saturated with sodium phosphate buffer, and spectra of Sephadex particles filled with buffer and dispersed in 1-butanol were also recorded using the same conditions.

Estimation of absorption flattening correction factor

To estimate the absorption flattening correction factor (Q_{CD}) using proposed simulation method ⁷, for each sample number of parameters had to be calculated: volume of particles within the cell, mean particle size and its fractional deviation, apparent absorbance of suspension. This was done exactly the same way as in previous chapters, using the same instruments constant $Z = 6.91$, therefore it will not be described here.

Volume fraction of the sample with the original loading of subtilisin of 4mg was calculated to be 0.20; with 10mg – 0.24; with 14mg – 0.21; with 15mg of α -chymotrypsin – 0.22. Mean particle size was measured to be 78.18 μ m. Fractional standard deviation 0.24.

Correction of CD spectrum and its comparison to the true one

Corrected CD spectrum of each sample was obtained by dividing each point from the raw CD data by the corresponding correction factor Q_{CD} and then subtracting blank CD spectrum.

In order to compare corrected CD spectrum to the true one concentration of protein inside the cell during measurements of suspension have to be calculated. This was obtained the same way as in previous chapter, therefore will not be described here. Average concentration of the protein in the sample with the original 4mg loading of subtilisin was calculated to be $3.18 \cdot 10^{-5} \text{M}$, with the original 10mg loading – $6.1 \cdot 10^{-5} \text{M}$; with 14mg – $9.84 \cdot 10^{-5} \text{M}$; with 15mg of α -chymotrypsin – $10.21 \cdot 10^{-5} \text{M}$.

A CD spectrum was measured for $1.29 \cdot 10^{-5} \text{M}$ subtilisin solution and $1.32 \cdot 10^{-5} \text{M}$ α -chymotrypsin solution in 20mM sodium phosphate buffer, pH 7.8. These control spectra were scaled up to give expected spectra of solutions having the same average concentration of protein in the cell as in suspensions. These spectra were compared with the corrected spectra of suspensions.

RESULTS AND DISCUSSIONS

Previous work on CD measurements of particle suspensions containing various chromophore solutions showed that in some cases it is possible to correct CD spectrum for the absorption flattening effect⁶. The main challenge is to see whether the same correction method can be applied to CD spectra of particle suspensions containing proteins.

CD measurements of subtilisin Carlsberg suspensions

Three samples with various amount of subtilisin within the Sephadex particles were prepared same way as in previous work with particles containing other compounds. Samples were then loaded into the cylindrical cell, having visibly the similar volume fraction of particles within each other (calculated afterwards to be 0.20, 0.24 and 0.21). CD spectra were then recorded on the Jasco J-810

spectropolarimeter and compared to the CD spectra of subtilisin solution in buffer. Fig.1 shows this comparison between solution and suspension samples.

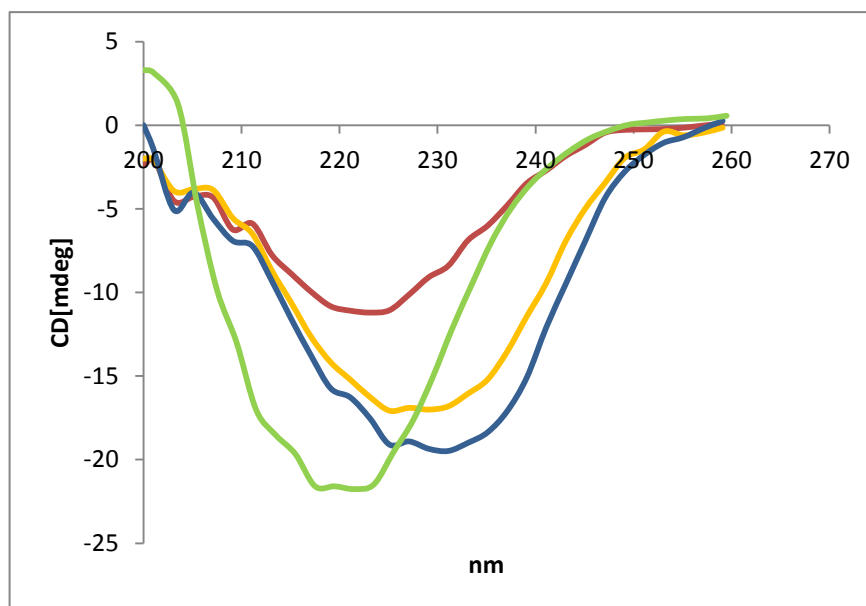


Fig.1. CD spectra of three subtilisin Carlsberg suspension samples with similar volume fractions of Sephadex particles (between 0.20 and 0.24) and various amounts of protein inside them: $3.18 \times 10^{-5} \text{ M}$ (red line), $6.1 \times 10^{-5} \text{ M}$ (yellow line), and $9.84 \times 10^{-5} \text{ M}$ (blue line). Compared with the CD spectrum of subtilisin solution in buffer (green line).

CD measurements show that the suspension sample with the $3.18 \times 10^{-5} \text{ M}$ average concentration of protein in the cell has its maximum at around 223 nm, sample with $6.1 \times 10^{-5} \text{ M}$ of protein at around 229 nm, and sample with $9.84 \times 10^{-5} \text{ M}$ at around 231 nm. The solution sample spectrum has its maximum peak at around 221 nm. So not only maximum of the suspension samples spectra are shifted from the maximum of the solution spectra but also they are shifted between each other. The higher the concentration of protein inside the particles the more its maximum peak is shifted into the longer wavelength region (red-shift).

In general, non-polar solvents have been observed to shift CD spectra of proteins in longer wavelength area when compared to their positions in aqueous solutions ^{11, 12}. Chen et. al.¹¹ showed that the red-shift occurs with the increase of refractive index and decrease of dielectric constant of the surrounding solvent. But in this work protein inside the particles and in solution are in the same environment (surrounded by the same solvent: water saturated with 1-butanol). But we still observe significant shift and even between suspension samples.

To get better understanding of the reasons behind this shift two samples with different volume fraction of Sephadex particles and same concentration of protein within them were measured (Fig.2). For better visual comparison between them, CD spectrum of sample with lower volume fraction of particles was scaled up (dashed blue line).

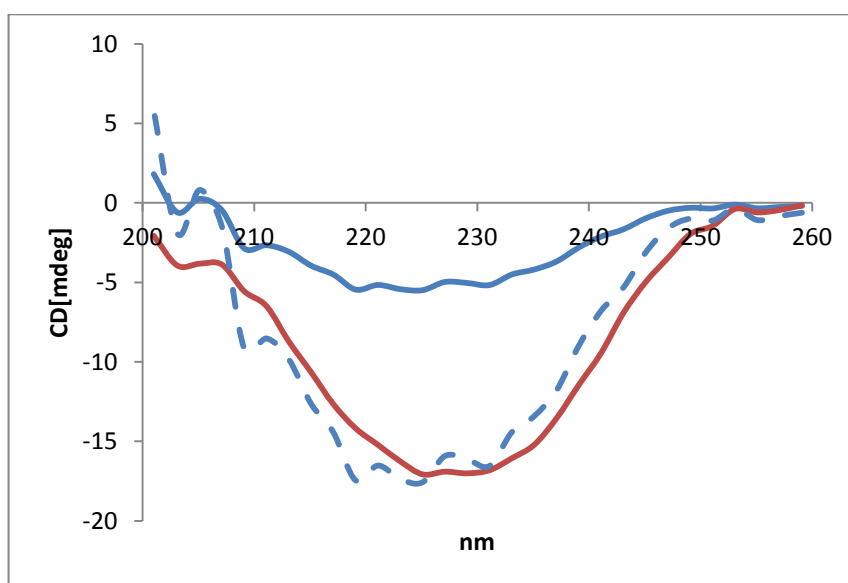


Fig. 2. CD spectra of samples with different volume fraction of Sephadex particles and same concentration of protein within them: blue line – lower volume fraction; red line – high volume fraction. Dashed blue line – scaled up CD spectrum of the sample with lower volume fraction of particles.

In this case there is still a slight red-shift of the peak maximum (around 2-3nm between each other), but not as significant as in previous samples with different concentrations of protein and similar volume fractions of particles. It looks like that concentration of protein plays a significant role in this shift, but is not the only reason.

There is no certain explanation to why this shift is observed. Number of reasons below, described later in the chapter, could influence it:

- Interaction between protein molecules (with high concentration clusters can be formed) – could be the main reason for shifts between maximum of suspension samples with different concentration of subtilisin within particles;
- Interaction with butanol results in change of subtilisin's structure;
- Absorption flattening ¹³;
- Differential scattering;
- Artefacts of the optics.

Correction of CD spectra for absorption flattening

The aim of the work is to see whether simulation method successfully used previously on suspension particles containing Ascorbic acid solutions and tris(ethylenediamine)cobalt II chloride solutions can be applied to particles containing proteins.

Proposed simulation programme ⁷ for absorption flattening correction has 3 inputs that have to be calculated for each suspension sample: volume fraction of the particles inside the cell, mean particle size and its fractional deviation. Result of these simulations is the relationship between apparent absorbance A_{SUS} and correction factor Q_{CD} . By using this relationship and calculating A_{SUS} from the HT spectra of CD measurements ⁶, one can obtain Q_{CD} for each point of the spectrum. By dividing each point from the CD spectrum by the appropriate correction factor and then subtracting blank a true spectrum can be obtained and compared to the

control solution spectrum – spectrum in which the same amount of chromophore was dispersed uniformly throughout the sample.

Once all the parameters were calculated a comparison graphs between corrected CD spectra and control solution spectra were plotted for each sample. Fig.3 shows the results of corrections for the suspension sample with $6.1 \times 10^{-5} \text{M}$ concentration of subtilisin within particles.

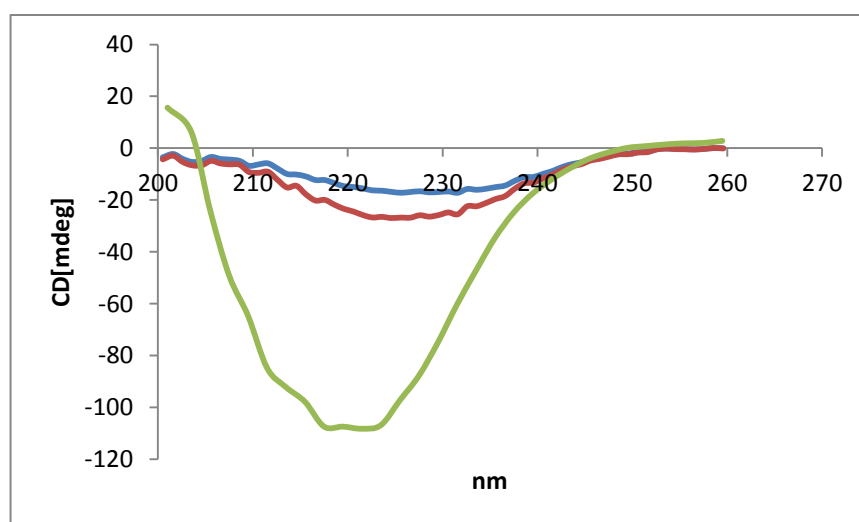


Fig.3. Comparison of corrected CD spectrum of suspension sample (red line) with spectrum of original suspension (blue line); and with control solution spectrum (green line). For the sample with $6.1 \times 10^{-5} \text{M}$ concentration of subtilisin in particles and in control solution.

Fig.3 shows that the suspension sample spectrum is much less intense than the control solution spectrum with the same amount of chromophore uniformly dispersed within it. This might be the result of the absorption flattening. Although proposed method changed original CD spectra by making it more intense by 50% and moving the peak maximum by couple nm into lower wavelength area, these corrections are still not enough comparing to the control solution spectrum with the same concentration of subtilisin. Correcting spectra of two other suspension samples with

different concentrations of subtilisin gave the same result of peaks being not as intense as they should be. It is clear that the correction model doesn't work properly in this case.

If presume that original inputs for the simulation programme were determined with an error, changing them manually until corrected and control spectra somewhat agree is the way to see whether the proposed method works at all for particles with protein. For the same sample with $6.1 \cdot 10^{-5} \text{M}$ concentration of subtilisin in Sephadex particles original input parameters were: volume fraction – 0.24; mean particle size - $78.18 \mu\text{m}$; fractional standard deviation – 0.24. An agreement between intensity of the spectra of corrected suspension sample and control solution sample was reached by:

- 1) Changing volume fraction to 0.1186 (twice smaller than calculated one) and leaving other parameters the same. Such a small volume fraction is not very realistic, because even visually particles in the cell take much more space than 10% of the cell.
- 2) Increasing mean particle size to $167.79 \mu\text{m}$ (about twice bigger than the calculated one using microscope). Such a big particle size means that particles are not individually dispersed in suspension but aggregate into clusters. This can look like a possible case, because during the measurements of suspensions the light can go through two particles that are stuck together and these small clusters are impossible to identify by eye. The repeat experiments show same results, meaning that whether particles are always combined into small clusters ($167.79 \mu\text{m}$ in diameter), or the model itself doesn't work. In previously studied cases with other chromophores inside Sephadex particles calculations showed that the mean particle size corresponding to single particle was the right input parameter into simulation programme. (Note, that particle size here is quoted very accurately, this is due to the correction model being very sensitive to the exact input values. This will be discussed in details later in the chapter.)
- 3) Decreasing volume fraction to 0.18 - more realistic then 0.1186, closer to the calculated 0.24; and increasing particle size to $121 \mu\text{m}$ - presumably the biggest particles were in the centre of the cell. Visual observation of the rotating

suspension sample show that the particles are distributed uniformly throughout the cell: big particles are observed both in the centre and away from it. Also the repeat experiments show same results each time, meaning that particles are uniformed. Thus these input parameters don't look very realistic either.

Fig.4 shows the comparison between the corrected CD spectrum with the new input parameters for the correction programme and control solution spectrum. (Note, corrected spectra for each set of different input parameters tested were all the same, therefore there is only one plot on Fig.4. This is because input parameters were chosen to make this happen). Shapes of two spectra agree well between 260nm and 220nm with the peak maximum at 221nm, but below 220nm suspension sample spectrum becomes narrower than the solution one. This means that either there is a change in the structure of the protein in the suspension sample or that the correction method does not work properly at that wavelength.

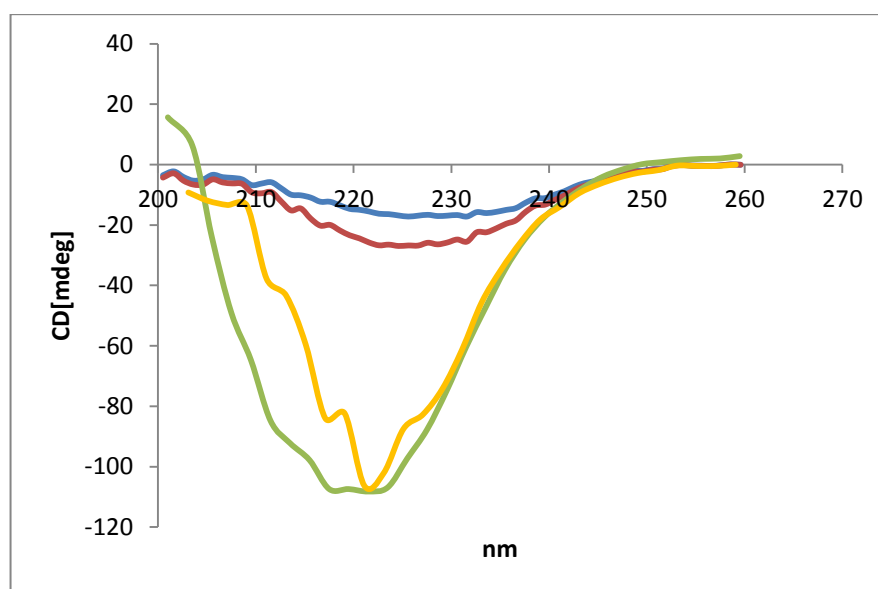


Fig.4. Comparison of the corrected CD spectrum of suspension sample using new input parameters (yellow line) with the control solution (green line). Raw CD spectrum of the suspension (blue line) and corrected CD spectrum with the original input data (red line) are also depicted for the reference. All data is for the sample with $6.1 \times 10^{-5} \text{M}$ concentration of subtilisin in particles and in control solution.

At the graph it is seen that the peak maximum for both corrected (with new input parameters) and control spectra is at 221nm. This means that the original peak shift of 8nm between the raw (uncorrected) CD spectrum and control spectrum was due to the absorption flattening and can be corrected with the right calculations. As discussed above, the required different input parameters are very unlikely to be correct, but just conceivable in the case if the particles are not individually dispersed in suspension but aggregate into clusters.

When changing volume fraction and particle size it was noticed that correction programme is very sensitive to the input data. This is demonstrated in Table 1 by couple examples of changing input parameters and their influence on the peak maximum at 221nm.

Table 1. Example of variation of input parameters for the correction model and its effect on CD data.

Input parameters			Wave-length, nm	Relationship of A_{sus} to Q_{CD}	Corrected CD	Control solution CD
Volume fraction	Mean particle size, μm	Fractional standard deviation				
1) Changing volume fraction						
0.1170	78.18	0.24	221	0.1691	-96.96	-109.729
0.1186 (1.4%)				0.1376 (18.6%)	-121.86 (25.7%)	
2) Changing mean particle size						
0.24	166.67	0.24	221	0.1873	-87.23	-109.729
	167.79 (0.7%)			0.1502 (19.8%)	-111.51 (27.8%)	
3) Changing volume fraction and particle size						
0.185	117.64	0.24	221	0.231	-69.52	-109.729
0.18 (2.7%)	121.21 (2.9%)			0.1566 (32.2)	-105.93 (52.3%)	

Even a slight deviation from each number changes the corrected spectrum significantly. This is shown in the table by numbers in brackets; for example, change in mean particle size by 0.7% changes relationship of A_{sus} to Q_{CD} by 19.8%, leading to a change in the CD signal by 27.8%. But in reality it is impossible to determine volume fraction and particle size with an ideal accuracy, at least with the determination methods used here. Therefore even if the values are correct, they cannot be measured accurately enough to use the flattening correction method.

Measurements on two other samples containing different concentration of subtilisin as well as samples with particle suspensions containing other protein (subtilisin was replaced by α -chymotrypsin) gave exactly the same results.

All above observations lead to a conclusion that the proposed correction method cannot be applied to the particle suspensions containing protein due to several reasons:

- the correction model requires almost an ideal accuracy in determining its input parameters, which cannot be achieved using methods applied here;
- the shape of the suspension sample spectra differs from the one in the solution sample below 220nm, possibly because of protein changing its structure in suspension sample.

CONCLUSIONS

Proposed theoretical model for absorption flattening correction ⁷ previously was successfully applied to particle suspensions containing Ascorbic acid solution and tris(ethylenediamine)cobalt chloride solution ⁶. This work demonstrated that unfortunately it cannot be used to correctly estimate effect of absorption flattening artefact on CD spectra of particles containing protein.

REFERENCES

1. Sreerama N., Woody R.W. On the analysis of membrane protein circular dichroism spectra. *Protein Sci.* 2004;13:100-112.
2. Swords N.A., Wallace B.A. Circular-dichroism analyses of membrane proteins: examination of environmental effects on bacteriorhodopsin spectra. *Biochem. J.* 1993;289:215-219.
3. Govorov A.O., Gun'ko Y.K., Slocik J.M., Gerard V.A., Fan Z., Naik R.R. Chiral nanoparticle assemblies: circular dichroism, plasmonic interactions, and exciton effects. *J. Mater. Chem.* 2011;21:16806-16818.
4. Sarmento B., Ferreira D.C., Jorgensen L., van de Weert M. Probing insulin's secondary structure after entrapment into alginate/chitosan nanoparticles. *Eur. J. Pharm. Biopharm.* 2007;65:10-17.
5. Wangoo N., Raman Suri C., Shekhawat G. Interaction of gold nanoparticles with protein: A spectroscopic study to monitor protein conformational changes. *Appl. Phys. Lett.* 2008;92:133104.
6. Gerdova A., Kelly S.M., Halling P.J. Experimental test of absorption flattening correction for circular dichroism of particle suspensions. *Chirality* 2011;23(7):574-579.
7. Halling P.J. Estimation of flattening coefficient for absorption and circular dichroism using simulation. *Anal. Biochem.* 2009;387:76-81.
8. Ganesan A., Price N.C., Kelly S.M., Petry I., Moore B.D., Halling P.J. Circular dichroism studies of subtilisin Carlsberg immobilised on micron sized silica particles. *Biochim. Biophys. Acta* 2006;1764:1119-1125.
9. Castillo M.P., Sola R.J., Griebenow K. On the role of protein structural dynamics in the catalytic activity and thermostability of serine protease subtilisin Carlsberg. *Biotechnol. Bioeng.* 2009;103(1):77-84.

10. Diego T.D., Lozano P., Gmouh S., Vaultier M., Iborra J.L. Fluorescence and CD spectroscopic analysis of the α -chymotrypsin stabilization by the ionic liquid, 1-Ethyl-3-methylimidazolium Bis[(trifluoromethyl)sulfonyl]amide. *Biotechnol Bioeng* 2004;88: 916–924.
11. Chen Y., Wallace B.A. Secondary solvent effects on the circular dichroism spectra of polypeptides in non-aqueous environments: influence of polarisation effects on the far ultraviolet spectra of alamethicin. *Biophys. Chem.* 1997;65:65-74
12. Wallace B.A., Lees J.G., Orry A.J., Lobley A., Janes R.W. Analyses of circular dichroism spectra of membrane proteins. *Protein Sci.* 2003;12(4):875-884.
13. Castiglioni E., Abbate S., Longhi G., Gangemi R. Wavelength shifts in solid-state circular dichroism spectra: a possible explanation. *Chirality* 2007;19:491-496.

CHAPTER IV

Circular dichroism measurements on individual 100 μm particles containing proteins using synchrotron light beam

Anna Gerdova,¹ Kusum Solanki,² Sharon M Kelly,³ Tamas Javorfi,⁴
Rohanah Hussain,⁴ Giuliano Siligardi,⁴ Gulam Mohmad,² Munishwar N. Gupta,²
Peter J. Halling¹

¹*WestCHEM, Department of Pure & Applied Chemistry, University of Strathclyde, Glasgow G1 1XL, UK*

²*Department of Chemistry, IIT Delhi, Hauz Khas, New Delhi 110016, India*

³*Faculty of Biomedical and Life Sciences, University of Glasgow, Glasgow G12 8QQ*

⁴*B23, Science Division, Diamond Light Source, Harwell Science and Innovation Campus, Chilton, Didcot, OX11 0DE, UK*

INTRODUCTION

There is considerable interest in proteins present in solid particles. These include immobilised enzymes, dried powder forms used for storage, biopharmaceutical formulations, precipitates formed deliberately or during storage of solutions, and of course natural solid structures like cartilage. Our understanding of the structure of proteins in the non-crystalline solid state is limited, because of problems with most of the physical techniques used in solution. Scattering is a serious difficulty for all optical techniques, while molecular scale physics affects methods like NMR. Even keeping particles in suspension can be an experimental problem.

CD gives valuable information about protein structure, and is widely used with solution samples to estimate secondary structure composition (far UV) and detect tertiary structure changes (near UV) ^{1,2}. There has recently been renewed interest in CD studies of proteins in nanoparticles ^{3,4}, particularly membrane fragments ^{5,6}. The use of synchrotron sources is being actively explored for membrane proteins in vesicle preparations, where the high intensities available are useful to overcome scattering ^{7,8}.

Until recently CD measurements had not been reported for suspensions of larger particles in the micrometer range. But we have demonstrated that measurements are possible on particles of 100 micrometres and larger ^{9,10}. This required a rotating sample cell, to keep the particles in suspension, and placement of the cell as close as possible to the detector, to minimise the effects of scattering. Transmitted intensities on a conventional bench-top spectropolarimeter were found to be sufficient to get CD spectra with good signal-to-noise ratios.

Measurements on particle suspensions have a number of limitations however. The spectra obtained are affected by absorption flattening, requiring often substantial corrections ¹¹. And they are necessarily an average over many different particles. An alternative approach for particles in the 100 micrometre size range would be to pass a tiny light beam entirely through a single particle. This would substantially reduce the artefact of absorption flattening, and allow detection of differences between

individual particles. To obtain a measurable signal from such a small beam would require very high intensity, but this is potentially obtainable from a synchrotron source. In this paper we report how it is in fact possible to obtain meaningful spectra from individual particles of around 100 micrometres diameter. This uses just a small fraction of the synchrotron beam, selected by a pinhole, and directed through the particle. Our work shows the difficulties associated with such measurements and challenges which have to be met before a completely satisfactory approach emerges. The systems chosen for this study include enzyme particles obtained by precipitation (and subsequent cross linking) of α -chymotrypsin. The enzyme has been widely used as a model protein in several earlier structural studies¹²⁻¹⁴.

MATERIALS AND METHODS

Alpha-chymotrypsin (protease from Bovine pancreas, Cat. No. C-4129), Ovalbumin (Albumin from chicken egg white, Cat. No A5503) potassium sulfate, ammonium sulphate were purchased from Sigma Chemical (St. Louis, MO, USA). (1S)-(+)-10-camphorsulfonic acid, ammonium salt was ordered from Jasco. *n*-Propanol obtained from Sigma Chemical (St. Louis, MO, USA) was of anhydrous grade and used after drying overnight over molecular sieves. *t*-Butanol was purchased from Merck Pvt. Ltd, Mumbai India.

Methods

Measurements were carried out at Diamond Light Source with B23 synchrotron radiation CD beamline, using end-station Module B, with a ring current of 200mA and slit width 0.5mm (equivalent to 1.2nm bandwidth)¹⁵.

All measurements were made with samples in a 0.2 mm pathlength cylindrical cell. In most cases some of the particles were seen to remain fixed in the middle and

upper parts of the cell, presumably because of contact with the cell faces. It was thus possible to align the sample such that individual particles would be in the beam transmitted by the pinhole. (It is possible that some of these particles were in fact aggregates of smaller particles, but these aggregates must have been already present in the sample suspension.) Detailed description of the cell holder will be given below in “Sample presentation” chapter.

TPP ovalbumin: Three phase partitioning generally consists of mixing appropriate amounts of *t*-butanol and ammonium sulphate to an aqueous solution of protein^{13,16}. After about 1 h, three layers are formed: lower aqueous layer, interfacial protein precipitate and upper *t*-butanol layer. In this case ovalbumin (0.4 mg/ml, pH 7.0) solution was mixed with 10 % (w/v) concentration of ammonium sulphate. The *t*-butanol was added to this solution in 1:1 (v/v) ratio, vortexed, and incubated at 25 °C. After 1 h, the mixture was centrifuged at 2,000g for 10 min for facilitating three phase formation. The upper *t*-butanol layer was pipetted out. Thereafter, the interfacial precipitate (of the ovalbumin) was pierced to collect the lower aqueous layer. The precipitated ovalbumin did not dissolve to a significant extent under several conditions which were tried including 50 mM phosphate buffer (pH 7.0). The amount of ovalbumin precipitated was calculated by measuring the amount in aqueous phase with the starting amount as 100 %. This precipitated amount was about 90 %.

EPRP and CLEA of alpha-chymotrypsin were prepared using standard procedures published in the work by K. Solanki et al.¹⁴

CD measurements of suspension samples were carried out on the conventional spectropolarimeter Jasco J-810. In order to avoid sedimentation of the particles in the cell during measurements, a rotating cell holder was used, applying methods previously described⁹.

RESULTS AND DISCUSSION

Sample presentation

The basic principle was to use a pinhole to select a small portion of the synchrotron beam. The selected beam is then passed through a sample particle and on to the detector (Fig.1).

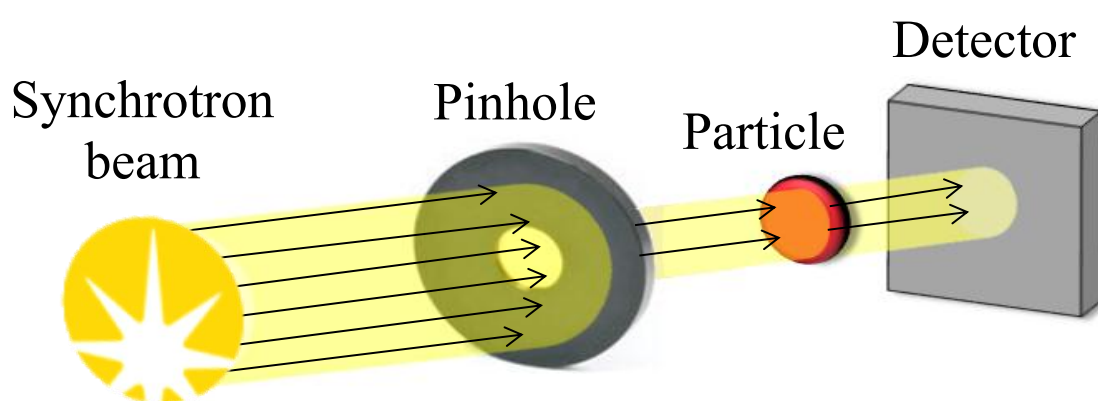


Fig.1. Schematic diagram of the sample presentation.

It was necessary to align the sample particle with the pinhole through which the selected part of the beam passes. The aligned pinhole and particle must then be aligned with the wavelength-selected synchrotron beam, so that a portion of this passes through the pinhole, then the sample, and goes on to hit the detector. To align the sample and pinhole we constructed a holder using the micrometer stage adjustment from an old microscope (Fig.2). With the pinhole fixed in a holder attached rigidly to the base, the two dimensional adjusters were used to move the sample cell until the particle was aligned. This was adjusted visually, aided by a light shone through the pinhole and/or a magnifying lens. The base was supported on

protruding bolts that rested on the floor of the sample compartment. By turning the bolts, it was possible to make a fine adjustment of the height of the base, and hence of the pinhole. The horizontal position of the pinhole was altered simply by sliding the whole assembly over the floor of the sample compartment.

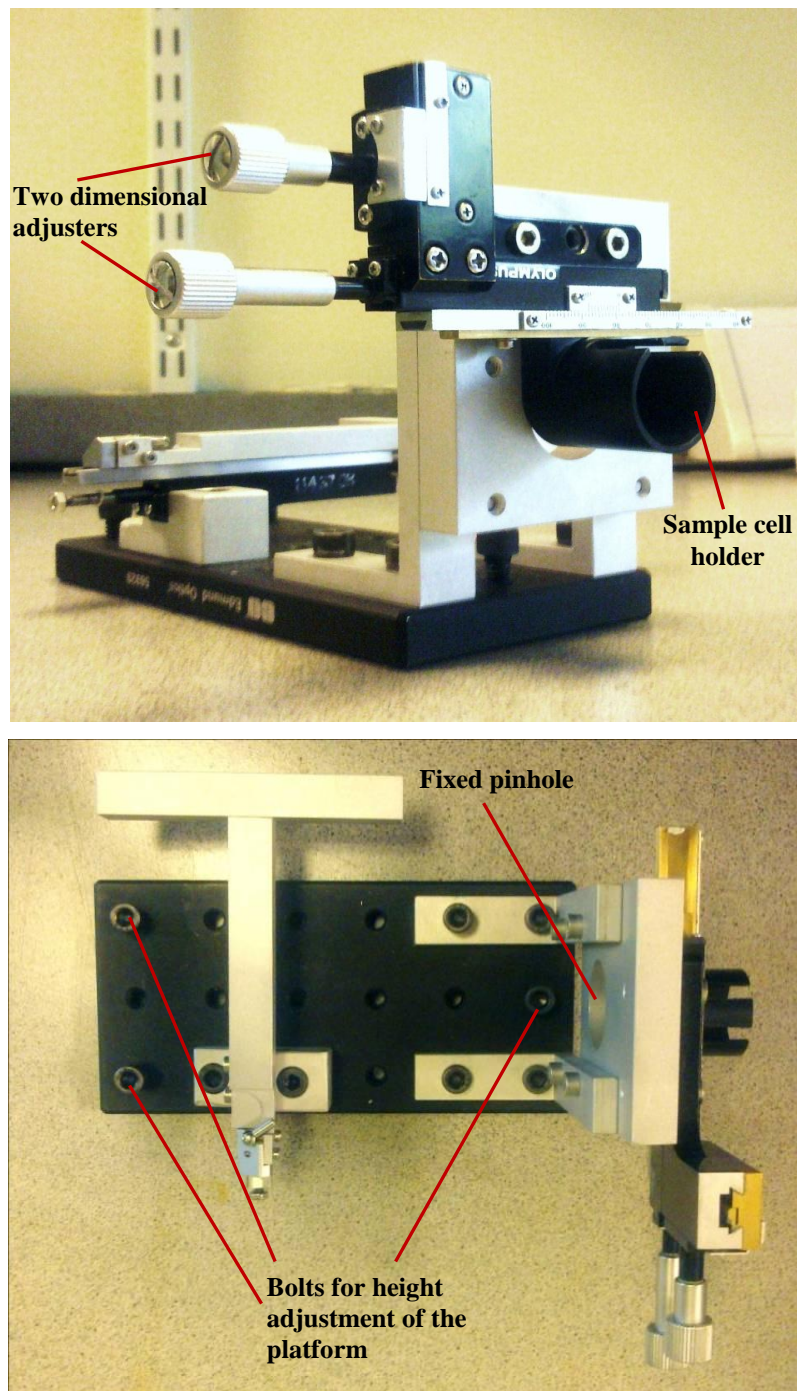


Fig.2. Pictures of the sample holder assembly.

To distinguish the two types of alignment adjustment, we will refer to: a) aligning the pinhole, which moves both the pinhole and the sample to the same extent, relative to the synchrotron beam; and b) aligning the sample, which moves the sample relative to the pinhole.

When making measurements on particles it is important to place the sample as close as possible to the detector window, to obtain maximum collection of scattered light. This is essential to minimise the effect of any differential scattering giving a false CD signal, but also important to get a better signal to noise ratio. We initially tried removing a barrier in the sample compartment of the CD instrument, so that the sample holder could be placed near the standard detector position. It was possible to obtain particle spectra in this way, but it was observed that the beam is rather larger in area here than at the normal sample position well in front of the detector. As a result the intensity of light at the pinhole, and hence illuminating the sample, will be reduced. So we moved the detector and re-mounted it with its window close to the normal sample position, where the beam is focussed to its smallest size. Then the pinhole and sample could be placed in this position of highest beam intensity.

It was observed that the position of the beam at the sample moved slightly (up to 2 mm) as the selected wavelength was varied, and perhaps also for other reasons. For a normal sample cell this would be immaterial, but in our case it could lead to the beam, or at least its brightest portion, missing the pinhole. The result was a very high HT value, and loss of any useful signal. To allow reasonable spectra to be collected, it was necessary to use a relatively narrow wavelength range, and to align the pinhole carefully to the beam in that wavelength range. Alignment was adjusted visually, aided by a piece of white paper stuck to the pinhole mount, and with a hole of about 0.7 mm diameter surrounding the pinhole. The beam position was clearly visible on the white surface, through autofluorescence of the paper when UV wavelengths were selected, which was viewed through UV protection glasses. The height and position of the sample and pinhole stand was adjusted until the illuminated spot appeared in the right position, with part of it now appearing dark as it hit the exposed black surface of the pinhole mount around the pinhole. One particular issue here is that the

beam actually consists of two bright spots separated by an almost dark horizontal band, due to the filter which absorbs hard X-rays component of the synchrotron radiation¹⁷. This was not easily seen by eye in the 1-2 mm spot where the beam hits the white surface. Hence the upper or lower part of the visible spot was aligned with the pinhole, rather than the very centre.

Measurements were made with samples in a conventional cylindrical CD cell of 0.2 mm pathlength. Some trials were made with a flattened capillary sample cell, as commonly used for synchrotron CD measurements^{15, 17}. However, particles would sediment to the lower part of the horizontally mounted capillary. Even with a blank liquid in the capillary, aligning the pinhole selected beam with this lower part of the capillary, where walls were strongly curved, led to very high apparent absorbance and high HT, preventing any useful CD data being collected.

Blank spectra

These were measured with the pinhole-selected portion of the beam passing through a sample cell containing either aqueous buffer or 1-propanol (the media in which particles were suspended). A selection of spectra are shown in Fig.3.

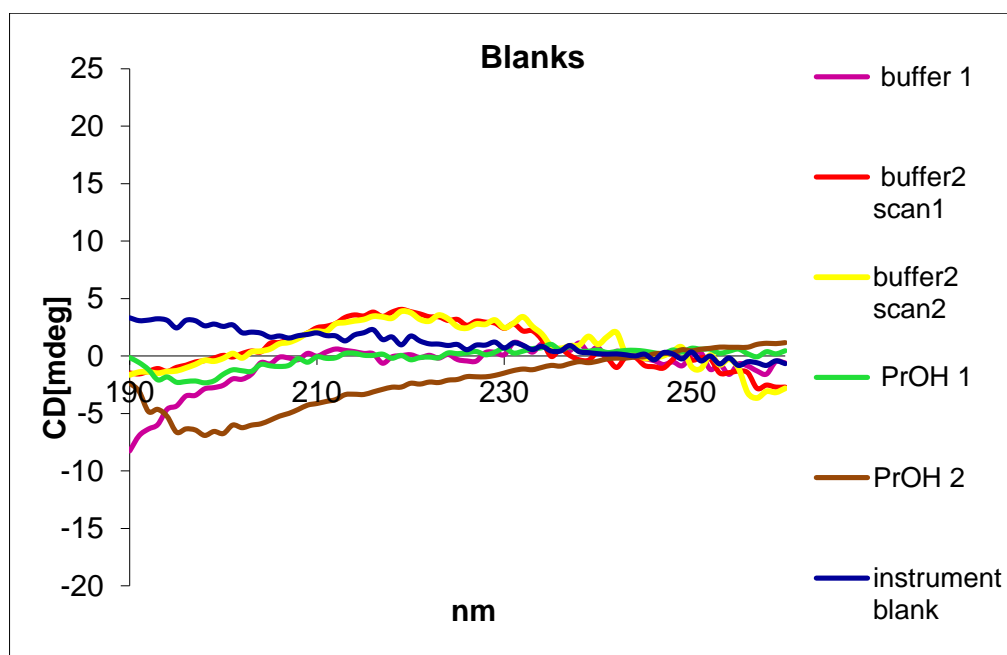


Fig. 3. Blank CD spectra with the synchrotron beam masked by a 150 μm pinhole. Each plot is the average of two successive scans with 5s integration time at each wavelength. First three experiments measured 20mM sodium phosphate buffer (pH 7.8) as a blank and in the fourth and fifth experiment 1-propanol was used as a blank. “Buffer2 scan1” and “Buffer2 scan2” were acquired successively with the same pinhole alignment, whereas different alignments were used for all others. “Instrument blank” was measured when the sample compartment of the instrument was absolutely empty: no pinhole, no sample holder.

The spectra in Fig.3 are quite noisy, compared with measurements in the absence of the pinhole, which showed noise of about 1 mdeg even with only 1 s integration time. This is no doubt because of the reduced intensity at the detector when using the pinhole. Repeat scans with exactly the same pinhole position were reproducible within the noise (e.g. Fig3, “buffer2 scan1” and “buffer2 scan2”). But after the pinhole was moved and then re-aligned, a significant change would often be observed (e.g.3, other plots). It was noted that turning the pinhole upside down led to a substantially and consistently different blank, so this aspect of its orientation was

kept constant. It would seem that some features on the surface of the pinhole can introduce artefactual signals. Some particularly large blank signals in early tests were traced to dust particles partly blocking the pinhole, so it was cleaned by blowing a N₂ stream through it. We speculated that alignment of the pinhole axis with the beam might be a variable, but a test with this deliberately misaligned by about 3 degrees gave a blank similar to others (data not shown). Since our test sample holder did not allow us to replace the pinhole in exactly the same position after changing sample, we have decided to subtract from measured sample spectra the “instrument blank”, which was measured with absolutely empty sample compartment (no pinhole, no sample holder).

Amount of light reaching detector

A major cause of the relatively high noise in these CD spectra is the limited amount of light reaching the detector. This is reflected in the rather high photomultiplier HT settings selected by the instrument electronics. It is informative to obtain an estimate of the amounts of light involved. The apparent absorbance of a sample in the spectropolarimeter can be estimated as:

$$A = Z \times \left(\log \frac{HT_s}{HT_b} \right) \quad (1)$$

where Z is an instrument constant, HT_s is HT of the sample and HT_b is HT of the blank¹⁸. Because the Olis electronics of SRCD vary the HT in a stepwise manner, the calculated absorbances will be rather more inaccurate, but are nevertheless a guide. From the HT values of a scan with an empty sample compartment, and with an A=2 neutral density filter in the beam, the instrument constant was estimated to be 9.2. Placing the pinhole in the light path at the point where the beam was smallest led to estimated absorbance of about 1.6 relative to the empty sample compartment, corresponding to between 2 and 3% of the light being transmitted. This is reasonable for a 150 μm pinhole in a beam of around 1 mm in size. No significant increase in absorbance was found on adding the blank liquid filled sample cell behind the

pinhole. If the pinhole was placed further back, near the standard detector position, the apparent absorbance was increased to about 2 (i.e. 1% transmission).

Standard spectrum of solution

To test the feasibility of obtaining reasonable spectra despite the limited light transmitted by the pinhole, we made measurements with the cell filled with a solution of ammonium camphor sulfonate. Fig.4 shows that the expected spectrum is observed, albeit more noisy than for normal measurements. For comparison, the same solution in the same cell was also measured on a conventional spectropolarimeter.

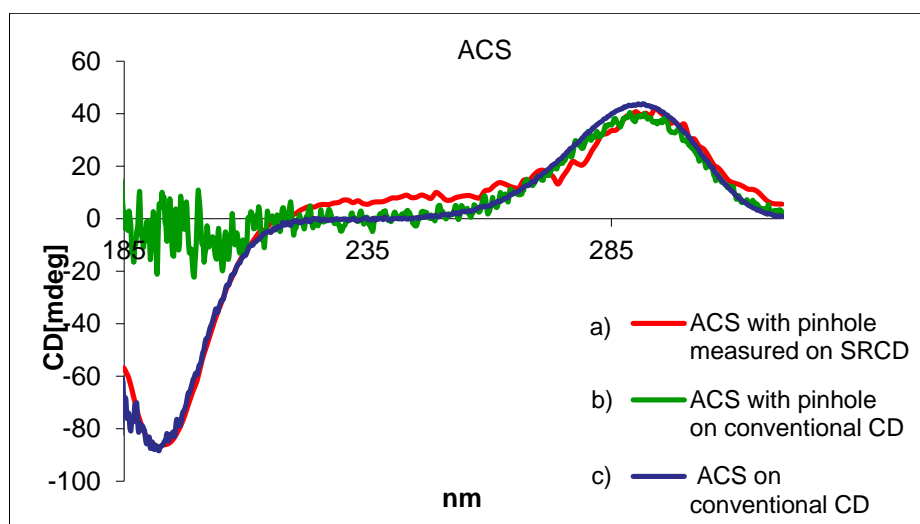


Fig. 4. CD spectrum of ammonium camphor sulfonate solution measured in different ways. The solution was 6.36 mg/mL ammonium camphor sulfonate in water, measured in a 0.02 cm pathlength cell. Spectra were measured: a) red line - using the synchrotron beam and a 150 μm pinhole, with 5 s integration time; b) green line - on a conventional spectropolarimeter with scan speed 10 nm/min and 4 s response time; and c) blue line - on the conventional spectropolarimeter with the 150 μm pinhole also inserted in the light beam. In case (c), the instrument HT was around 700 V at longer wavelengths, rising to 800 V at 220 nm and 900 V at 200 nm.

As can be seen (Fig.4), there is rather good agreement between the spectra, with perhaps a slightly lower maximum CD intensity on the synchrotron measurements. For comparison, measurements were also made on the conventional spectropolarimeter with the same pinhole placed in the light beam (Fig.4). The 291 nm peak was still visible, although somewhat reduced in intensity, and much noisier, no doubt due to the increase in HT from around 250 to 700 V, reflecting the much reduced light intensity after selection by the pinhole. But below 220 nm, the signal became very noisy, and there was no real indication of the usual prominent negative peak. Undoubtedly this reflects the relatively weak beam intensity in the far UV on the lab spectropolarimeter, such that after most of it is masked by the pinhole, too little light remains for meaningful measurements. In contrast the synchrotron beam has high intensity in this wavelength range, so the negative peak is still clearly measured.

Protein-containing particles: ovalbumin prepared by TPP

We proceeded to make measurements on a number of protein-containing particles. Fig.5 shows a series of spectra measured on particles in a preparation of ovalbumin treated by the process of three-phase partitioning (TPP). This is known to lead to changes in the structure of many proteins^{19, 20}, and significant enhancement in the activity of several enzymes both in aqueous and low water media²¹.

As can be seen, all spectra show shapes typical of proteins, with a broad negative peak around 220-230 nm, and then becoming positive at shorter wavelengths. Repeat scans with the same sample and pinhole alignment were reproducible within the noise (Fig.5, “particle 1 scan 1” and “particle 1 scan 2”). If the sample alignment was moved slightly, then the same particle brought back into the beam, the measured spectrum had a similar shape down to about 220 nm, but slightly different in lower wavelength and was apparently offset by 1.6 mdeg (not shown on the Fig.5). Note that with our current sample holder, re-aligning the sample necessarily also involved re-aligning the pinhole, and we have shown how this can alter the blank spectrum. Protein CD spectra normally have little intensity in the region of 250-260 nm, so it is

plausible to suggest that the difference in signal in this region just reflect offsets. Hence scans 1 and 2 of the particle 1 in Fig.5 have been offset to bring them to zero in this wavelength range. The shape of these spectra also resemble quite well those of a suspension of the same particles, measured using the rotating cell method (Fig.5 “suspension measurements”). Estimation of apparent absorbance (as described above) relative to the blank showed values increasing from near zero at 250 nm to around 0.8 at 210 nm.

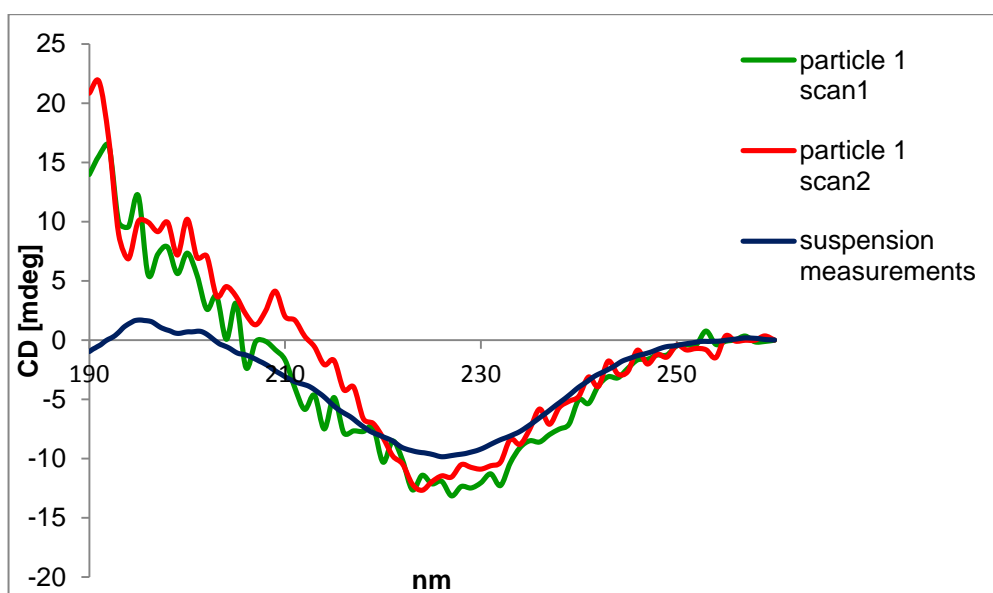


Fig.5. CD spectra of ovalbumin treated by three phase partitioning. Two were obtained from the same particle with the synchrotron beam and pinhole: repeat scans (1 and 2) with the same alignment of both pinhole and sample (green and red lines). “Suspension measurements” scan (blue line) was measured on a suspension of the ovalbumin particles in a rotating cell on a conventional spectropolarimeter. Particle scans have been blanked against “instrument blank” and slightly offset “scan 1” by +3mdeg, “scan 2” by +4.2 mdeg, to be around zero at 250-260 nm. The similar intensity of suspension scan with the others may be purely coincidental, because effective protein concentrations may differ in the suspension and single particle.

Measurements were also attempted using the conventional spectropolarimeter with the pinhole in the beam, on various protein-containing samples (solutions as well as suspensions). But no significant signals could be detected above very high noise levels, undoubtedly due to the low intensity passing the pinhole and hence very high HT values.

The very high intensity of the synchrotron beam means that radiation damage to the sample must be considered²². This is a greater concern in our measurements because of the relatively long acquisition times needed on account of the low amounts of light reaching the detector. A single scan from 260 to 190 nm involved the particle being exposed to UV for about 10 min. To examine this, repeated scans were made on the same particle (Fig.6).

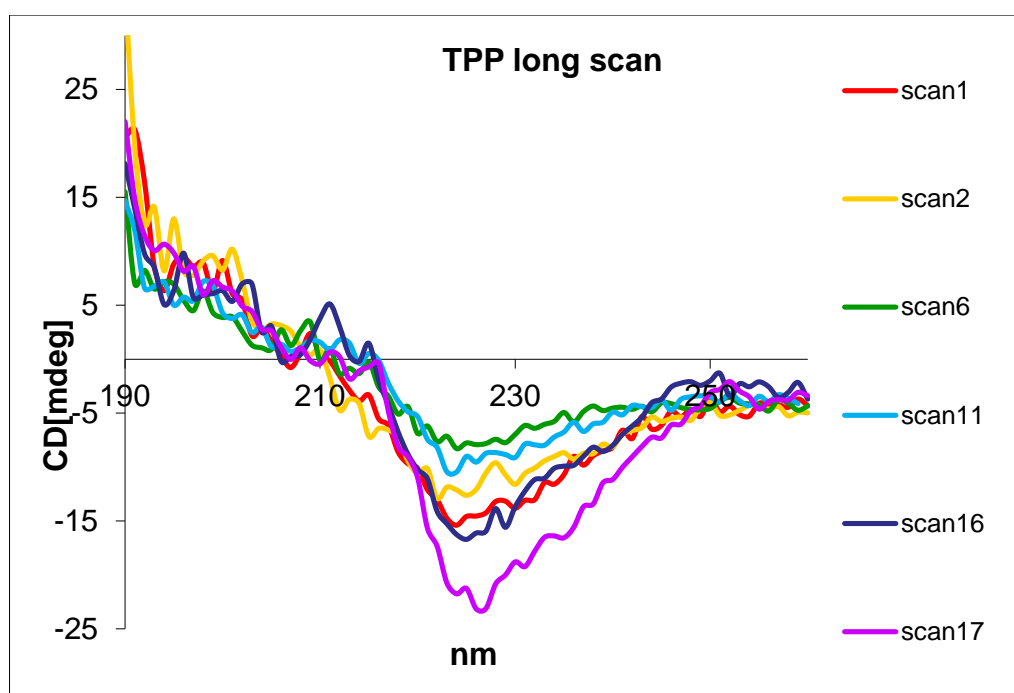


Fig.6. CD spectra observed on 17 repeated scans of the same particle of TPP treated ovalbumin. Scans were recorded without changing alignment of particle or pinhole, each lasting about 10 min. Shown here are scans 1, 2, 6, 11, 16, 17. Each spectrum was blanked against “instrument blank”.

The first 3 or 4 scans were essentially identical, but the subsequent scans showed a progressive reduction in (negative) signal around 225 nm, indicating that illumination was possibly damaging the protein. The essential shape of the spectra, particularly above 210 nm did not change substantially. It would appear that at least 2 scans can be acquired under our normal conditions without significant damage, so this was adopted for subsequent measurements.

Examination of a different particle would often, however, lead to a significantly different spectrum (Fig.7). In part the effect was a change in signal intensity, which may reflect just a different amount of protein in the beam path, because of differences in particle size, structure or porosity. But scaling of the spectra revealed significant changes in shape as well. For example, the differences in wavelength at which they cross the zero signal axis are clearly visible in Fig.7.

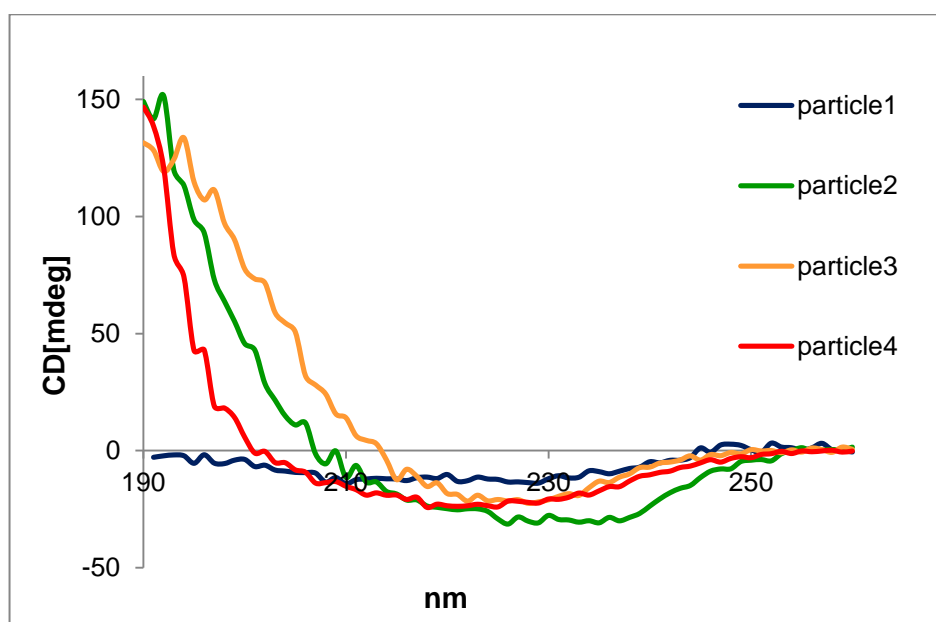


Fig.7. CD spectra of four different particles in the suspension of TPP treated ovalbumin. Each is the mean of two successive scans, which agreed within the noise. All four spectra were blanked against “instrument blank” and were offset to be around zero at 250-260nm (particle 1” was offset by -2.5mdeg, “particle 2” by +2mdeg, “particle 3” by +21mdeg, and “particle 4” by +4mdeg).

It is of course entirely possible that individual particles in a suspension have differences in protein conformation, which these spectra appear to suggest. Such differences would never be detectable through averaged measurements on a suspension of many particles. The possibility of differing blank contributions must be acknowledged here, as discussed above. But it is worth noting that some other particle preparations showed much more similar spectra for different particles, as shown below.

Chymotrypsin EPRPs

We proceeded to study a different type of preparation, an enzyme precipitated and rinsed in propanol (EPRP). The EPRP of alpha-chymotrypsin (and other of enzymes) show much higher activity than lyophilized powders in low water media ²³. Fig.8 shows spectra obtained from 3 different particles in an EPRP of alpha-chymotrypsin suspended in n-propanol. With these particles the apparent absorbance relative to the blank was higher (rising from 0.4 at 250 nm to 1.2 at 210 nm), so the spectra are noisier. A typical protein CD spectrum is however still detectable. Within the noise, there is no evidence that these particles have different spectra from each other. Fig.8 also shows the spectrum measured on a suspension of these same EPRP particles using the rotating cell method ²⁴. The shape of the longer wavelength part of the spectrum is similar to that of the individual particles, but there are significant deviations at lower wavelengths. One factor here may be the effect of absorption flattening, which will be much more severe for the suspension, especially where its absorbance is higher ¹¹.

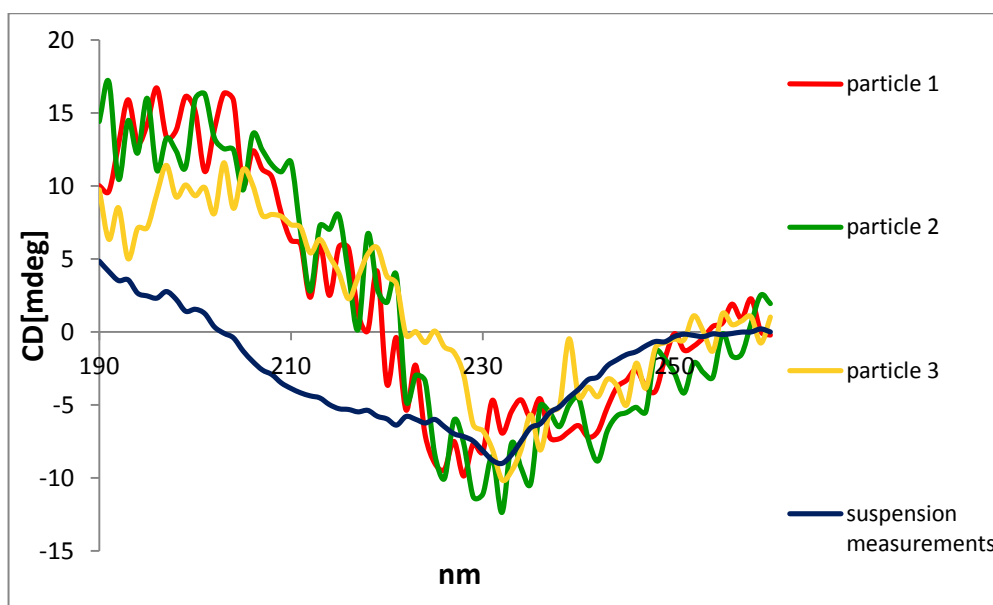


Fig.8. CD spectra of alpha chymotrypsin EPRP preparations suspended in propanol. Mean of two scans on 3 different particles in the suspension (red, green, yellow lines), and mean of two scans of suspension measured by rotating cell method (blue line). Spectra on three different particles were blanked against “instrument blank” and were offset to be around zero at 250-260nm: particle 1 by +9, particle 2 by +7.5, particle 3 by +6.5. To allow easier comparison of the shapes of the spectra, the CD signals measured on the suspension have been multiplied by 1.5 (comparison of absolute intensities are not meaningful because of different effective protein concentrations).

Chymotrypsin CLEAs

The EPRP particles may be treated with a cross-linking reagent (glutaraldehyde) to give a form of cross-linked enzyme aggregate (CLEA)²⁵. This leads to some loss of catalytic activity, which might reflect changes in structure²⁴. Fig.9 shows spectra acquired from 3 different particles from chymotrypsin CLEAs prepared in this way. The spectra have the same general shape as those for the EPRPs from which they were made (Fig.8). However, they are probably somewhat changed, and there also

seem to be significant differences in the spectra between the 3 particles. When preparing CLEAs, it is known that the extent of crosslinking dictates thermal stability, catalytic efficiency and enantioselectivity²⁵. Hence, the ability to detect structural changes in single particles would be of immense help in ‘fine tuning’ CLEA design. The spectrum obtained for measurements on the suspension of CLEA particles is similar to that for the EPRP suspension above (Fig.8), and plausibly could be seen as an average of what the individual particles show.

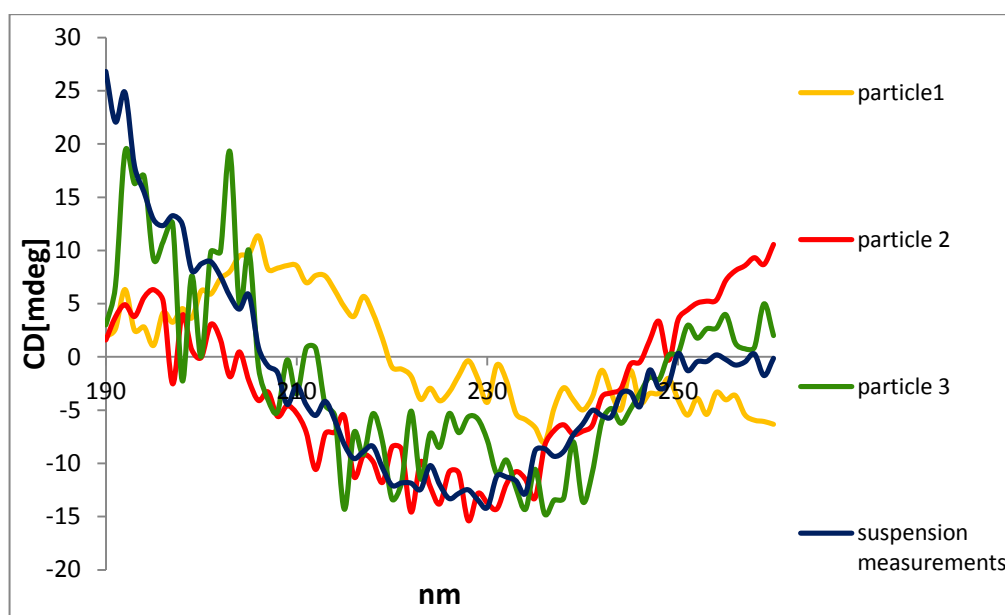


Fig.9. CD spectra of alpha chymotrypsin CLEA preparation suspended in propanol. The CLEA suspension was produced by cross-linking of EPRPs, as used for Fig.8. Mean of two scans on 3 different particles in the suspension (yellow, red and green lines), and mean of two scans of suspension measured by rotating cell method (blue line). Spectra on three different particles were blanked against “instrument blank”. To allow easier comparison of the shapes of the spectra, the CD signals measured on the suspension have been multiplied by 10 (comparison of absolute intensities are not meaningful because of different effective protein concentrations).

CONCLUSIONS

It is particularly important to point out that measurements on individual particles can reveal differences between particles in the same suspension. We have shown that these can be detected, certainly in the case of TPP ovalbumin. This would of course be undetectable by measurements on the whole suspension. But it is valuable information to aid understanding of the nature of the system. It is of course quite plausible that molecules in different particles in a suspension have had different histories during preparation, and therefore differences in structure.

Our approach could also be used to examine spatial differences in CD spectra in different parts of an inhomogeneous sample. For example, CD measurements can give useful information about the proteins in a section of muscle tissue²⁶. Measurements on different regions with dimensions of the order of 100 μm would allow investigation of whether changes in protein structure are spatially different within the sample. This would effectively be CD imaging, on a scale useful in understanding biological and disease mechanisms. Another key area is to be able to determine the consequence of moving from micron sized protein containing particles (especially protein immobilized on solid supports) to nanosized particles.

We have demonstrated that it is feasible to obtain CD spectra from single protein-containing particles using the synchrotron light beam masked by a 150 μm pinhole. At the same time, we have identified a number of factors that should be addressed in order to improve such measurements in terms of better reproducibility and better signal to noise ratio. In particular there should be a mechanism to replace the pinhole in exactly the same alignment relative to the beam, so that appropriate blanks may be recorded and subtracted.

REFERENCES

1. Berova, N., Nakanishi, K., Woody, R.W. Circular dichroism: Principles and Applications. 2nd edition, Wiley-VCH, New York, 2000.
2. Kelly, S.M., Jess, T.J., Price, N.C. How to study proteins by circular dichroism. *Biochimica et Biophysica Acta* 2005;1751: 119-139.
3. Wangoo N., Raman Suri C., Shekhawat G. Interaction of gold nanoparticles with protein: A spectroscopic study to monitor protein conformational changes. *Appl.Phys.Lett.*; 2008(92):133104-133107.
4. Sarmiento B., Ferreira D.C., Jorgensen L., van de Weert M. Probing insulin's secondary structure after entrapment into alginate/chitosan nanoparticles. *Eur. J. Pharm. Biopharm.* 2007;65:10-17.
5. Pebay-Peyroula E. Biophysical Analysis of membrane proteins. WILEY-VCH Verlag GmbH&Co; 2008: 243-258.
6. Wallace B.A., Mao D. Circular dichroism analysis of membrane proteins: an examination of light scattering and absorption flattening in large membrane vesicles and membrane sheets. *Anal. Biochem.* 1984;142: 317-328.
7. Wallace B.A., Janes R.W. Modern Techniques for circular dichroism and synchrotron radiation circular dichroism spectroscopy. *Advances in biomedical spectroscopy – vol.1*, IOS Press 2009.
8. Patching S.G., Edara S., Ma P., Nakayama J., Hussain R., Siligardi G., Phillips-Jones M.K. Interactions of the intact FsrC membrane histidine kinase with its pheromone ligand GBAP revealed through synchrotron radiation circular dichroism. *Biochim. Biophys. Acta* 2012;1818(7):1595-1602.
9. Ganesan A., Price N. C., Kelly S. M., Petry I., Moore B. D., Halling P. J. Circular dichroism studies of subtilisin Carlsberg immobilised on micron

- sized silica particles. *Biochimica et Biophysica Acta* 2006;1764(6): 1119-1125.
10. Ganesan A., Moore B. D., Kelly S. M., Price N. C., Rolinski O. J., Birch D. J. S., Dunkin I. R., Halling P. J. Optical spectroscopic methods for probing the conformational stability of immobilised enzymes. *Chem. Phys Chem* 2009;10(9-10): 1492-1499.
 11. Halling P. J. Estimation of flattening coefficient for absorption and circular dichroism using simulation. *Analytical Biochemistry* 2009;387: 76-81.
 12. Solanki K., Gupta M.N., Halling P.J. Examining structure–activity correlations of some high activity enzyme preparations for low water media. *Biores. Techn.* 2012;115:147-151.
 13. Rather G.M., Mukherjee J., Halling P.J., Gupta M.N. Activation of alpha-chymotrypsin by three phase-partitioning is accompanied by aggregation. *PLoS ONE* 7(12): e49241. doi:10.1371/journal.pone.0049241.
 14. Tomimatsu Y., Jansen E.F., Gaffield W., Olson A.C. Physical chemical observations on the α -chymotrypsin glutaraldehyde system during formation of an insoluble derivative. *J.Coll.Interf.Sci.* 1971;36(1):51-64.
 15. Hussain R., Javorfi T., Siligardi G. Circular Dichroism beamline B23 at the Diamond Light Source. *J. Synchrotron Rad.* 2012;19:132-135.
 16. Pike R.N., Dennison C. Protein fractionation by Three Phase Partitioning (TPP) in aqueous/t-butanol mixtures. *Biotech. Bioeng.* 1989;33:221-228.
 17. Javorfi T., Hussain R., Myatt D., Siligardi G. Measuring circular dichroism in a capillary cell using the B23 synchrotron radiation CD beamline at Diamond Light Source. *Chirality* 2010;22:149-153.
 18. Arvinte, T., Bui, T.T.T., Dahab, A.A., Demeule, B., Drake, A.F., Elhag, D., King, P. The multi-mode polarization modulation spectrometer: part 1:

- simultaneous detection of absorption, turbidity, and optical activity. *Analytical Biochemistry* 2004;33: 46-57.
19. Singh R. K., Gourinath S., Sharma S., Roy I., Gupta M. N., Betzel C., Srinivasan A., Singh T.P. Enhancement of enzyme activity through three phase partitioning: Crystal structure of a modified serine protease at 1.5 Å resolution. *Protein Engineering* 2001;14: 307-313.
 20. Lovrien R.E., Conroy M.J., Richardson T.I. Molecular basis for protein separations. In: Gregory R.B., editor. *Protein-solvent interactions*. Marcel Dekker; New York: 1995; 521–553.
 21. Roy I., Gupta M. N. α - chymotrypsin shows higher activity in water as well as organic solvents after three phase partitioning. *Biocat. Biotrans.* 2004;22:261-268.
 22. Orry A., Janes R.W., Sarra R., Hanlon M.R., Wallace B.A. Synchrotron radiation circular dichroism spectroscopy: vacuum ultraviolet irradiation does not damage protein integrity. *J. Synchrotron Rad.* 2001;8:1027-1029.
 23. Roy I., Gupta M.N. Preparation of highly active α -chymotrypsin for catalysis in organic media. *Bioorg.Med.Chem.Lett.* 2004;14:2191-2193.
 24. Solanki K., Gupta M.N., Halling P.J. Examining structure-activity correlations of some high activity enzyme preparations for low water media. *Bioresour.Technol.* 2012;115:147-151.
 25. Majumder A.B., Mondal K., Singh T.P., Gupta M.N. Designing cross-linked lipase aggregates for optimum performance as biocatalysts. *Biocat.Biotransform.* 2008;26:235-242.
 26. Kelly S.M., Price N.C. The use of circular dichroism in the investigation of protein structure and function. *Curr.Prot.Pept.Sci.* 2000;1:349-384.

CONCLUSION AND FUTURE WORK

The aim of this research work was to correct the effect of absorption flattening on the CD spectra of protein-containing particle suspensions. This was done by testing the simulation method recently developed by Halling (2009).

The results of correction for absorption flattening may be plausible CD spectra, agreeing with the expected spectra of protein molecules in the sample (when the same amount of chromophore is uniformly distributed throughout the entire volume of the cell). But in the absence of other methods to determine the structure experimentally, there remains doubt as to whether the corrected spectra are actually accurate. It was desirable to make some tests with non-protein samples in which the true spectrum can be known more confidently, and be used to compare with that obtained after correction for flattening. First two chapters of the thesis describe development and tests of such models.

In the first chapter chiral tris (ethylenediamine) Co(III) complex was chosen as its CD spectrum can be easily determined. It is a commonly used compound for CD calibration, with CD bands arising at near UV – Visible wavelength region. Tests were done on the Co(III) complex dispersed in small Sephadex particles, suspended in a chromophore free medium of 1-butanol. Once CD spectrum of this suspension sample was corrected for absorption flattening it showed good agreement with the expected CD spectrum. This demonstrated that the absorption flattening can be correctly estimated by using the appropriate theoretical model, at least at near UV-Visible region.

Because proteins absorb light in the UV, it was useful to test the correction model in this wavelength range. In Chapter II a number of samples with different chromophores with CD bands between 200 and 300 nm were studied. But only suspension containing ascorbic acid appeared to be suitable for the proposed model. Its CD spectrum when corrected for absorption flattening agreed well with the expected spectrum. This indicated that proposed simulation method can also be used to correct CD spectra in UV region, when applied to suitable samples.

In chapter III CD spectra of protein-containing particle suspensions were studied. Samples were prepared and measured same way as with previous chromophores. But, unfortunately, this time corrected CD spectra didn't agree with the expected ones (when the same amount of chromophore was uniformly distributed throughout the cell volume). Even the shape of the suspension sample spectra was different from the one in the solution sample. Studies also revealed that in this case simulation programme required almost ideal accuracy in determining the input parameters, which was not possible with the methods applied.

This leads to an overall conclusion, that although the simulation method can correctly estimate effect of absorption flattening artefact on CD spectra of some particle suspensions, it is not suitable for protein-containing particles (at least when using the proposed sample model).

Further studies are required to develop a suitable correction method for absorption flattening of CD spectra of suspensions with proteins. In future, the proposed correction method can be tested on other sample models, for example using different supports and solvents.

When the CD spectra of enzyme particles can be accurately estimated it would be useful to look at the different enzyme preparation methods for use in organic media. For example: propanol rinsed enzyme preparations (PREPs), enzymes treated by three phase partitioning (TPP), cross-linked enzyme aggregates (CLEAs), etc. Such preparations differ in activity and operational stability. Knowing the state of the enzyme molecules will benefit in understanding the reason behind this activity

variations, leading to developing an efficient and robust catalysts that can be used in low-water media.

Chapter IV suggests an alternative approach to solving the problem with artefacts of CD measurements of particle suspensions. The use of intensive synchrotron source allowed collecting feasible CD spectra on single protein-containing particles (100 μm in diameter), thus reducing effect of absorption flattening. This approach also revealed structural differences between particles in the same suspension, which would be undetectable by measurements on the whole suspension. Also this work identified a number of problems that should be addressed in order to improve such measurements.

In future it would be advantageous to further exploit such single-particle measurements. They need improvement, especially in reproducibility (of both alignment and spectra) and better signal to noise ratio. This can be done by modifying instrument and sample holder. In particular, the pinhole should be placed in exactly the same alignment relative to the beam, allowing to record appropriate blanks. Also the photomultiplier tube should be placed as close as possible to the sample, thus improving signal to noise ratio.

SRCD measurements of single particles show a great potential in better understanding of proteins structure that are in particulate form. These measurements not only reduce the absorption flattening affect but also can show differences between particles in the suspension, thus giving valuable information to help understanding of the nature of the system.

Further from this it would be advantageous to do imaging experiments and examine spatial differences in CD spectra in different parts of an inhomogeneous sample. This would be very useful in understanding biological and disease mechanisms.

APPENDIX

Enhancing activity and stability of alpha-chymotrypsin by entrapment inside dextran beads.

Kusum Solanki¹, Anna Gerdova², Peter J. Halling² and Munishwar N. Gupta¹

¹ *Department of Chemistry, Indian Institute of Technology Delhi, Hauz Khas, New Delhi, 110016, India.*

² *WestCHEM, Department of Pure and Applied Chemistry, University of Strathclyde, Glasgow G1 1XL, UK.*

ABSTRACT A method for preparing crosslinked enzyme aggregates (CLEA) of α -chymotrypsin inside dextran beads is described. This was possible by precipitating the enzyme inside the beads by *n*-propanol and subsequently crosslinking with glutaraldehyde. The V_{\max}/K_m for esterase activity of entrapped CLEA and free CLEA (as control) were 1520 and 1670 $\text{min}^{-1} \text{mg}^{-1} \text{ml}$ respectively. For caseinolytic activity, the corresponding values were 53 and 67 $\text{min}^{-1} \text{mg}^{-1} \text{ml}$ respectively. In low water media, both preparations gave similar initial rates for transesterification. The half lives of CLEA and entrapped CLEA at 50°C in aqueous conditions were 41 min and 100 min respectively. The CD spectra of the suspensions recorded with a special accessory confirmed the presence of the enzyme inside the beads and indicated the protein particles in the entrapped CLEA were less clumped than in the standard preparation.

INTRODUCTION

Enzyme immobilization is now an established approach for using enzymes in both aqueous and nonaqueous media ¹⁻⁴. Crosslinked enzyme aggregates (CLEA) have emerged as a robust biocatalyst design ⁵⁻⁷. In recent years entrapment of enzyme aggregates in silica ⁸ and CLEA in Lentikats ⁹ have been reported as further variation of the CLEA design. While it introduces a matrix (like most of the immobilization approaches) in the CLEA design, the entrapped CLEA design is more robust. The preparations are easier to handle, recover (after the reaction) and pack in column reactors. The present work is an extension of much older work from this laboratory wherein proteins were entrapped in Sephadex beads by aggregating the protein molecules by extensive crosslinking ¹⁰. The easy availability of these dextran beads with well defined porosities still makes them an attractive matrix. As recent work clearly shows that CLEA (made by crosslinking enzyme precipitates) are far more robust catalysts than earlier reported "chemical aggregates" ¹¹ (made by direct chemical crosslinking of enzymes in solution), the present method was developed in order to form CLEA inside the Sephadex beads.

It is shown that it is possible to form CLEAs inside Sephadex beads with complete retention of activity. Sephadex G 100 was chosen as a matrix because from the earlier work it was found that an appropriate pore size range is required for successful entrapment of the enzyme aggregates inside the beads. The present work was mostly carried out with alpha-chymotrypsin (Mol. Wt. 25 KDa). For an enzyme of molecular weight around 25000 Da, Sephadex G-100 gave the maximum yield of entrapment ¹⁰. These preparations show very high activity in organic solvents (just like CLEA) and high thermal stability in aqueous media (just like CLEA). In as much as such beads have been used extensively in gel filtration chromatography, the entrapped CLEA in Sephadex G-100 should work well in packed beds. Use of CD (with a special accessory which allows us to work with suspensions) ^{12, 13} has enabled us to look at structural aspects of the enzyme precipitates/aggregates inside the beads.

MATERIALS AND METHODS

Alpha-chymotrypsin (from Bovine pancreas, Cat. No. C-4129), *N*-acetyl-L-phenylalanine ethyl ester and *N*-benzyl tyrosine ethyl ester (BTEE) were obtained from Sigma Chemical Co., St. Louis, USA. All solvents were of low water grade (< 0.005 % water (v^v⁻¹)) and obtained from Sigma Chemical Co., St. Louis, USA. These solvents were further dried by gentle shaking with 3 Å molecular sieves (E. Merck, Mumbai, India). All others chemicals used were of analytical grade. Sephadex G 100 beads were purchased from Pharmacia Fine chemicals, Sweden. Recombinant green fluorescent protein (GFP_{uv}) overexpressed in *E. coli* BL21 (DE3) was purified by the method described elsewhere¹⁴.

Preparation of CLEA of alpha-chymotrypsin entrapped in the Sephadex G-100

Six samples with various concentrations of enzyme (alpha-chymotrypsin) and suspensions of Sephadex G-100 were prepared as follows: Different amounts of alpha-chymotrypsin were dissolved in the sodium phosphate buffer (10 mM, pH 7.5) and were added to dry Sephadex G-100 beads in different proportions (Table 1).

Table1. Concentrations of enzyme and sephadex beads while preparing samples.

Sample No.	Concentration of alpha-chymotrypsin, mg/ml	Concentration of Sephadex G-100, mg/ml
0	-	66
1	250	66
2	50	94
3	50	69
4	25	69

The mixtures were kept to swell overnight at 4°C. (The Sephadex concentrations used were high so as to get all the enzyme solution absorbed by the beads; the amount of liquid used was less than amount that gives complete swelling.) After that 500 µl of chilled anhydrous *n*-propanol was added to each sample to precipitate the enzyme (320 µl of enzyme solution absorbed by beads). After keeping mixtures on shaker for 30 min (at 4°C) at the speed of 150 rpm, 22 µl of aqueous glutaraldehyde was added so that the final concentration in the mixture became 100 mM. Mixtures were left on shaker at 4°C for 3 h at 175 rpm. At the end of the reaction time, samples were centrifuged at low speed of 664 x g (to minimize Sephadex beads breakage) for 15 min. Supernatants were removed and samples were then used for carrying out aqueous assays. Samples were further washed 3 times with anhydrous *n*-propanol, followed by 3 times of washing with anhydrous *n*-octane before carrying out transesterification reactions in organic solvents.

Preparation of CLEA

CLEA were made as described earlier^{5,6}. Alpha-chymotrypsin (8 mg) was dissolved in 320 µl of sodium phosphate buffer (10 mM, pH 7.5) and precipitated by adding 500 µl of *n*-propanol at 4 °C. After incubating the mixtures on a shaker for 30 min (at 4°C) at the speed of 150 rpm, 100 mM of glutaraldehyde was added to crosslink the precipitate, with constant orbital shaking at 4°C for 3 hours at 175 rpm. At the end of the reaction time, samples were centrifuged for 15 min, at 664 x g. Supernatants were removed and samples were washed 3 times with anhydrous *n*-propanol, followed by 3 times of washing with anhydrous *n*-octane.

Transesterification reaction by alpha-chymotrypsin

The catalytic activities of preparations of alpha-chymotrypsin in organic solvents were measured by transesterification reaction between *N*-acetyl-L-phenylalanine ethyl ester (10 mM) and *n*-propanol (1 M) with *n*-octane as a reaction medium¹⁵. Enzyme preparations (equivalent to 8 mg of original enzyme powder) were introduced to

transesterification reaction by suspending them in 10 ml of anhydrous *n*-octane, and to these mixtures a solution of *N*-acetyl-*L*-phenylalanine ethyl ester in anhydrous *n*-propanol were added. The reaction mixture was incubated at 30 °C and the progress of reaction was monitored by withdrawing aliquots at different time periods. The samples were analyzed by HPLC ¹⁵. Initial rates were calculated from the aliquots taken within 0.25 to 2 h. The percentage conversions during these time periods were in the range of 1-30 % and were in linear range. Reactions were done in triplicate and the value for initial rates reported is mean of all three. Individual values within all sets of triplicates were within ± 5 %.

HPLC analysis

The samples were analyzed by HPLC using ZORBAX SB-C18 column (Agilent Technologies, USA). The eluent consisted of 5 % (v/v) glacial acetic acid, 55 % (v/v) water and 40 % (v/v) acetonitrile with a flow rate of 1 ml min⁻¹ and detection was carried out with a UV detector at 258 nm ¹⁵.

Determination of kinetic parameters

K_m and V_{max} values of different formulations of alpha-chymotrypsin for two substrates, BTEE (*N*-Benzyl-tyrosine ethyl ester in 0.1 M Tris-HCl buffer, pH 7.8) ¹⁶ and casein (in 50mM Tris-HCl buffer, pH 7.8) ¹⁷ were determined. Initial rates of hydrolysis were measured with various concentrations of substrates. Hanes-Woolf plots were drawn for determination of K_m values for native enzyme solution, CLEA and entrapped CLEA in beads. Each of the above experiment was carried out in duplicate and difference in the initial rate values within a pair was found to vary within 5 %.

Preparation of the green fluorescent protein (GFP) sample

320 μ l of GFP solution (25 mg/ml) was added to 22 mg of Sephadex G-100 and left to swell overnight at 4°C. Rest of the procedure for the preparation of CLEA (entrapped in Sephadex G 100 beads) was same as used for alpha-chymotrypsin.

Protein Determination

Protein concentration was determined according to the procedure described by Bradford using bovine serum albumin (BSA) as the standard protein ¹⁸.

Circular Dichroism

CD measurements of biocatalyst formulations in *n*-propanol were done on Jasco J-810 using a rotating sample cell holder fabricated at University of Strathclyde ^{12, 13}, and a cylindrical quartz cell of pathlength 0.5 mm. The spectra were corrected for the background.

Confocal Laser Scanning Microscopy

The GFP samples were mounted on slides and images were taken on a Leica TCS-SP2 confocal microscope (Leica). Images were processed using Leica confocal software (LCS, Biolabs) and Adobe Photoshop version 7.0.

Thermal stability study

Thermal stability of alpha-chymotrypsin (free enzyme, free CLEA and CLEA entrapped in beads) was studied at 50 °C (in 50 mM Tris-HCl buffer, pH 7.8). An appropriately diluted sample of free enzyme and CLEA was withdrawn at different time intervals, cooled to assay temperature and then assayed by BTEE hydrolysis to measure activity.

RESULTS AND DISCUSSIONS

In order to test the conceptual design, Green fluorescent protein (GFP), was initially used as a model protein. This made it easy to determine whether all the protein was entrapped inside the beads. The GFP molecular weight is 26 KDa hence Sephadex G100 beads were appropriate choice for this protein as well.

Figure 1 shows the confocal image of CLEA of Green fluorescent protein (GFP) entrapped inside Sephadex G 100 beads.

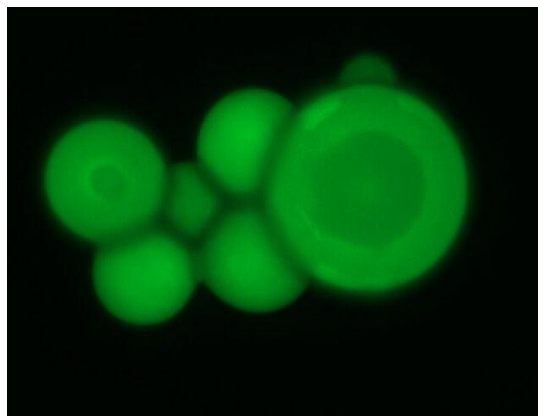


Fig.1. Green Fluorescent Protein as a marker for entrapping enzyme inside dextran beads for low water media.

For protein solution to be completely absorbed by the beads, only small amount (320 μ l) of enzyme solution in 10 mM sodium phosphate buffer (pH 7.5) was added to the 22 mg of dry Sephadex G-100 beads. Also, due to the low amount of liquid available, all the beads were not swollen completely and different sizes of beads were observed. Figure 1 shows that no protein aggregates are present outside the beads. Entrapped GFP CLEA did

not show any leaching up to 6 cycles (1 cycle corresponds to 1 h incubation in 50 mM sodium phosphate buffer (pH 7.5) at 50 rpm followed by centrifugation and then resuspension in same buffer) (Figure 2). After 6 cycles also, it was shaken with buffer overnight and even after 12 h of shaking no GFP was released from beads. In case of GFP absorbed in the beads (no precipitation and crosslinking), there was nothing retained within the beads after 4 h.

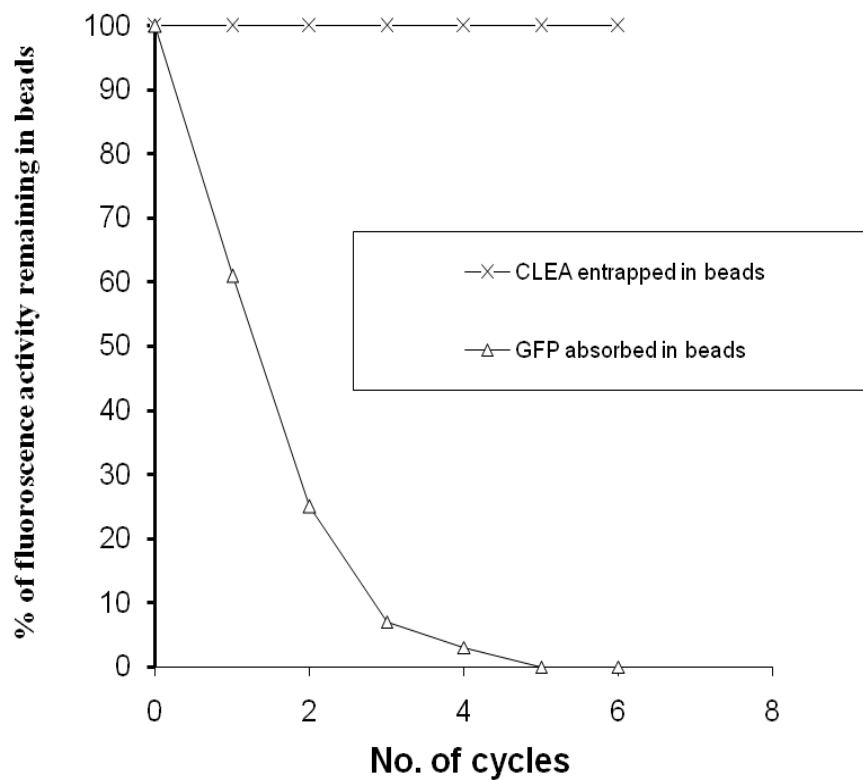


Fig.2 Release of entrapped GFP from sephadex G-100 beads by washing with Tris buffer (0.5 M, pH 7.5).

Encouraged by these results, we proceeded to work with alpha-chymotrypsin. After precipitating enzyme with anhydrous *n*-propanol all samples were examined under the microscope to see if all protein was entrapped into the Sephadex beads (Figure 3).

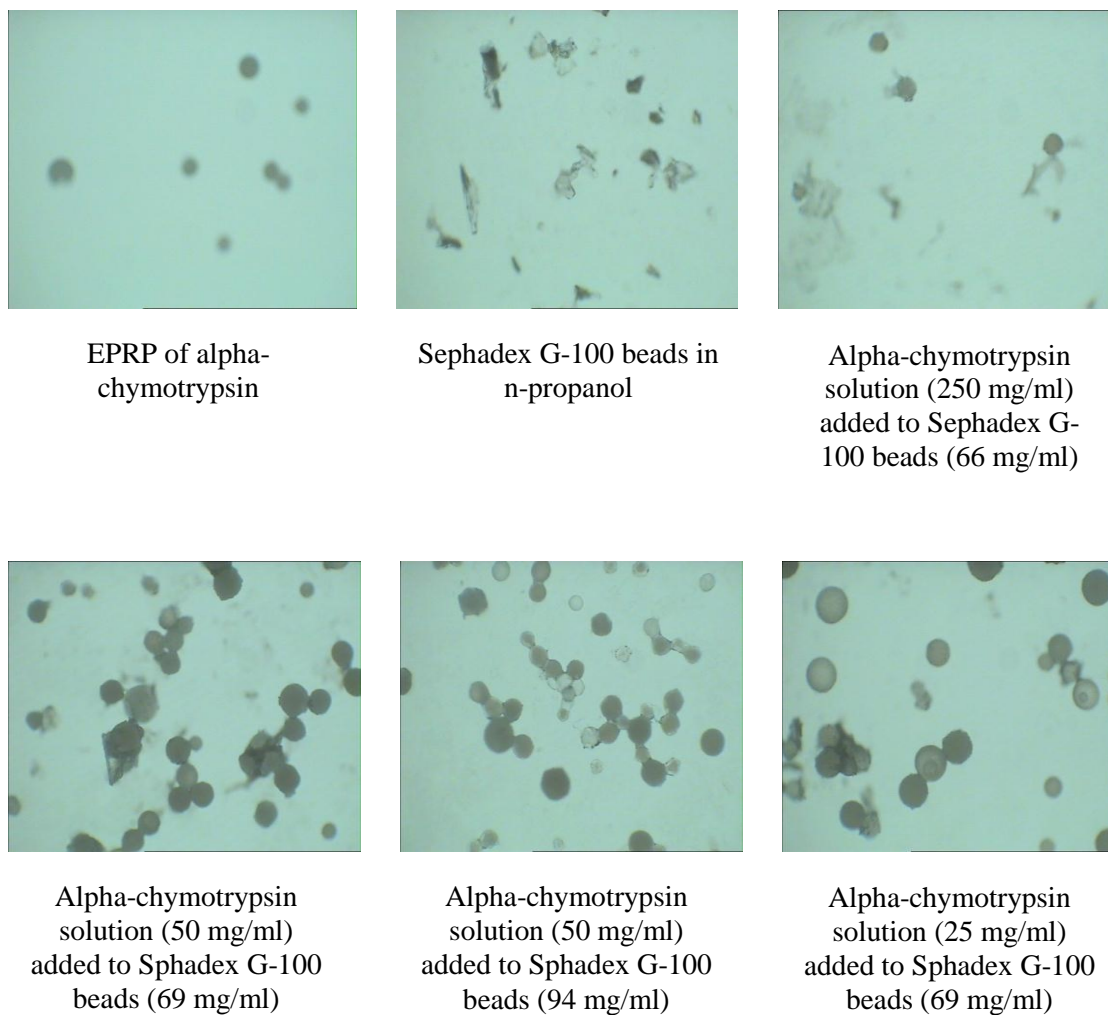


Fig.3. Microscopic pictures of alpha-chymotrypsin entrapped inside Sephadex G-100 beads. (Sephadex beads were incubated overnight with enzyme solution. After the absorption of enzyme by beads, *n*-propanol was added to precipitate the enzyme inside the beads followed by the crosslinking of aggregates by addition of glutaraldehyde.)

As can be seen, there were some precipitated protein particles around the beads, and these were more numerous when more protein had been added to a fixed amount of beads. The best results were found to be for the Sample 3 (Table 1) (with 50 mg/ml of enzyme solution added to 69 mg of dry Sephadex beads per ml) and Sample 4 (Table 1) (with 25 mg/ml of enzyme solution added to 69 mg of dry Sephadex beads per ml), where the amount of protein precipitates surrounding the beads were minimum.

The optimized alpha-chymotrypsin concentration used for entrapment was 25 mg/ml. The clear enzyme solution was made at 4 °C and immediately added to 69 mg of dry Sephadex beads. As a control, free CLEA were also prepared using same enzyme concentration (25 mg/ml) at 4 °C.

The specific activity of CLEA entrapped was 62.3 U/mg of enzyme as compared to 63.5 and 55.1 U/mg protein for straight out of bottle enzyme (free enzyme solution) and free CLEA formulation of alpha-chymotrypsin respectively (Table 2A). The activity recovery after entrapping the CLEA in sephadex G 100 beads was around 98 % whereas for free CLEA it was only 87 %. This could be due to the fact that free CLEA tend to aggregate and form clusters. As reported earlier, CLEAs look like a continuous mass¹³.¹⁴. On the other hand, when entrapped inside the beads, CLEA material is present as discrete portions. Former, thus are expected to show greater mass transfer constraints.

Table 2A: Esterase activity of alpha-chymotrypsin (determined by BTEE assay)

Enzyme formulation	Specific activity (U/mg protein)	% activity
Straight out of bottle	63.5	100
free CLEA	55.1	87
CLEA entrapped in sephadex beads G - 100	62.3	98

Table 2 B & C summarize the V_{\max}/K_m values of different formulations of alpha-chymotrypsin using BTEE and Casein respectively as substrates.

Table 2B: Determination of kinetic parameters for different formulations of alpha-chymotrypsin with Benzoyl tyrosine ethyl ester (BTEE) as a substrate.

(The experiments were done in triplicate and the percentage error in each set of readings was within 4 %.)

Enzyme formulation	K_m (mM)	V_{max} ($\mu\text{molmin}^{-1}\text{mg}$ (protein)⁻¹)	V_{max}/K_m ($\text{min}^{-1}\text{mg}^{-1}\text{ml}$)
Straight out of bottle	0.039	63.5	1630
CLEA (100 mM)	0.038	63.3	1670
CLEA entrapped in sephadex beads G-100	0.042	63.0	1520

The V_{\max}/K_m measured towards BTEE as a substrate, for CLEA entrapped in beads (1520 $\text{min}^{-1}\text{mg}^{-1}\text{ml}$) was perhaps marginally lower than CLEA (1670 $\text{min}^{-1}\text{mg}^{-1}\text{ml}$) and free native enzyme (1630 $\text{min}^{-1}\text{mg}^{-1}\text{ml}$) (Table 2B).

The CLEA entrapped inside the beads showed V_{\max}/K_m better than CLEA but worse than the native free enzyme solution for caseinolytic activity (Table 2C).

Table 2C: Determination of kinetic parameters for different formulations of alpha-chymotrypsin with Casein as a substrate.

(The molecular weight of casein used to get molar concentration was 23,700 gmol⁻¹. The experiments were done in triplicate and the percentage error in each set of readings was within 4 %.)

Enzyme formulation	K_m (mM)	V_{max} (μmolmin⁻¹mg (protein)⁻¹)	V_{max}/K_m (min⁻¹mg⁻¹ ml)
Straight out of bottle	0.00097	0.21	216
CLEA (100 mM)	0.0036	0.19	53
CLEA entrapped in sephadex beads G-100	0.0018	0.12	67

The V_{max}/K_m values determined were 216, 53 and 67 min⁻¹mg⁻¹ml for enzyme solution, CLEA and CLEA entrapped inside beads respectively. This casein vs. ester data is expected as larger substrate would show greater mass transfer constraints for the particulate CLEA preparations. The better V_{max}/K_m for entrapped rather than standard CLEA in case of caseinolytic activity is interesting. As discussed above, CLEA look like a continuous mass whereas discrete particles^{5,6} could have been formed by entrapment, so better mass transfer was observed.

There was an enhancement in the thermal stability of CLEA of alpha-chymotrypsin after its entrapment in the beads. The half lives of “straight out of bottle” native enzyme and CLEA were 25 and 41 min respectively at 50 °C (in 50 mM Tris-HCl buffer, pH 7.8). Upon entrapment of CLEA in beads the half life increased to 100 min (Data not shown).

The synthetic activity in non-aqueous media was also determined using transesterification reaction between *N*-acetyl-*L*-phenylalanine ethyl ester (10 mM) and *n*-propanol (1 M) with *n*-octane (10 ml) as a reaction medium. Table 2D shows the initial rates for transesterification reaction for CLEA entrapped in beads (24 nmoles min⁻¹ mg⁻¹), determined by HPLC, was similar to the rates of free CLEA enzyme preparations (26 nmoles min⁻¹ mg⁻¹).

Table 2D: Transesterification activity of CLEA of alpha-Chymotrypsin entrapped inside different beads.

(CLEA of alpha-chymotrypsin entrapped in beads was made by incubating 22 mg of different beads with 8mg of alpha-chymotrypsin in 320 µl of 10 mM sodium phosphate buffer (pH 7.8). Details of transesterification reaction are given in materials and methods.)

Biocatalytic preparations	Initial rates (nmolmin ⁻¹ mg ⁻¹)
Straight out of bottle	0.7
CLEA	26
CLEA entrapped in Sephadex beads G-100	24
CLEA entrapped in Superdex 75 beads.	200

To demonstrate the generality of the described entrapment procedure and to improve the mechanical properties of CLEA entrapped in beads, a rigid matrix – superdex 75 beads - was also tried for CLEA entrapment (Table 2D). Initial rate of transesterification for CLEA of alpha-chymotrypsin entrapped in superdex 75 beads was measured as 200 nmolesmin⁻¹mg⁻¹ respectively as compared to 0.7 nmolesmin⁻¹mg⁻¹ for straight out of bottle enzyme (Table 2D).

Figure 4 represents the far UV CD spectra of different formulations of alpha-chymotrypsin i.e. enzyme solution in aqueous buffer, CLEA and entrapped CLEA in Sephadex G-100 suspended in *n*-propanol.

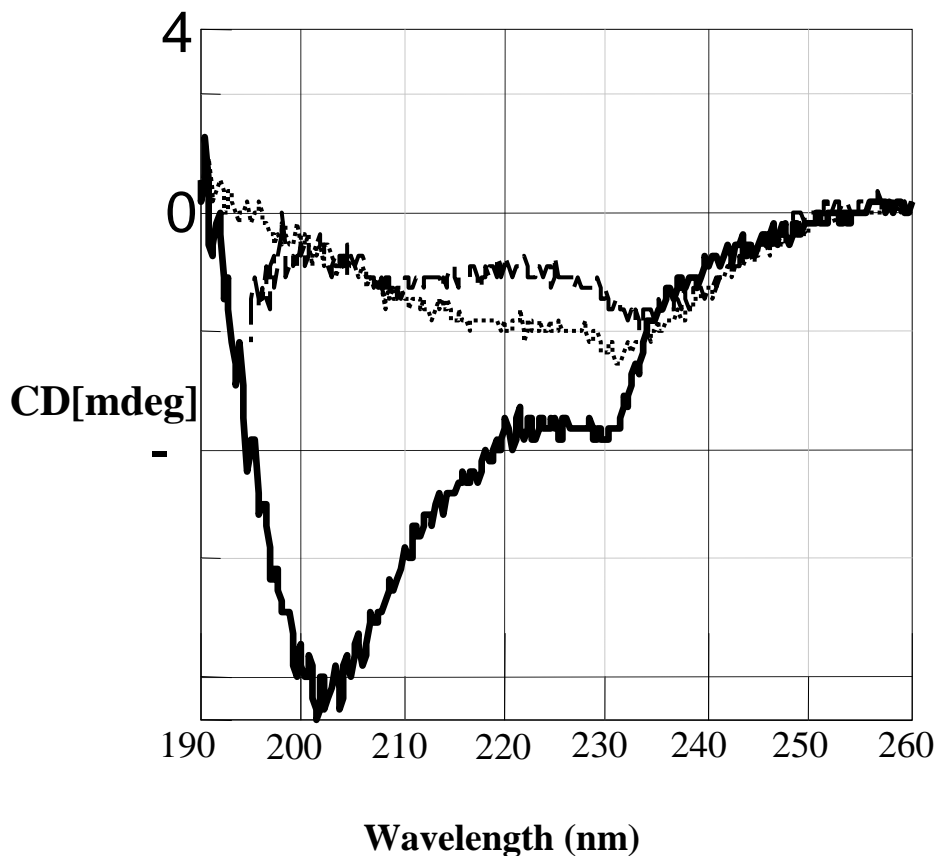


Fig. 4. Far UV CD spectra of different formulations of alpha-chymotrypsin. Solid line – alpha-chymotrypsin solution in 20 mM phosphate buffer (pH 7.8);
..... – CLEA suspension (not entrapped in beads) suspended in *n*-propanol;
----- CLEA entrapped in sephadex G-100 suspended in *n*-propanol.

Far UV CD spectrum of alpha-chymotrypsin consists of two minima, one at 230 nm (due to antiparallel beta sheets) and another at 202 nm (parallel beta sheets) ¹⁹. The spectrum of free CLEA shows that the characteristic negative peak at 230 nm is there but the minimum at 202 nm has completely disappeared (could be due to absorption flattening). Far UV spectra of CLEA entrapped in Sephadex beads consists of negative peaks at 230 nm and 205 nm. The appearance of negative peak at 205 nm in case of CLEA entrapped in beads could be due to either less absorption flattening or due to different secondary structure than free CLEA (not entrapped in the beads). This shows that there is less clumping in case of CLEA entrapped in beads than free CLEA.

CONCLUSION

The above results show preparation of a high activity alpha-chymotrypsin preparation which shows better catalytic properties and enhanced thermal stability. While some other procedures for entrapment of CLEAs have been described ^{8,9}, the method described here is simple and does not require any special equipment or material. Both Sephadex beads and superdex beads are readily available commercially. We are aware that the method can work equally well with beads made of other materials with different characteristics. The work with variety of such beads is in progress.

REFERENCES

1. G. Carrea, S. Riva, Properties and synthetic applications of enzymes in organic solvents, *Angew. Chem. Int. Ed.* 39 (2000) 2226-2254.
2. E.P. Hudson, R.K. Eppler, D.S. Clark, Biocatalysis in semi-aqueous and nearly anhydrous conditions, *Curr. Opin. Biotechnol.* 16 (2005) 637-643.
3. J.M. Guisan, (2006) In *Immobilization of enzymes and cells*. Guisan, J.M.(Ed.); Humana Press: New Jersey.
4. L. Cao, (2005) In *Carrier bound immobilized enzymes: principles, applications and designs*. Wiley-VCH verlag GmbH & Co.
5. R. Schoevaart, M.W. Wolbers, M. Golubovic, M., Ottens, A.P.G. Kieboom, F. van Rantwijk, L.A.M. van der Wielen, R.A. Sheldon, Preparation, optimization, and structures of cross-linked enzyme aggregates (CLEAs), *Biotechnol. Bioeng.* 87 (2004) 754-762.
6. S. Shah, A. Sharma, M.N. Gupta, Preparation of cross-linked enzyme aggregates by using bovine serum albumin as a proteic feeder, *Anal. Biochem.* 351 (2006) 207-213.
7. M.N. Gupta, S. Raghava, (2009) Enzyme stabilization via cross-linked enzyme aggregates In: *Methods in Molecular Biology: Enzyme Stabilization: Methods and Protocols* (Shelley D. Minter, Ed), Humana Press Inc., Totowa, NJ.

8. M. Il Kim, J. Kim, J. Lee, H. Jia, H. B. Na, J. K. Youn, J. H. Kwak, A. Dohnalkova, J. W. Grate, P. Wang, T. Hyeon, H. G. Park, H. N. Chang, Crosslinked enzyme aggregates in hierarchically-ordered mesoporous silica: A simple and effective method for enzyme stabilization, *Biotechnol. Bioeng.* 96 (2007) 210-218.
9. L. Wilson, A. Lllanes, C.C.P. Benevides, O. Abian, R. Fernández-Lafuente, J.M. Guisán, Encapsulation of crosslinked Penicillin G acylase aggregates in lentikats: evaluation of novel biocatalyst in organic media. *Biotechnol. Bioeng.* 88 (2004) 558-562.
10. S.K. Khare, S. Vaidya, M.N. Gupta, Entrapment of proteins by aggregation within Sephadex beads, *App. Biochem. Biotechnol.* 27 (1991) 205-216.
11. G. B. Broun, Chemically aggregated enzymes, *Methods Enzymol.* 44 (1976) 263-280.
12. A. Ganesan, B.D. Moore, S.M. Kelly, N.C. Price, O.J. Rolinski, D.J.S. Birch, I.R. Dunkin, P.J. Halling, Optical spectroscopic methods for probing the conformational stability of immobilised enzymes, *Chem. Phys. Chem.* 10 (2009) 1492-1499.
13. A. Ganesan, N.C. Price, S.M. Kelly, I. Petry, B.D. Moore, P.J. Halling, Circular dichroism studies of subtilisin Carlsberg immobilised on micron sized silica particles, *Biochim. Biophys. Acta* 1764 (2006) 1119-1125.
14. S. Dalal, S. Raghava, M.N. Gupta, Single step purification of recombinant green fluorescent protein on expanded beds of immobilized metal affinity chromatography media, *Biochem. Eng. J.* 42 (2008) 301-307.

15. M.T. Ru, J.S. Dordick, J.A. Reimer, D.S. Clark, (2001) Salt-induced activation of enzymes in organic solvents: optimizing the lyophilization time and water content. In *Enzymes In Nonaqueous Solvents* (Vulfson EN, Halling PJ & Holland HL, eds.), pp. 3-11. Humana Press Inc., NJ.
16. K.A. Walsh, P.E. Wilcox (1970) Serine proteases. In *Methods Enzymol* (Perlmann GE & Lorand L, eds), pp31-41 Vol 41. Academic Press, NY.
17. M. Fujimora, T. Mori, T. Tosa, Preparation and properties of soluble-insoluble immobilized proteases, *Biotechnol. Bioeng.* 29 (1987) 747-752.
18. M.M. Bradford, A rapid and sensitive method for the quantitation of microgram quantities of protein utilizing the principle of protein-dye binding, *Anal. Biochem.* 72 (1976) 248-254.
19. M.S. Celej, M.G. D'Andrea, P.T. Campana, G.D. Fidelio, M.L. Bianconi, Superactivity and conformational changes on alpha-chymotrypsin upon interfacial binding to cationic micelles, *Biochem. J.* 378 (2004) 1059-1066.